

Manuscript Number: JTB-D-18-00514R2

Title: Adaptive damage retention mechanism enables healthier yeast population

Article Type: Regular paper

Keywords: damage retention, replicative ageing, pedigree-tree model, ageing, unicellular organisms, yeast, dynamical modelling

Corresponding Author: Professor Marija Cvijovic, PhD

Corresponding Author's Institution: University of Gothenburg

First Author: Qasim Ali

Order of Authors: Qasim Ali; Riccardo Dainese; Marija Cvijovic, PhD

**Abstract:** During cytokinesis in budding yeast (*Saccharomyces cerevisiae*) damaged proteins are distributed asymmetrically between the daughter and the mother cell. Retention of damaged proteins is a crucial mechanism ensuring a healthy daughter cell with full replicative potential and an ageing mother cell. However, the protein quality control (PQC) system is tuned for optimal reproduction success that suggests optimal health and size of the population, rather than long-term survival of the mother cell. Modelling retention of damage as an adaptable mechanism, we propose two damage retention strategies to find an optimal way of decreasing damage retention efficiency in order to maximize population size and minimize the damage in the individual yeast cell. A pedigree model is used to investigate the impact of small variations in the strategies over the whole population. These impacts are based on the altruistic effects of damage retention mechanism and are measured by a cost function whose minimum value provides the optimal health and size of the population. We showed that fluctuations in the cost function allow yeast cell to continuously vary its strategy, suggesting that optimal reproduction success is a local minimum of the cost function. Our results suggest that a rapid decrease in the efficiency of damage retention, at the time when the mother cell is almost exhausted, produces fewer daughters with high levels of damaged proteins. In addition, retaining more damage during the early divisions increases the number of healthy daughters in the population.

#### Research Data Related to this Submission

There are no linked research data sets for this submission. The following reason is given:

No data was used for the research described in the article

Gothenburg, November 5, 2018

Journal of Theoretical Biology, editorial board

Dear Professor Chaplain,

On behalf of the authors, I thank you and the referees for the careful assessment of resubmission. As both reviewers noted, we have clearly improved our manuscript. We now submit a second revised version where we have addressed the points raised as outlined in our response to reviewers.

We have received the comments from two reviewers:

**Reviewer 2** Was very positive with our revision and had minor cosmetic comments regarding the figure and model description. We have taken these two points into the consideration and have updated our manuscript accordingly.

**Reviewer 3** Was also positive with our latest improvements of the manuscript and had comments related to the language and conclusions. Several typos are now corrected, however some concerns and comments raised by this reviewer left a feeling that s/he doesn't possess a knowledge on yeast ageing and is more focused on mathematical conclusions. Although this is completely understandable and we agree with it, we would like to draw attention that reviewers comments should be taken with consideration.

In both first and now second revision, we have provided extensive biological motivation for the problem we are analyzing and cannot agree with some of the points raised.

Our responses to all the points raised are detailed in the Rebuttal. We hope that with these changes, you will find our manuscript suitable for publication.

Thank you for your consideration.

Sincerely,

Marija Cvijovic, on behalf of all authors

## \*2. Response to Reviews (for Revision)

Reviewer #2: The authors have addressed the major concerns by the reviewer.  
We would like to thank to the reviewer for careful and thorough evaluation of our revision.

I have a couple of minor discretionary revisions:

(1) Figure 3 is too busy, and difficult to follow. Maybe the authors can select the most important curves that illustrate the feature of the models they wish to highlight.

After testing several versions of this figure, we decided to keep the original version.

(2) The paper might benefit of moving the model from the appendix/supplementary material to the body of the paper. There is an interruption in the flow of the manuscript by having core features of the model in the appendix instead of the body of the paper.

We have now included an abbreviated summary of the model in the main text.

Reviewer #3: This manuscript is much improved. Two significant concerns remain, however.

We would like to thank to the reviewer for careful and thorough evaluation of our revision.

Language: Throughout, the use of English needs improvement. Much of this is minor, but in some places it obscures meaning. These need to be resolved.

Specifics from the first few pages:

line 85: 'rejuvenated daughter'. Odd choice of words: the daughter has just been born. 'Re'-juvination is not possible.

The term 'rejuvenated daughter' is widely used in ageing research, meaning that the daughter's age is 'reset to zero' when it arises from an ageing mother.

For yeast specifically, first-born daughters are referred to 'rejuvenated-daughters' as they are born damage-free with full replicative potential. The last daughters are born with substantial amounts of damage and are referred to as 'prematurely old' and they exhibit reduced replicative potential.

line 104 'is vaguely understood the terminology used...'

This is not corrected

line 106: 'A population's success is in the asymmetric division...'

This is not corrected

line 121: '\_The\_ natural selection ...\_The\_ asymmetric division' (Articles not needed.)

This is not corrected

line 130: 'in spatially sequester regions...'

This is not corrected

line 133: 'In previously computational models...'

This is not corrected

line 152: damaged  
This is not corrected

Conclusions: The main conclusions are still largely intuitive statements. E.g. from the abstract: "Our results suggest that a rapid decrease in the efficiency of damage retention, at the time when the mother cell is almost exhausted, produces fewer daughters with high levels of damaged proteins. In addition, retaining more damage during the early divisions increases the number of healthy daughters in the population." No mathematical analysis is needed to reach these conclusions. I recommend reorganizing the document to highlight your less intuitive findings (on e.g. altruism and local minima).

We cannot agree with the reviewer on this comment. Experimentally it is still not feasible to understand mechanisms of damage retention, more specifically to what level mother cell is retaining damage and more importantly when it starts to pass damage to her daughters. We tried to answer these questions theoretically, and even though results might sound intuitive they represent an important contribution to the understanding of yeast ageing. During the first revision, we have provided detailed (biological) reasoning for these questions. Also, these findings can be very useful in designing new targeted experiments to test this hypothesis. For example, with the development of microfluidics systems, we hope that this work can serve as a starting point for experimental design and can pinpoint to the specific mechanism to look at experimentally.

Analysis of Altruism concluded that distance strategy provides healthier populations than division strategy (see section Altruism Provides Healthy but a Small Population). In case of global minima of cost function we conclude that the distance strategy is preferred. The cost function for the species following either of the two strategies can never stay at the global minima as species keep looking for a better choice.

# Adaptive damage retention mechanism enables healthier yeast population

Qasim Ali<sup>1,2</sup>, Riccardo Dainese<sup>1,3</sup>, Marija Cvijovic<sup>1\*</sup>

<sup>1</sup>Department of Mathematical Sciences, Chalmers University of Technology and University of  
Gothenburg, Gothenburg, Sweden

<sup>2</sup> Department of Mathematics, North Carolina State University, NC 27607, USA (current  
affiliation)

<sup>3</sup> Laboratory of Systems Biology and Genetics, Institute of Bioengineering, School of Life  
Sciences, École Polytechnique Fédérale de Lausanne (EPFL), Lausanne, Switzerland (current  
affiliation)

\*Corresponding author

Marija Cvijovic

Department of Mathematical Sciences

Chalmers University of Technology and University of Gothenburg

Chalmers tvärgata 3

SE-41296 Gothenburg, Sweden

Phone: +46 31 772 53 21

Email: marija.cvijovic@gu.se

## 24 Highlights

- 25       ▪ retaining more damage by a yeast cell during the early divisions increases the number of  
26       healthy daughters in the population
- 27       ▪ a rapid decrease in the efficiency of damage retention, at the time when the mother cell is  
28       almost exhausted, produces fewer daughters with high levels of damage
- 29       ▪ fluctuations in the cost function allow yeast cell to continuously vary its strategy, suggesting  
30       that optimal reproduction success is a local minimum of the cost function

31

32 Keywords: yeast, asymmetrical division, damage retention, dynamical modelling, pedigree-  
33 tree model

34

35

36

## Abstract

37 During cytokinesis in budding yeast (*Saccharomyces cerevisiae*) damaged proteins are  
38 distributed asymmetrically between the daughter and the mother cell. Retention of damaged  
39 proteins is a crucial mechanism ensuring a healthy daughter cell with full replicative potential  
40 and an ageing mother cell. However, the protein quality control (PQC) system is tuned for  
41 optimal reproduction success that suggests optimal health and size of the population, rather  
42 than long-term survival of the mother cell. Modelling retention of damage as an adaptable  
43 mechanism, we propose two damage retention strategies to find an optimal way of decreasing  
44 damage retention efficiency in order to maximize population size and minimize the damage  
45 in the individual yeast cell. A pedigree model is used to investigate the impact of small  
46 variations in the strategies over the whole population. These impacts are based on the  
47 altruistic effects of damage retention mechanism and are measured by a cost function whose  
48 minimum value provides the optimal health and size of the population. We showed that  
49 fluctuations in the cost function allow yeast cell to continuously vary its strategy, suggesting  
50 that optimal reproduction success is a local minimum of the cost function. Our results suggest  
51 that a rapid decrease in the efficiency of damage retention, at the time when the mother cell  
52 is almost exhausted, produces fewer daughters with high levels of damaged proteins. In  
53 addition, retaining more damage during the early divisions increases the number of healthy  
54 daughters in the population.

55

Abbreviations	Description
$RE_{div/dist}$	Division / distance strategy of damage retention
$g$	Division number
$\alpha, n$	repressor activation constant, repressor Hill constant
$\tau_i, \tau_D$	Time required for intact/damage component to reach division/ death
$I_{div}$	Intact component threshold
$R_t$	Ratio between the times required for division and death threshold
$I_g$ and $D_g$	Intact and damage component of mother cell after division
$re$	Damage Retention with altruist effect
$re_{max}$	Maximum possible damage retention
$A$	Altruist value to make a variation in the strategy
$D, D_{death}$	Damage variable, Damage threshold
$N_{daugh/mot/pop}$	Daughter/mother/accumulated cells
$P_{daugh}, P_{mot}, P$	Population distribution for daughter/mother/accumulated
$D_{daugh/mot/pop}$	Damage in daughter/mother/accumulated cells population
$C_{daugh/mot/pop}$	Cost function for daughter/mother/accumulated cells population



## 59    **Introduction:**

60    Aging is a conserved scale-invariant phenomenon that exploits the entire organism  
61    simultaneously, from the organelles involved in the cellular processes to the organs and body  
62    structure. Aging factors like damage accumulation and its asymmetric segregation through  
63    retention mechanism during growth and division processes respectively have been frequently  
64    studied in the past few decades and are proposed to promote ageing from simple unicellular  
65    organism like budding yeast to higher eukaryotes (Bufalino et al., 2013; Erjavec et al., 2007;  
66    Hill et al., 2016; Katajisto et al., 2015; Kennedy et al., 1994; Kruegel et al., 2011; Zhou et al.,  
67    2014). Retention of damage during the process of cell division is an evolutionary conserved  
68    mechanism whose efficiency decreases gradually and leads to the senescence state where  
69    basic cellular processes are unable to produce enough proteins to have subsequent divisions  
70    (Aguilaniu et al, 2003; Ackermann et al., 2003; Erjavec et al., 2008; Rujano et al., 2006).  
71    Budding yeast, *Saccharomyces cerevisiae* (*S. cerevisiae*) has been widely studied in aging  
72    research and has contributed to the identification of many genes involved in mammalian aging  
73    (Longo et al, 2012). Ageing in yeast can be studied by two main approaches: replicative aging,  
74    which is measured by the number of divisions that a cell performs before senescence, and  
75    chronological aging, which corresponds to the time before a cell enters senescence in a non-  
76    dividing state (Longo, 2012). Experiments targeting replicative aging showed that yeast cells  
77    give rise to a limited number of daughter cells, usually around 20–25 (Mortimer and Johnson  
78    1959, Longo, 2012). Throughout its lifespan, a cell accumulates different types of ageing  
79    factors, like extra chromosomal RNA circles (ERCs), increased intracellular oxidative stress,  
80    mitochondrial dysfunctions and accumulation of damaged proteins (Aguilaniu 2003, Sinclair  
81    1998). It has been shown that asymmetric distribution of damaged proteins in the unicellular  
82    organisms is evolutionarily beneficial for the whole progeny thus ensuring the highest level of  
83    fitness for the daughter cells (Waddington, 1953; Eshel and Matessi, 1998; Crispo, 2007,  
84    Kaberlein, 2010). This unequal distribution of damage results in an ageing mother cell and a  
85    rejuvenated daughter with full replicative potential (Eglimetz and Jazwinski, 1989). In the early  
86    divisions, a mother cell is able to retain most of the damage, giving rise to fully healthy  
87    daughter cells. However, in the late stages of a mother cell's lifespan, damage retention  
88    becomes less effective, and aging factors begin to be passed to the daughters which, thus, are  
89    born prematurely old (Kennedy et al, 1994; Sinclair et al, 1998a; Sinclair et al, 1998b). This

trend reaches a climax in the last 5% of a mother's lifespan when divisions are often symmetric, and the daughter inherits a consistent amount of cellular damage from the mother. The gradual decline in the organelles performance during replicative aging results in cells with a unique way of damage retention that is well conserved across natural selection and provide a distinctive reproduction strategy among the different yeast strains (Erjavec et al., 2008; Kirkwood and Rose, 1991; Nyström and Liu, 2014).

From the evolutionary perspective of Darwinism, the variation in the genetic material of a trait is a random process that is passed on to its progeny by means of natural selection. These variations are negligible, preserving the structure and function during the lifespan of a particular species (Konieczny et al., 2014). However, there are several characteristics, e.g. age, size and reproduction, which are uniquely identifiable within the same species. Bringing all the characteristics together outlines an evolutionary survival strategy of the population that leads to its reproduction success (Berg et al., 2002; Brooks and Garratt, 2017).

Optimal reproduction success **is a term** used to define the replicative lifespan of a yeast cell that has evolved the organelles to adopt the finest route for the healthy survival of the yeast population. **A success of the population is in the asymmetric distribution of damage during the cell division that ensures the low amount of damage in the progeny and its long replicative lifespan** (Chao et al., 2016; Nyström and Liu, 2014). However, healthy progeny and long replicative lifespan are inversely proportional to each other since it is asserted that, during the replicative lifespan, yeast strains sacrifice their long-term survival over the health of their progeny by retaining the aging factors (Aguilaniu et al., 2003; Hill et al., 2017; Kirkwood and Rose, 1991). Therefore, it is interesting to find a strategy for optimal retention of aging factors in such a way that yeast population accumulates less damage in the living cells and provides maximum population.

Theoretical models have played a critical role in understanding the ageing process in the unicellular organisms (Ackermann et al., 2007; Chao, 2010; Chao et al., 2016; Clegg et al., 2014; Coelho et al., 2014; Erjavec et al., 2008; Lindner et al., 2008; Stewart et al., 2005; Vedel et al., 2016). A recent theoretical study has shown that symmetric division alone can lead to a senescence state where the cell can no longer divide while some stochastic effects on the damage distribution between mother and daughter cells can protect cells from early damage

(Chao et al., 2016). Moreover, natural selection adapts the protective mechanism into the subsequent progeny in a genetically controlled manner. Asymmetric division in yeast cells increases the population fitness in case of high damage propagation rates and therefore increases the proliferating capacity of the progeny (Erjavec et al., 2008). It has been suggested that the optimal aging strategy is to repair the transcriptional errors and mal-functionalities by recycling the damaged material to maintain the quality rather than segregating the damaged portions (Clegg et al., 2014). However, the protein quality control system is not sufficiently effective to maintain the proteostasis and therefore cellular health is sacrificed over the continuous production of proteins (Nyström and Liu, 2014; Orgel, 1963). Therefore, the segregation of damaged proteins in spatially sequestered regions of a cell becomes a necessity in order to maintain the performance of the organelles involved in the fundamental cellular processes (Hill et al., 2017; Tyedmers et al., 2010).

In previous computational models, retention of damage is, due to simplicity, assumed to have the same efficiency throughout the cells replicative life, thus it is treated as a constant (Erjavec et al., 2008; Clegg et al., 2014). Here, based on several experimental evidences reported in yeast (Kennedy et al, 1994; Sinclair et al, 1998a; Sinclair et al, 1998b), we consider that damage retention, like many other processes, loses its efficiency during the replicative lifespan of the yeast cell. However, the exact mechanisms of damage retention remain unclear. We propose two strategies named as *distance strategy* and *division strategy*, to investigate the efficiency and stability of damage retention during the replicative lifespan of the single cell. We ask whether it be possible that any two yeast strains following different strategies of damage retention converge to a unique optimal reproduction success. We also investigate whether a yeast population following a well-defined strategy of damage retention reaches a specific optimal reproduction success that her fellow mutated species cannot reach until it follows the same strategy.

## Mathematical Modelling

Mathematical model presented here is built on a model published by Erjavec et al, 2008 and comprises of division and growth processes for each cell using the discrete-continuous model. We provide here an abbreviated summary (for detailed derivation and parameters see Appendix 1).

150 Each cell increases its intact ( $I$ ) and damaged ( $D$ ) components during the growth process (Eq.  
 151 1) and asymmetrically distributes these components between mother  $R_m$  (Eq.2) and daughter  
 152  $R_d$  (Eq.3) cells during the division process.

$$\begin{aligned} \dot{I} &= k_1 \left( 1 - \frac{I + D}{K} \right) - k_2 I - k_3 I \\ \dot{D} &= k_3 I - k_4 D \end{aligned} \quad (1)$$

$$\begin{aligned} I_{in}(g+1) &= I_{end}(g) \cdot R_m - D_{end}(g) \cdot R_d \cdot re(g) \\ D_{in}(g+1) &= D_{end}(g) \cdot R_m + D_{end}(g) \cdot R_d \cdot re(g) \end{aligned} \quad (2)$$

$$\begin{aligned} I_{in}(g+1) &= I_{end}(g) \cdot R_d + D_{end}(g) \cdot R_d \cdot re(g) \\ D_{in}(g+1) &= D_{end}(g) \cdot R_d - D_{end}(g) \cdot R_d \cdot re(g) \end{aligned} \quad (3)$$

153 The damage retention mechanism allows mother cell to retain part of the damaged proteins  
 154 from the daughter cell and, in return, give part of the intact portion. The efficiency of damage  
 155 retention decreases during the whole replicative lifespan in a specified manner termed as a  
 156 strategy of premiere cell. This strategy is followed by the cell and its whole progeny during  
 157 their respective replicative lifespans. A pedigree-tree model follows the whole population and  
 158 provides a discrete population distribution function over the damaged component.

159 In this work, we consider two yeast strains following distinct strategies of decreased efficiency  
 160 of damage retention during the cell division. These strategies are based on the assumption  
 161 that each strain is tuned for a long replicative lifespan and not for its own long-term survival  
 162 (Kirkwood and Rose, 1991; Nyström and Liu, 2014). Small variations in a strategy are  
 163 implanted to alter the way of decreasing the efficiency of damage retention. It is considered  
 164 that each variation in the strategy represents an altruistic behaviour of a mother cell for her  
 165 progeny. However, for each variation, the whole pedigree-tree model is simulated, and cost  
 166 functions are calculated. These cost functions are based on the damage proportion of the alive  
 167 cells and their population size.

## 168    **Damage retention strategies**

169    Retention parameter can be varied considerably in multiple ways while each one can provide  
170    a significant effect on the population in the long run. However, it is not feasible to follow all  
171    plausible ways of reducing the efficiency of damage retentions due to computational limits.  
172    Therefore, it is inevitable to develop strategies by means of well-defined functions for the  
173    efficiency of damage retention. Two strategies, named as *division strategy* and *distance*  
174    *strategy*, are defined to investigate the efficiency of damage retention during the replicative  
175    lifespan of the single cell. Strategies have been developed in such a way that a mother cell  
176    following distance strategy retains more damage than a mother cell following division strategy  
177    during the early divisions.

### 178    **Division Strategy**

179    In a division strategy, we define retention efficiency as a repressor Hill function in the  
180    following way

$$RE_{div}(g + 1) = 1 - \frac{g^n}{g^n + \alpha^n} \quad (4)$$

181    where  $\alpha > 0$  and  $n \geq 1$  are constants. Increasing these constant values can slow down the  
182    decrease in the efficiency of damage retention in the subsequent divisions of the mother cell  
183    (Figure 1).

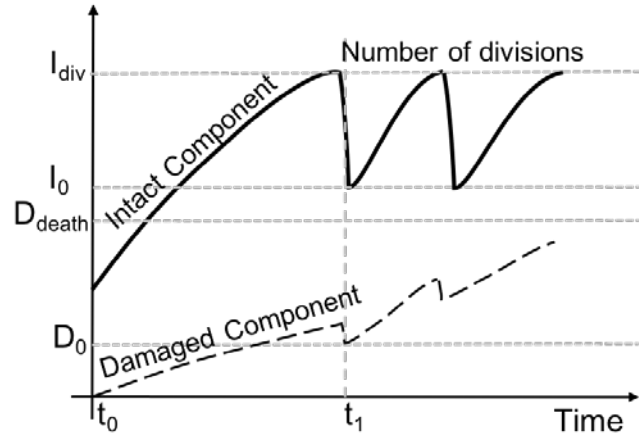


Figure 1: Division strategy: Efficiency in damage retention decreases with the increase in number of divisions. Mother cell is able to retain maximum damage in the beginning but loses its efficiency of damage retention as the number of divisions increases. The intact component decreases from its threshold  $I_{div}$  to  $I_{g=0}$  after division and the damaged component decreases to  $D_{g=0}$ . The cell death threshold is represented by  $D_{death}$ .

## Distance Strategy

In distance strategy, the efficiency of retaining damage (RE) decreases with the increase in the number of cell divisions and is also modelled by repressor Hill function as:

$$RE_{dist}(g + 1) = 1 - \frac{R_t^n(g)}{R_t^n(g) + \alpha^n} \quad (5)$$

The parameters  $n > 1$  and  $\alpha > 0$  can be set according to the  $R_t$  value; however, these parameters are the same as in the previous strategy (see Appendix 1). The variable  $R_t$  is the ratio between the time required for the intact component to reach division level ( $\tau_I$ ) and the time required for damage component to reach cell death ( $\tau_D$ ).

$$R_t = \frac{\tau_I}{\tau_D} \quad (6)$$

Due to the increase in damage during the replicative lifespan of a cell, the retention becomes more difficult. After every division cell anticipates the possibility of the next division. If the damage is high enough such that the next division is not possible then cell further decreases

its retention to the minimum level ( $RE_{\text{dist}} = 0$ ) as in the division strategy. The required times ( $\tau_I$  and  $\tau_D$ ) are calculated by taking the ratio between remaining distance and the mean rate of change in the corresponding intact ( $Avg(\dot{I})$ ) and damage ( $Avg(\dot{D})$ ) component.

$$\tau_I = \frac{I_{\text{div}} - I_g}{Avg(\dot{I})}, \tau_D = \frac{D_{\text{death}} - D_g}{Avg(\dot{D})} \quad (7)$$

In the distance strategy (Figure 2), cell composition is divided into two components which are increasing during their growth process. The increase in the damage component is represented by long-dashed lines (— —) that starts from zero and passes through  $D_0$  and intact component by continuous lines that starts from a minimum amount of intact proteins. At time  $t_1$ , the cell reaches the division threshold ( $I_{\text{div}}$ ) where it is ready to bud a daughter with asymmetric distribution of intact and damage component. After division, mother cell has intact component  $I_g$  and damage component  $D_g$ . At this point, the distance strategy comes into action. The parametric value of retention set by the strategy is used to anticipate the success in completing the next division by the above-defined procedure (see Eq. 5). If the next division is possible then the cell will divide according to the defined strategy. Otherwise, the cell will decrease the retention to its minimum value so that the next division becomes possible.

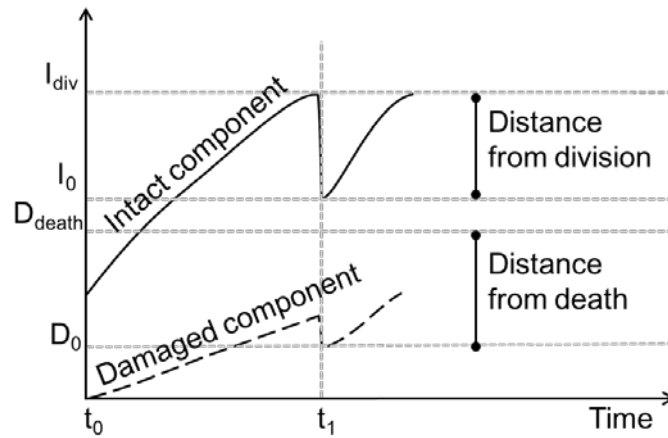


Figure 2: Mother cell decreases damage retention by anticipating her next reproduction success. Cell increases its initial intact and damage component from  $t_0$  and divides at time  $t_1$ . The intact component decreases from its threshold  $I_{\text{div}}$  to  $I_{g=0}$  after division and the damaged component decreases to  $D_{g=0}$ . The cell death threshold is represented by  $D_{\text{death}}$ .

## 214 Altruistic Variation in the Efficiency of Damage Retention

215 The strategies provide a unique way of decreasing the efficiency of damage retention which  
216 can be varied by using an altruist factor ( $A$ ) as defined in Eq. (8). The parameter  $A$  is based on  
217 the consequences of the actions performed for the replicative lifespan of a mother cell and  
218 for the reproductive fitness of the offspring that is measured by determining their health  
219 status. The parameter  $A = 0.5$  is defined as a neutral value when it has no effect on the  
220 strategies of damage retention and therefore follows the asymmetric division as defined in  
221 Eqs. (4) and (5). For  $A < 0.5$ , cells show selfish behaviour to their progeny by retaining less  
222 damage than being neutral during their replicative lifespan, whereas for  $A > 0.5$ , cells show  
223 selfless behaviour by retaining more damage than the one defined in a neutral strategy. At  
224 the extreme values, the cells show either no retention ( $re = 0$ ) or full retention ( $re = 1$ ) during  
225 their replicative lifespan.

226 At the time of division, damage retention is set in two stages. Firstly,  $RE(g)$  is calculated by  
227 means of a defined strategy (distance or division strategy). Secondly, altruism parameter is  
228 used to alter the strategy. When no more divisions are possible, the retention decreases to  
229 zero allowing another division without taking the altruist effect into account. The equation for  
230 altruist retention is written as:

$$re(A, g) = RE(g) + 2 \left( A - \frac{1}{2} \right) ((1 - A)RE(g) + A(re_{max} - RE(g))) \quad (8)$$

231 The parameter  $re$  is the altruism-dependent efficiency of damage retention and  $re_{max}$  is the  
232 maximum attainable retention, i.e. 1.

## 233 Pedigree-tree model

234 Here we develop a pedigree-tree model to follow the complete population with variable  
235 retention parameter (Eq(1-3) and Appendix 1). The cellular growth is represented by an  
236 increase in the number of intact and damage components and the division is represented by  
237 the asymmetric distribution of growth components (intact and damage) between mother and  
238 daughter cells. The advantage of this model is that the cells are instantly counted when bud  
239 out from their mothers while their growth components are tracked throughout their



240 replicative lifespan. At the end of the simulation, the cells are distributed according to their  
 241 intact and damage components in a discrete manner. Moreover, the variable retention of a  
 242 single cell during its lifespan can be applied over the whole population in an appropriate  
 243 manner. Following this procedure leads us to find the population distribution function for  
 244 damage component and to investigate the differences between strategies by using cost  
 245 functions.

## 246 **Population distribution function for intact/damage component**

247 Each cell is born with a specific level of damage and intact components and grows accordingly  
 248 until it reaches the division threshold that leads to its asymmetric binary division. The division  
 249 leads to a new daughter cell which follows the same growth and division strategy as her  
 250 mother. During this process the population increases, generating cells with a diverse level of  
 251 intact/damage components. These components can be distributed over the whole population  
 252 at any time  $t = t_0$  and can be represented by a population distribution function  $P(A, D)$ .  
 253 Therefore, for each altruist value  $A$  and accumulated damage  $D$ , the population distribution  
 254 function for the damaged component is written as,

$$P(A, D) = \frac{\sum_{D=a}^{D=b} (N_{daugh}(A, D) + N_{mot}(A, D))}{N_{pop}(A)}. \quad (9)$$

255 where  $a$  and  $b$  are the minimum and maximum accumulated damage, respectively. The  
 256 functions  $N_{daugh}(A, D)$  and  $N_{mot}(A, D)$  represent the number of daughter and mother cells with  
 257  $D \in [0, D_{death}]$  amount of damage component at a given altruist value  $A$ . The population  
 258 distribution function is normalized by total population of alive cells  $N_{pop}(A) = \sum (N_{daugh}(A, D) +$   
 259  $N_{mot}(A, D))$ . The variation in  $N_{pop}$  due to altruism  $A$  is well-intended to ensure the total size of  
 260 the population at any time  $t = t_0$ . Similar kind of distribution functions can be defined for the  
 261 normalized population distribution of daughter cells,  $P_{daugh}(A, D)$ , and mother cells,  $P_{mot}(A, D)$   
 262 as follows:

$$P_{mot}(A, D) = \frac{\sum_{D=a}^{D=b} N_{mot}(A, D)}{\sum_D N_{mot}(A, D)},$$

$$P_{daugh}(A, D) = \frac{\sum_{D=a}^{D=b} N_{daugh}(A, D)}{\sum_D N_{daugh}(A, D)}. \quad (10)$$

## 263 Cost Functions

264 The calculation of cost function is performed at the end of the discrete-continuous model  
 265 while the objective is to find the minimum cost function so that smallest amount of damage  
 266 and a maximum number of cells exist in the population. The damaged component and the  
 267 total population is calculated for the virgin cells – the cells that have not undergone any  
 268 division yet, for the mother cells and for the whole population. These calculations are then  
 269 normalized, defined by  $\tilde{N}(X)$ , where  $X$  is any population distribution of either mother, daughter  
 270 or total cells with a given altruist value and damage  $D$ . This helps to eliminate the redundancy  
 271 between the cellular components and the population.  $\tilde{N}(X)$  can be defined as,

$$272 \quad \tilde{N}(X) = \frac{X - X_{min}}{X_{max} - X_{min}}$$

273 The normalization is carried out by finding the extreme values from the deterministic model  
 274 for the total damage in the cells and the total population. The extreme values for each cost  
 275 function exist at unique values of altruism  $A \in [0,1]$ .

276 Cost function at any given altruism value  $A$  in case of daughter cells is the sum of normalized  
 277 accumulated damage of all the daughter cells,  $\tilde{N}(\sum_{D_{daugh}} D_{daugh}(A))$ , and difference between  
 278 normalized maximum number of daughter cells during  $A \in [0,1]$ , i.e. equals to 1, and  
 279 normalized alive daughter cells,  $\tilde{N}(N_{daugh}(A, D))$ , present in the system at any time  $t = t_0$ .

$$C_{daugh}(A) = \tilde{N}\left(\sum_{D_{daugh}} D_{daugh}(A)\right) + \left(1 - \tilde{N}\left(\sum_D N_{daugh}(A, D)\right)\right) \quad (11)$$

280 The cost function for damage component in the mother cells at a given value of  $A$  is similar to  
 281 the cost function defined for damage component in the daughter cells. The only difference is  
 282 that we calculate damage in those cells that have been divided at least once. We write this  
 283 cost function as,

$$C_{mot}(A) = \tilde{N} \left( \sum_{D_{mot}} D_{mot}(A) \right) + \left( 1 - \tilde{N} \left( \sum_D N_{mot}(A, D) \right) \right) \quad (12)$$

284 Damage in a mother cell is denoted by  $D_{mot}$  and a total population of the mother cells is  $N_{mot}$ .  
 285 For the damage proportion in the total yeast population at a given altruism  $A$ ,  $N_{pop}(A)$ , the cost  
 286 function is the sum of the normalized damage in the total population,  $\tilde{N}(D_{pop})$ , and the  
 287 difference between the normalized maximum and the normalized current population sizes,  
 288 i.e.  $1 - \tilde{N}(N_{pop})$ . It is given by the following formula,

$$C_{pop}(A) = \tilde{N} \left( \sum_{D_{pop}} D_{pop}(A) \right) + \left( 1 - \tilde{N}(N_{pop}(A)) \right) \quad (1)$$

## 289 Variation in Altruism

290 Altruism parameter  $A$  is varied deterministically as well as stochastically. The deterministic  
 291 way is quite straightforward as it formulates the normalized distribution of cells at discrete  
 292 values of  $A$  and calculates cost functions for each value of  $A$  that varies in the interval  $[0,1]$ .  
 293 These cost functions are further used in the stochastic model to help find the minimum value  
 294 of cost function.

295 The stochastic settings involve individual-based modelling approach in which altruist  
 296 parameter  $A$  is randomly chosen from its neighbouring values. Small variations bring changes  
 297 in the strategy of damage retention and mimic the concept of mutation which directly affects  
 298 the cost function. The cost of following an individual's strategy of damage retention by its  
 299 progeny is deterministically calculated using Eqs. (11), (12) and (13) which involves simulation  
 300 of the pedigree-tree model for a specific period of time. The method allows the cell to follow  
 301 the direction where it finds minimum cost function. The direction of the altruist value is  
 302 chosen on the basis of current and preceding cost functions by using the signum function while  
 303 the magnitude of the variation is set by choosing a random value in the interval of  $[0, \varepsilon]$ .

$$A_{i+1} = A_i \pm \text{rand}(0, \varepsilon) \text{sgn}(C(A_{i-1}) - C(A_i)) \quad (14)$$

304 This process continues for a set period of time and is terminated by the following criteria,

$$\sum_{i=S_N+l}^{S_N+j+l} |A_{i-j} - A_{i-(j+k)}| < \varepsilon. \quad (15)$$

305 In the above equation, sign  $\pm$  are set according to the direction of altruist value and the index  
 306 of altruism  $A$  indicates the strategy variation number. The positive sign is used when the  
 307 direction of altruism is upward, i.e.  $A_{i-1} < A_i$ , whereas the negative sign is used in case altruism  
 308 is decreasing, i.e.  $A_{i-1} > A_i$ .

## 309 **Results:**

310 Initially, there is a single daughter yeast cell present in the system that has a sufficient amount  
 311 of intact proteins to grow and doesn't contain any damaged proteins. A general behaviour of  
 312 the model is described in Figure S1.

313 In the course of this work, we sought to establish a relationship between strategies followed  
 314 by distinct yeast strains and relationship among yeast strains following the same strategy. The  
 315 former is followed deterministically to find the reproduction success by using the given cost  
 316 functions whereas in the later the optimality is investigated by making stochastic variations in  
 317 the strategies.

## 318 **Relation Between Strategies**

319 Damage retention strategies follow a defined way to decrease the retention efficiency of a  
 320 mother cell. However, there are unique routes associated with each value of altruism that is  
 321 followed according to their intrinsic behaviour represented by Eqs. (4) and (5). The distance  
 322 strategy keeps the damage retention high and decreases the efficiency at an increasing rate  
 323 whereas the division strategy was defined in an opposite fashion by showing a sharp decrease  
 324 during the early replicative lifespan of a mother cell.

325 The strategies are defined using Hill function in the equations (4) and (5) with  $\alpha = 1$  (Figure  
 326 3). A comparison between the symmetric and asymmetric cell divisions has been performed  
 327 to observe the effect of strategies over the number of divisions while choosing different sizes  
 328 of the cells. The variations in the strategies are given by altruist parameter  $A$  with  $A_{max} = 1$ . It  
 329 is interesting to note that both strategies provide the same behaviour at the endpoints of  $A$ ,  
 330 i.e. 0 and 1 (Figure 3).

331

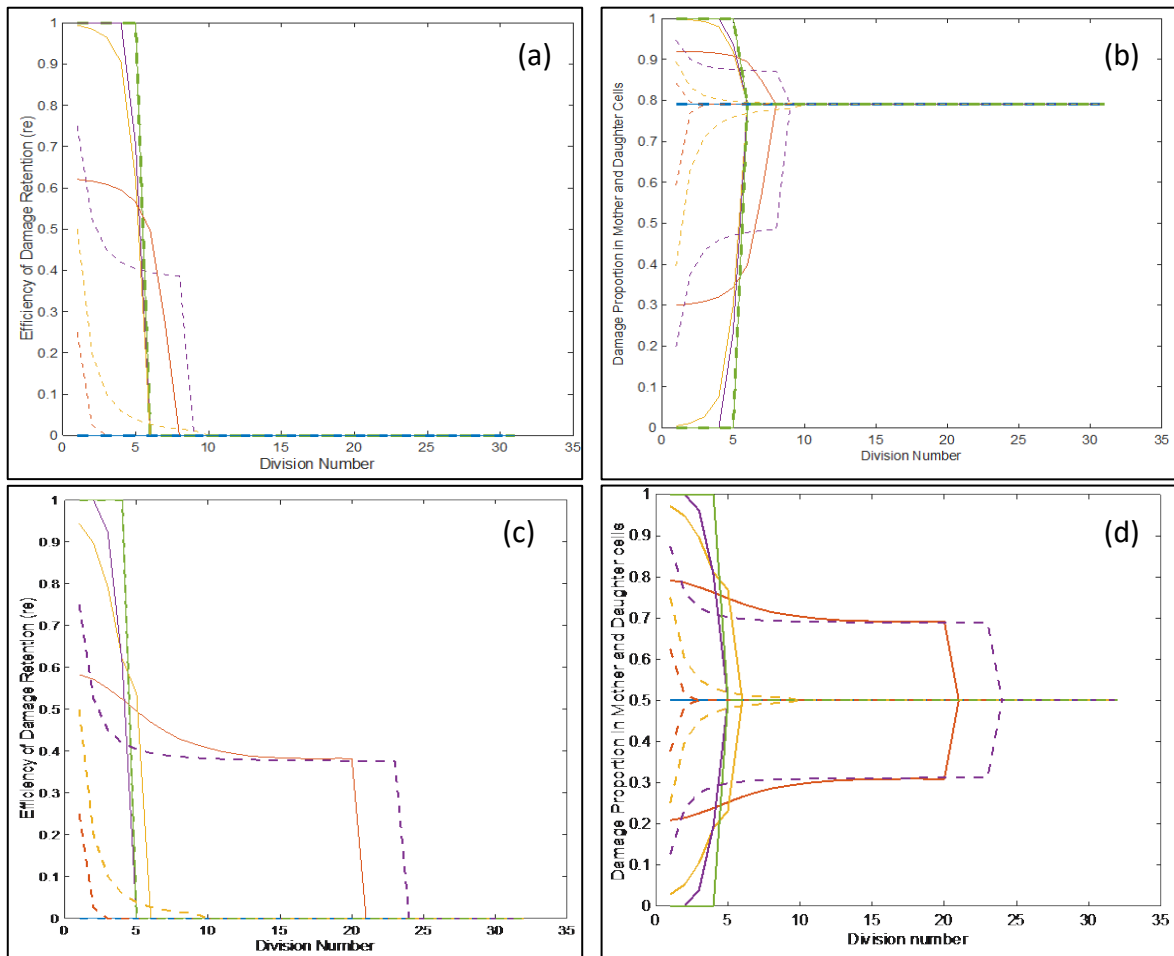


Figure 3: Damage retention efficiency ( $RE$ ) for altruist parameter values  $A = 0$  (blue), 0.25 (red), 0.5 (yellow), 0.75 (violet) and 1 (green). The dashed lines represent division strategy and continuous lines represent distance strategy. Colours are drawn to match the altruist parameter values between the two strategies. Left hand side panels (a) and (c) shows the damage retention by mother cell while the right-hand side panels (b) and (d) are obtained by relating size-wise damage distribution among mother and daughter cells. The cell sizes after division of cells are chosen asymmetric ( $R_m = 0.79$ ) for panel (a) and (b) and symmetric ( $R_m = 0.5$ ) for panel (c) and (d).

At  $A = 0$ , yeast cell does not retain any damaged portion ( $re(0, g) = 0$ ) during its replicative lifespan and therefore share damage with her daughter according to the division size of the cell  $R_m$ . Consequently, yeast survives for a longer replicative time and buds off 31 daughters when  $R_m = 0.5$  and 32 daughters when  $R_m = 0.79$  (Figure 3). On the other hand, at  $A = 1$ , yeast cell retains all the damage ( $re(1, g) = 1$ ) and buds a completely healthy daughter cell each time which affects its lifespan and brings it to 5 divisions. For all the other altruist values, i.e.  $0 < A < 1$ ,  $A$  does not provide the same retention function for both strategies. It can be observed that cell with division strategy retains less damage than distance strategy; however, the former retains damage for a longer period of time during its lifespan. After the critical damage level when no more retention possible, the cell loses all the retention and share the damage according to the cell sizes.

### **Population Distribution of Damaged Proteins**

The pedigree-tree model provides a large population of cells where intact and damage components are individually tracked throughout their replicative lifespan. This provides a non-uniform distribution of alive cells over damaged components. Therefore, the cell population is clustered according to the accumulated damage in each cell (with cluster size of 60 and number of clusters of 10 in the interval  $[0, 600]$ ) for five values of altruism  $A = 0, 0.25, 0.5, 0.75$  and  $1$  (Figure 4, Figure 5 and Figure 6). The maximum attainable damage is bounded by the threshold  $D_{\text{death}} = 600$ ; however, the figures show that the cell could have accumulated damage at most in the interval  $[480, 540]$ . These clustered populations are normalized in order to calculate the proportion of cells with respect to the total population. Moreover, the error bars are drawn to find the mean and standard deviation of the proportion of cells attaining specific proportion of accumulated damage at the four simulation times  $t = 1.5, 1.75, 2$  and  $2.25$ .

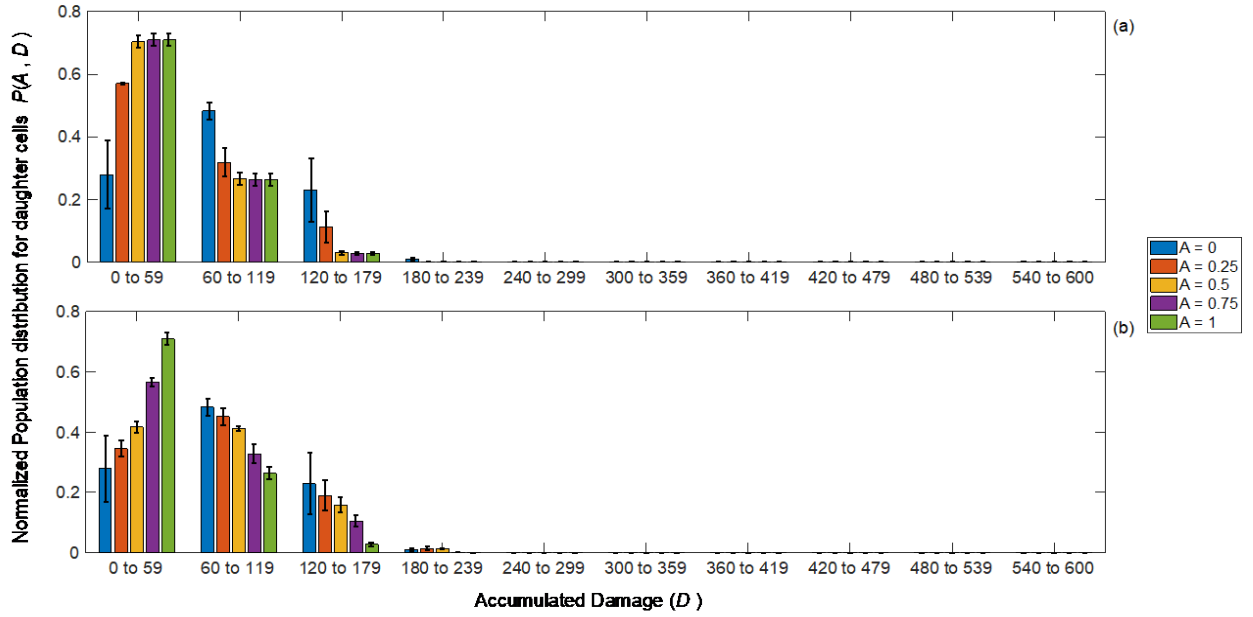


Figure 4: Mean and standard deviation of the daughter distribution of damaged proteins by using distance (a) and division (b) strategies, see Eq. (11). Mean of the distribution is taken for the simulation time  $t = 1.5, 1.75, 2, 2.25$ . The accumulated damage in the span of 600 is clustered into subintervals each of length 60.

The population distribution of daughter cells is present only in the first three clusters of damage component (Figure 4). In the first cluster,  $D_{\text{daugh}} \in [0, 59]$ , the mean proportion of cells,  $P(A, D)$ , increases when altruism  $A$  goes from 0 to 1 while the succeeding clusters show a reverse behaviour. The error bars represent the standard deviation of the mean distribution values for simulation time  $t = 1.5, 1.75, 2, 2.25$ . For  $A = 0$ , the standard deviation is quite high because the cell proportion was higher in the first and third clusters ( $P(A = 0, D = [0, 60]) \approx 0.38$ ) during the early simulation time,  $t = 1.5$ . However, it decreased to below 0.2 in the later simulation time,  $t = 2.25$ . Moreover, for  $A \geq 0.5$ , the proportion of cells with least damage is much high and have a very small standard deviation.

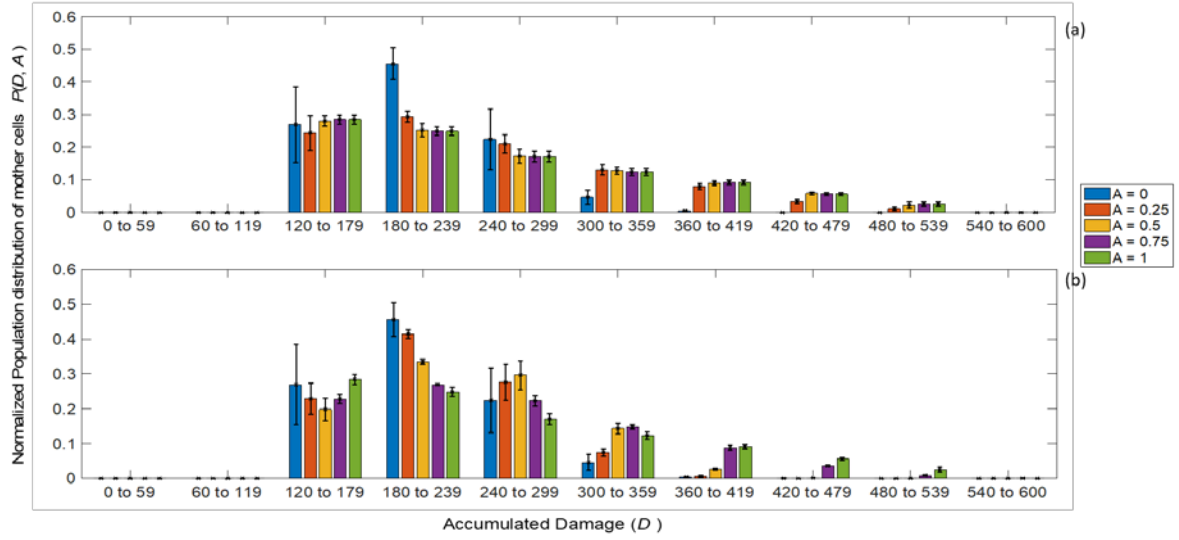


Figure 5: Mean and standard deviation of the mother distribution of damaged proteins by using distance (a) and division (b) strategies, see Eq. (10). Mean of the distribution is taken for the simulation time  $t = 1.5, 1.75, 2, 2.25$ . The accumulated damage in the span of 600 is clustered into subintervals each of length 60.

The number of daughter cells gradually increases in the first cluster of accumulated damage as  $A$  goes from 0 to 1 however it shows opposite behaviour in the second and third cluster (Figure 4b). It can be observed that the mean proportion of daughter cells following the distance strategy is higher than the mean proportion following the division strategy in the first cluster for all values of  $A$ , except the extreme values where both strategies provide the same result. However, the behaviour is opposite in the next two clusters. This suggests that the distance strategy, i.e. keeping the retention high in the early divisions, accumulates less damage in the population.

Mother cells distribution for damaged component is also normalized and its mean and standard deviation is calculated for the given simulation times  $t = 1.5, 1.75, 2$  and  $2.25$  and altruism values  $A = (0, 0.25, 0.5, 0.75, 1)$  and accumulated damage component in mother cells is shown in the third and succeeding clusters (Figure 5). This means that cells become a mother in the third cluster of damage accumulation however the highest proportion of cells are present in the fourth cluster where damage is in the interval  $[180, 240)$ . The standard deviation of the mean proportion of mother cells is similar to the mean proportion of daughter cells and therefore cellular health becomes better as  $A$  goes from 0 to 1. In comparison between the two strategies, the mothers following the distance strategy have higher damage than mothers



following division strategy. In addition, the mean proportion of mother cells containing high damage is comparatively lower than the ones containing the low damage.

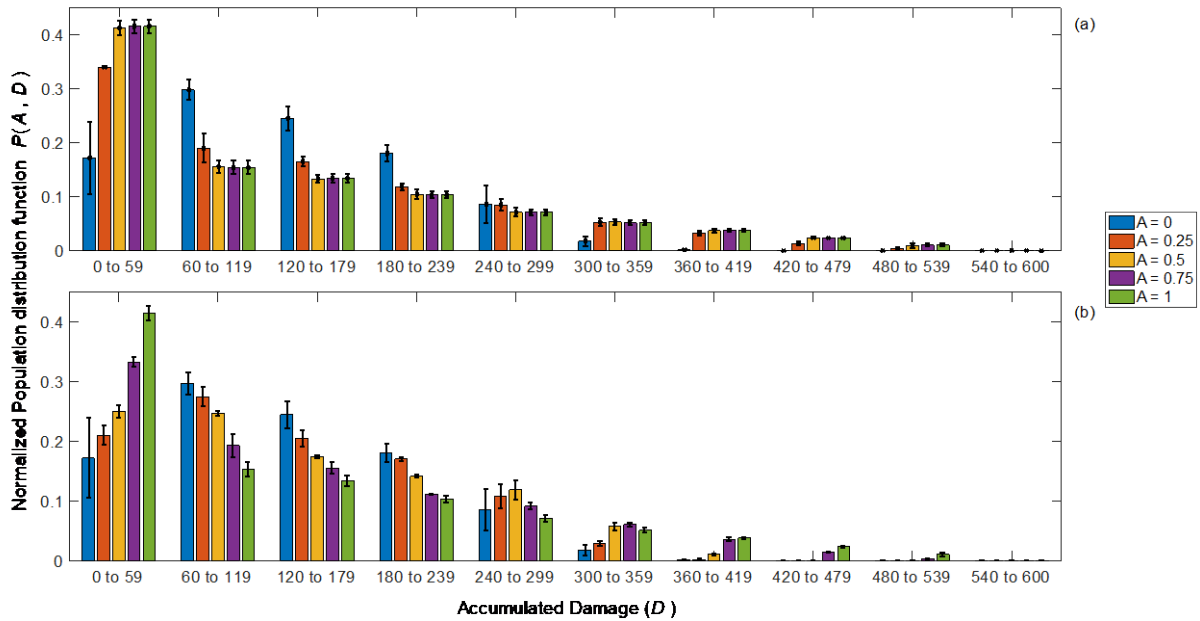


Figure 6: Mean and standard deviation of the normalized population distribution of damaged proteins by using (a) distance and (b) division strategies as defined in Eq. (9). Mean of the distribution is taken for the simulation time  $t = 1.5, 1.75, 2, 2.25$ . The accumulated damage in the span of 600 is clustered into subintervals each of length 60.

Mean and standard deviation of the normalized distribution of cells over the accumulated damage in alive cells show the behaviour similar to the above distributions at different values of  $A$ , however, there is a significant decline in the proportion of healthy cells, i.e. first cluster (Figure 6). At  $A = 0$ , the standard deviation gives comparatively high values. This is due to the fact that premier cells do not have enough damage to share with their daughter cells for short time scale ( $t = 1.5$ ) and therefore most of the daughter cells born with damage are grouped in clusters 1 and 2. Moreover, the proportion of cells is significantly decreased to below 0.2 when time duration is increased to  $t = 2.25$ .

### Optimal Reproduction success

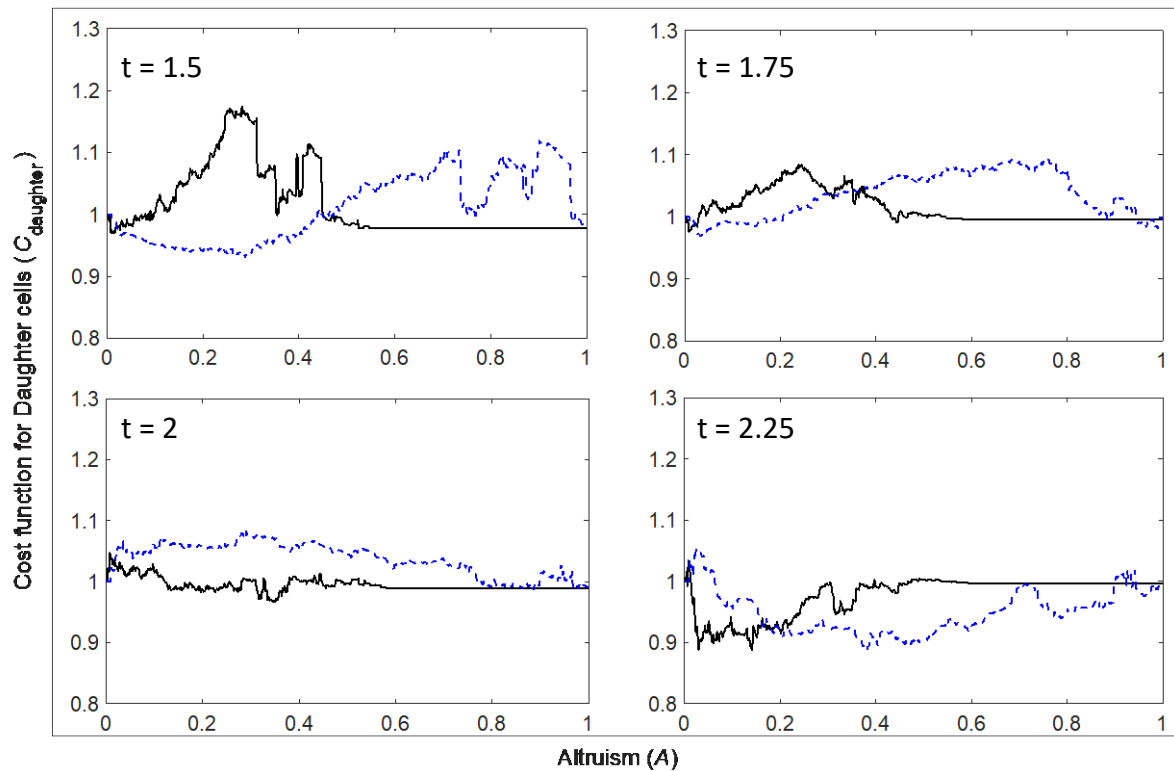
Models are simulated in deterministic as well as stochastic settings to find the cost functions. These cost functions represent reproduction success by taking into account the cellular health status and population size. The deterministic model provides a cost for predefined values of

411 altruism  $A$  whereas the stochastic model tracks the minimum value for cost function by taking  
412 random steps towards the lowest value of the cost function.

### 413 Deterministic outcomes

414 The deterministic modelling approach is used to evaluate the cost functions by varying the  
415 altruist parameter  $A$  between 0 and 1 with the step size  $\Delta A = 10^{-3}$ . The results are obtained for  
416 the cost functions defined in Eqs. (11), (12) and (13) and are presented in Figure 7 (for  
417 daughter cells), in Figure 8 (for mother cells) and in Figure 9 (for a total number of alive cells)  
418 respectively each at four different times  $t = 1.5, 1.75, 2$  and  $2.25$ . Computationally, it becomes  
419 very expensive to go beyond the time point  $t = 2.25$ . Therefore, this is the maximum time point  
420 chosen. Other time points are chosen to understand the behaviour of cost function over the  
421 altruism parameter  $A$ . The cost function is modelled by taking this fact into consideration that  
422 the replicative lifespan decreases with the increase in damage retention by the cell. In such a  
423 scenario, it would be interesting to see the effect of replicative lifespan over the damage  
424 accumulation in the population.

425 Altruistic effects on the daughter cells provide a time-variant response to its cost function.  
426 Due to asymmetric division, mother cells require less time to reproduce than the daughter  
427 cells. Therefore, the longer lifespan of mother cells will quickly increase the population;  
428 however, in case of low damage retention, high amount of damage is passed on to the newly  
429 born daughter cells. In case of distance strategy, this phenomenon quickly increases the  
430 damage in the population and raises the cost function to a high level during the early time, i.e.  
431  $t = 1.5$  and  $1.75$  (Figure 7, Figure 8 and Figure 9). However, with the progression of time, i.e.  $t$   
432 goes to  $2$  and  $2.25$ , the cost function gives a surprising outcome by replacing the high values  
433 with the lower ones, exposing that for large time scale, population size can dominate over the  
434 total damage present in the population. For instance, the distance strategy (continuous lines)  
435 near  $A = 0.3$ , the cost function that was at maximum, i.e.  $C_{\text{daugh}} = 1.2$  at time  $t = 1.5$ , goes below  
436 the value of  $C_{\text{daugh}} = 1$  at time  $t = 2.25$ .



438 Figure 7: Cost function for the distance (continuous lines) and division (dashed lines) strategies of  
 439 daughter cells  $C_{Daugh}$  at four time-points  $t = 1.5, 1.75, 2$  and  $2.25$  against the altruist values  $A$  in the  
 440 interval  $[0,1]$  and step size  $0.001$ . The cost function is defined in Eq. (11) while the deterministic model  
 441 used to simulate the results is described in Appendix 1.

442 Division strategy provides the opposite response than the distance strategy during the early  
 443 simulation time by showing a small decrease in the payoff function for early altruism values.  
 444 The reason is clearly that the proportion of cells in the population decreases slightly slower  
 445 than the increase in the proportion of damage accumulation (Figure S2). For a longer period  
 446 of time,  $t = 2.25$ , both strategies decrease their cost function for early values of  $A$ , however,  
 447 their optimal reproduction success varies.

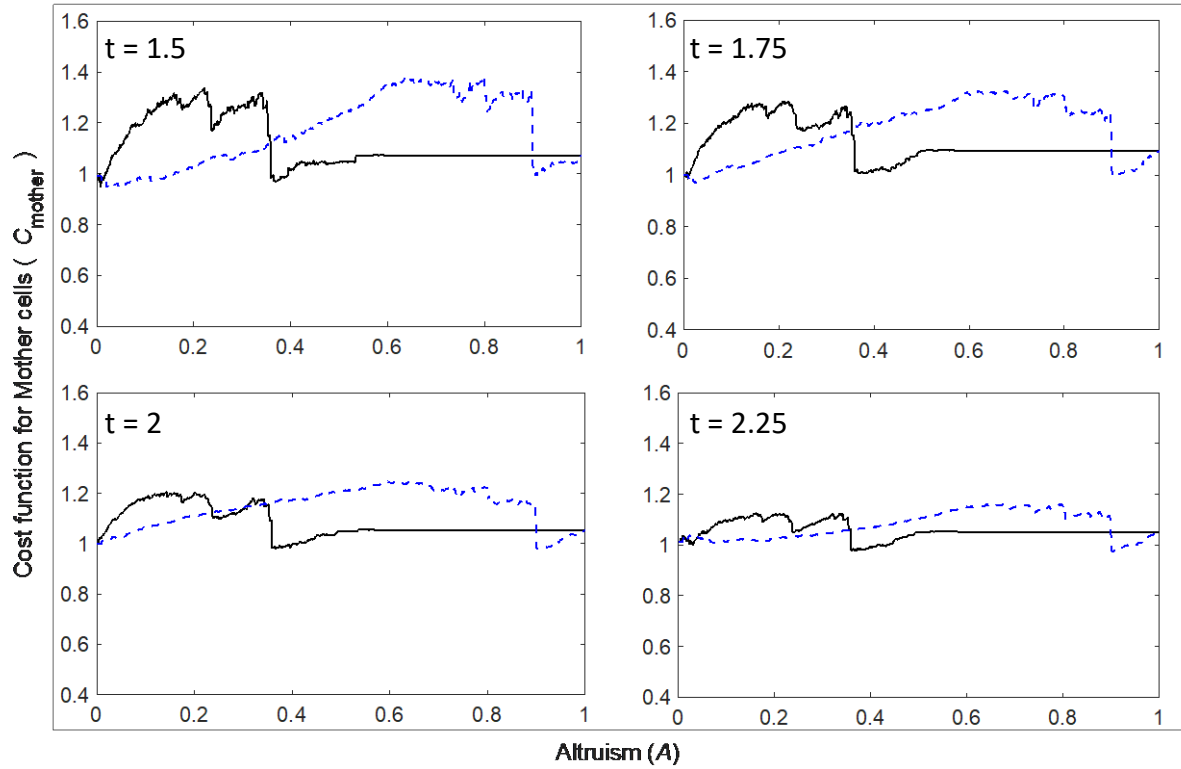


Figure 8: Cost function for the distance (continuous lines) and division (dashed lines) strategies of mother cells  $C_{\text{Mot}}$  at four time-points  $t = 1.5, 1.75, 2$  and  $2.25$  against the altruist values  $A$  in the interval  $[0,1]$  and step size  $0.001$ .

Taking the final time into consideration, the results provide several interesting outcomes regarding the least value for the cost function, i.e. the optimal reproduction success. Firstly, the optimal reproduction success for both strategies requires selfish behaviour of mother cells when altruism parameter  $A < 0.5$ . However, a complete selfish behaviour is not a good strategy which may increase the damage in the population. It is important to note that the cost function varies significantly from one simulation time to the next one, e.g.  $t = 2$  to  $2.25$  which means that the cost function is not in an equilibrium state. Conversely, it is interesting to note that the cost function is squeezing around  $C_{\text{Daugh/Mot/Tot}} = 1$  by reducing the drastic changes. These drastic changes cause fluctuations in the cost function whose local minimum is termed as “evolutionary ditch”. These ditches may not provide the least cost function; however, it becomes difficult to come out from such ditches since these are surrounded by high values of cost functions.

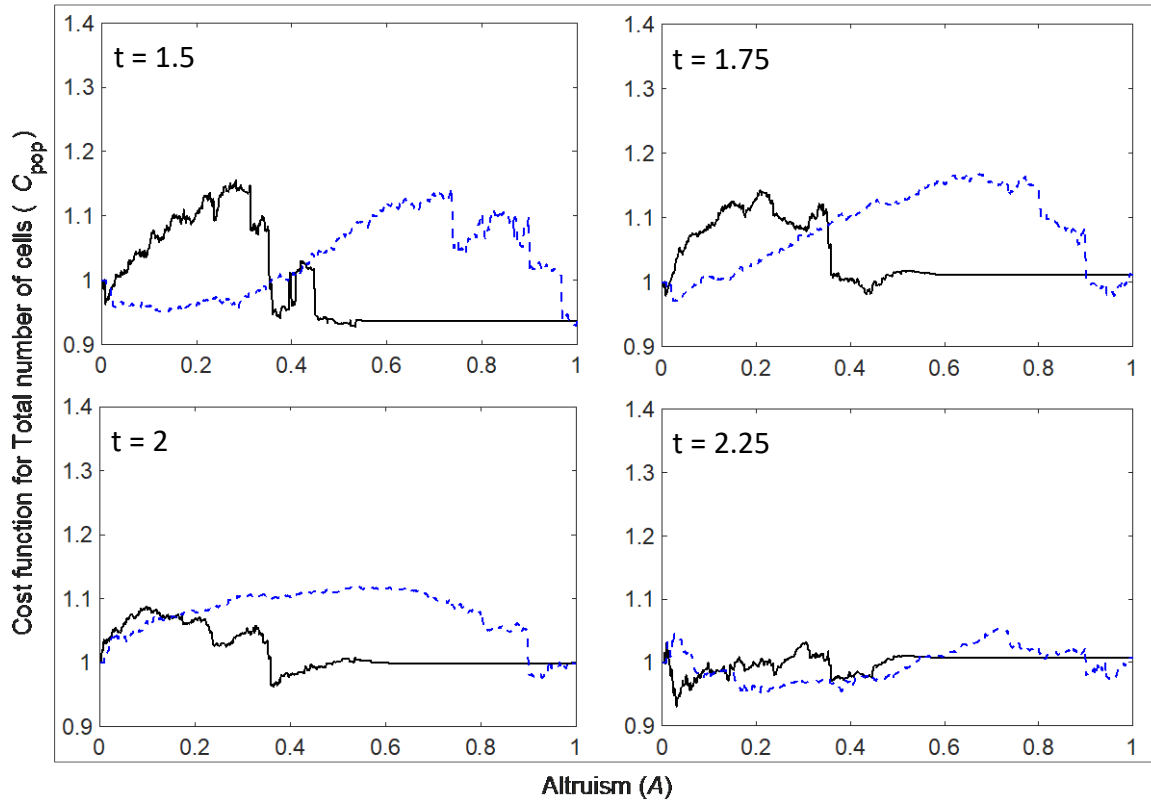


Figure 9: Cost function for the distance (continuous lines) and division (dashed lines) strategies of total cells  $C_{pop}$  at four time-points  $t = 1.5, 1.75, 2$  and  $2.25$  against the altruist values  $A$  in the interval  $[0,1]$  and step size  $0.001$ .

#### Stochastic Simulations

Stochastic settings are implemented to observe the behaviour of the cost function for total cells calculated at the simulation time  $t = 1.5$ . The strategies starting points are chosen for altruist values  $A$  between  $0$  and  $1$  with a step size of  $0.1$  (Figure 10). At each altruist value, cost functions are calculated which are then compared to their previous values. The strategies vary in the direction where small values of cost function are found by using Eq. (14). However, the least value is not predefined in the stochastic settings and therefore the simulation continues even after reaching the least cost function. The cost function is very sensitive in the sense that a small variation in altruist parameter can vary the yeast efficiency of retaining damage which may result in the decrease/increase in the yeast cell population and damage accumulation in the population. This fallouts fluctuation in the cost function which sets the direction by varying altruism values as shown in Figure 10. In the simulations, an important aspect to analyse is that most of the fluctuations occurred at some specific altruism values. The stopping criteria

481 is implemented after 1000 variations, strategy variation number ( $S_N$ ) = 1000, by the following  
482 inequality

$$\sum_{i=S_N+l}^{S_N+j+l} |A_{i-j} - A_{i-(j+k)}| < \varepsilon \quad (15)$$

483 The index values are  $j = k = 10$  and the epsilon  $\varepsilon = 0.02$ . The parameter epsilon provides the  
484 maximum possible variation in the altruism value and is used in the Eq. (14). The stopping  
485 criteria are defined by the summation expression that stops the simulation if the  $\varepsilon$  condition  
486 is fulfilled consecutively for five values of index  $l$ .

487 The altruist effects on distance strategy (Figure 10a), have revealed clear differences between  
488 the values of  $A$  chosen above and below the neutral one, i.e. 0.5. For a yeast population  
489 following its strategy with altruism  $A \geq 0.5$ , the cost function decreases as  $A$  increases and  
490 eventually,  $A$  reaches to the maximum value. On the other hand, when  $A < 0.5$ , the strategy  
491 varies most of the time around the values  $A = 0$  and 0.4 that are surrounded by evolutionary  
492 ditches. Since strategies are tuned to keep varying  $A$  in the direction where least value of cost  
493 function (minimum of the cost function) is found, therefore, the sensitivity in cost function  
494 against the altruist values allows cells to alter their strategy which creates a safe escape from  
495 the evolutionary ditch. In a similar way, these strategies escape from the least values of the  
496 cost function. Such escapes are made possible due to the involvement of randomness in the  
497 altruism.

498 The division strategy also shows similar behaviour as distance strategy however the strategy  
499 is more frequently observed around the extreme values of altruism, i.e.  $A = 0, 0.1, 0.9$  and 1  
500 (Figure 10b). The simulations show that strategy started around  $A \leq 0.4$  could not escape from  
501 the local minimum of the cost function while the starting value of  $A$  above 0.8 eventually  
502 reached to their evolutionary ditch.

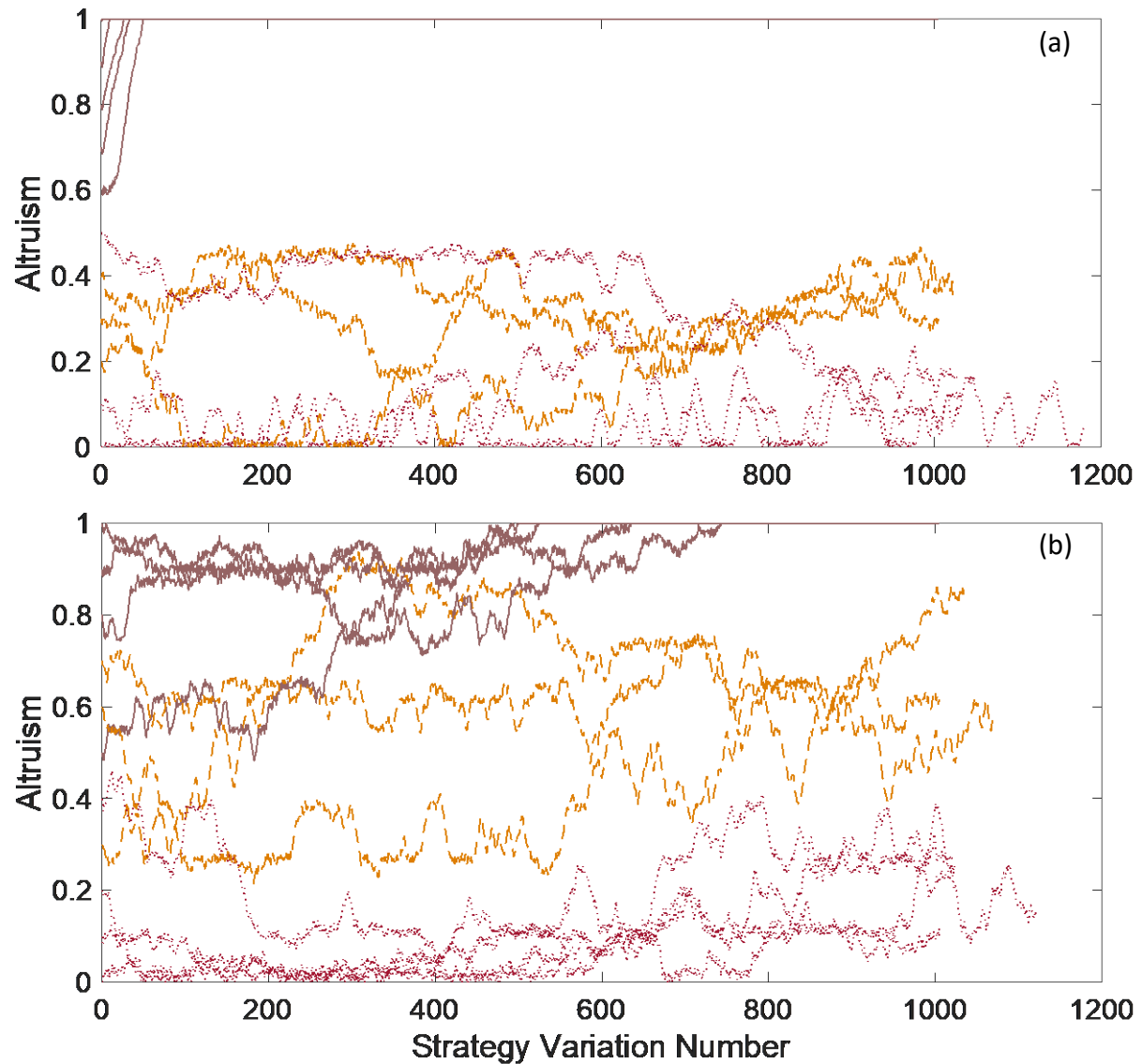


Figure 10: Stochastic simulations of (a) distance and (b) division strategies at time  $t = 1.5$ . The altruism parameter  $A$  is varied randomly for each strategy variation number in the interval  $[0, \varepsilon = 0.02]$ . The lines styles are used to clear up the tracking of each simulation.

## Conclusions

The efficiency of damage retention provides a monotonically decreasing function in which a mother cell retains lower amounts of damage in each subsequent division. The defined strategies have provided unique ways for decreasing the efficiency during cell replicative lifespan of a budding yeast while the altruism factor was used to make deviations in the strategy. For each deviation, a well-defined cost function is computed. Deterministic settings were adopted to analyse the behaviour of cost functions for each strategy. It has also provided the extreme values of the cost function which were further used under the stochastic settings. The cost functions were varied by means of random altruistic effects given to the strategies.

These variations were tuned to find the optimal reproduction success of the population. However, the strategies that started at different altruist values, ended up optimizing in a local fashion rather than approaching a global minima of the cost function.

### **Distance vs Division Strategy**

Our results show that retaining more damage, in the beginning, provides healthy daughter cells which plays a significant role in maintaining the accumulated health of the population. Moreover, the daughters born with high damage did not replicate as often as daughters born with low damage. In the case of division strategy, the mother cell shared more damage in the early divisions, leading to the poor health of progeny. At the later stage of replication, when the damage efficiency is low, the mother cell shared a high level of damage with its daughter cells. Consequently, these daughter cells could not provide healthy progeny to the population.

### **Altruism Provides Healthy but a Small Population**

Increase in the altruist values increases the efficiency of damage retention of the mother cell. A complete altruist behaviour allows a mother cell to retain all the damage at the time of division which reduces its replicative lifespan while giving birth to completely healthy daughter cells (Figure 3). In the case of whole pedigree, the same phenomenon is followed (Figures S1). When both factors, health and population size are considered (Figures 7 – 9), the cost functions of each strategy provided different global minima, while the distance strategy provides lower cost than the division strategy. This shows that a yeast following division strategy can never achieve a better health and population status than a yeast following a distance strategy.

Population size and population health have shown reverse behaviours. Increasing population size affects the health of the population and brings more damage to the cells while a better health keeps the population size small. In addition, yeast cells with altruistic behaviour do not give a boost to the population health as compared to selfish yeasts who although increase the damage but doubles the size of the population. Providing good health to new buds significantly increases damage in the mother cells which results in an early senescence state where no more replications are possible (Aguilaniu et al., 2003; Denoth Lippuner et al., 2014;



543 Jazwinski and Wawryn, 2001; Liu et al., 2011; Spokoini et al., 2012). On the other hand, selfish  
544 behaviour allows a long replicative lifespan.

### 545 **Optimal Reproduction Success represents Local Minima of Cost Function**

546 Strategies were adopted for the continuous search for the minimal value of the cost function.  
547 Since the function values could not be anticipated in the stochastic simulations, the altruist  
548 value varied continuously to search for it. Therefore, the cost function never converged to any  
549 specific value. This interprets the physical phenomenon where mutations in a yeast strain  
550 could vary the strategy that is followed by its progeny. It is observed that when yeast varied  
551 its state from the minima of the cost function, the subsequent mutations could not reverse  
552 mutation due to stochastic effects and therefore the trait is able to reach local minima of the  
553 cost function. Thus, the optimal reproduction success would never be able to show stable  
554 behaviour near the minima of the cost function. At the same time, when cells opted for a  
555 minimum value of cost function, the optimal reproduction success trapped for a long period  
556 of time to local minima which were surrounded by high cost functions.

### 557 **Evolutionary Ditches can make a Trait Maladaptive**

558 Evolutionary ditches became evolutionary traps in certain cases when the yeast species were  
559 unable to escape from local minima because the cost function is surrounded by higher values.  
560 With distance strategy, the cost function at  $A = 1$  is lower than  $0.5 < A < 1$ , however it is  
561 sufficiently higher than the minimum value of cost function (Figures 7 – 9). Consequently, in  
562 the stochastic simulation, the cells with  $A > 0.5$ , have rapidly adapted complete altruist  
563 behaviour,  $A = 1$ , and couldn't manage to escape from there. This behaviour showed sufficient  
564 potential in the yeast strategy to follow an extinction, especially when it is competing against  
565 the other species with lower values of the cost function. In summary, our results suggest that  
566 damage retention during the early divisions (distance strategy) increases the number of  
567 healthy daughters in the yeast population. In addition, a rapid decrease in the efficiency of  
568 damage retention, at the time when the mother cell is almost exhausted, produces fewer  
569 daughters with a very high amount of damage. Next, the two proposed strategies have distinct  
570 cost functions, implying that a strategy may not attain the same minima of cost function as  
571 the other. The minimum value attained by distance strategy has provided the minimal value

572 of cost function. And finally, fluctuations in the cost function allow yeast cell to continuously  
573 vary its strategy, suggesting that optimal reproduction success is a local minimum of the cost  
574 function.

575 Acknowledgement

576 This work was supported by the Swedish Foundation for Strategic Research.

577

## 578 **Appendix 1**

### 579 **A mathematical model for yeast cell growth and division processes**

580 The replicative lifespan of a yeast cell is comprised of two major processes: cellular growth in  
581 which the intact and damage components of a cell increase, and cell asymmetric division in  
582 which cell buds out a new daughter cell. A pedigree-tree modelling approach is used so that  
583 the cellular processes can be tracked for each cell individually. A similar modelling approach  
584 has been used in the literature where the retention parameter was kept constant (Erjavec et  
585 al., 2008), however, it followed the fate of the progenitor and the progeny, separately,  
586 through a number of generations. We could thus draw a “mother lineage” and a “daughter  
587 lineage”, whereby we would, after every division, follow respectively the next generation of  
588 mothers only, or the next generations of daughters only. However, these do not represent a  
589 realistic population that consists of intermediated branches as well. Thus, in the model  
590 presented here, we simulate the realistic population, including all intermediated branches and  
591 mixed-linages.

592 During the growth process, the number of healthy protein (intact protein) molecules increases  
593 in the cell at the rate constant  $k_1$  and dissolves into the system due to half-life phenomenon  
594 at the rate equals to  $k_2$ . At the rate,  $k_3$  damage proteins are formed. The degradation rate for  
595 damaged molecules is denoted by  $k_4$ . The modelled equations can, therefore, be written as,

$$\begin{aligned} \dot{I} &= k_1 \left( 1 - \frac{I + D}{K} \right) - k_2 I - k_3 I \\ \dot{D} &= k_3 I - k_4 D \end{aligned} \quad \text{Eq. 1}$$

596 The increase in the number of damaged proteins  $D$  becomes lethal if the cell reaches death  
597 threshold value  $D = D^*$  whereas the intact component  $I$  increases inside the cell to division  
598 threshold  $I = I^*$ . If the cell reaches division threshold first, the cell divides and produces a  
599 daughter cell with a mother to daughter cell size ratio  $R_m : 1 - R_m$ . During the early cell  
600 divisions, the mother cell retains maximum damage while its retention efficiency decreases in  
601 the later divisions until it reaches the minimum value  $re(g)=0$ , i.e. no retention.

602

Parameter	Description	Values	Assumptions and source
$I^*$	cell division threshold, in the number of intact proteins	1500	amount of intact proteins (Erjavec et al., 2008)
$D^*$	cell death threshold, in number of damaged proteins	600	
$k_1$	rate maximal protein production	$1.5 \times 10^4$	adjusted by hand to allow steady-state (Erjavec et al., 2008)
$k_2$	the rate of degradation of intact proteins	$\ln 2$	the half-life of 1 time unit (Erjavec et al., 2008)
$k_3$	rate of damaging of intact proteins	[0.1,2.3] by 0.75	(Erjavec et al., 2008)
$k_4$	the rate of degradation of damaged proteins	$\ln 2$	the half-life of 1 time unit (Erjavec et al., 2008)
$K$	carrying capacity	2500	adjusted by hand
$re$	retention coefficient	[0, 1] by 0.125	(Erjavec et al., 2008)
$R_m$	size of the progenitor after division	0.79	$R_m + R_d = 1$ (Erjavec et al., 2008)
$R_d$	size of the progeny after division	0.21	$R_m + R_d = 1$ (Erjavec et al., 2008)

Table 1: **Model parameters with default values and assumptions made**

606 The division process is modelled as a discrete set of equations for mother and daughter cells.

607 For the mother cell, the intact and damage portions can be calculated as:

$$\begin{aligned} I_{in}(g+1) &= I_{end}(g) \cdot R_m - D_{end}(g) \cdot R_d \cdot re(g) \\ D_{in}(g+1) &= D_{end}(g) \cdot R_m + D_{end}(g) \cdot R_d \cdot re(g) \end{aligned} \quad \text{Eq. 2}$$

608 The intact and damage portions for daughter cells have the similar equations

$$\begin{aligned} I_{in}(g+1) &= I_{end}(g) \cdot R_d + D_{end}(g) \cdot R_d \cdot re(g) \\ D_{in}(g+1) &= D_{end}(g) \cdot R_d - D_{end}(g) \cdot R_d \cdot re(g) \end{aligned} \quad \text{Eq. 3}$$

609 where the parameter  $R_d = 1 - R_m$  size of the daughter cell after division and  $g$  is division  
610 number. The index terms *in* and *end* are the initial value after division and end value before  
611 division respectively. The equations 2 and 3 are based on the principle of mass conservation  
612 over generations (Erjavec et al., 2008). In particular, this means that the total cellular content  
613 ( $I+D$ ), in the original cell equal the sum of the total cellular content of the mother and daughter  
614 cell. The conditions are also based on mass conservation with respect to intact component  $I$   
615 and damage  $D$ .

## 616 The general behaviour of Model

617 The processes described in the above model involving cell growth and division are simulated  
618 in the Figure S1. The figure describes a general behaviour of the modelled system without  
619 including the strategies and their altruist behaviour. Three parameters are investigated at  
620 different values to understand their effect on the overall dynamics of the modelled system.  
621 We observe that cell undergoes more divisions with the decrease in the values of  $k_3$ ,  $R_m$  and  
622  $re$ . In the case of finite replications, cell generally takes more time in the later divisions to grow  
623 and reach the division threshold. On the other hand, increasing the cell size ratio from mother  
624 to daughter cells ( $R_m$ ) decreases the time to the next division. Damage retention also plays an  
625 important role in the replicative lifespan of a cell. However, this parameter is chosen constant  
626 here for the sake of simplicity. It is interesting to observe that a total number of divisions  
627 drastically decreases with the increase in retention parameter. We study the retention  
628 parameter as a variable, dependent upon a number of divisions of the mother cell.

629

630

631

632

633

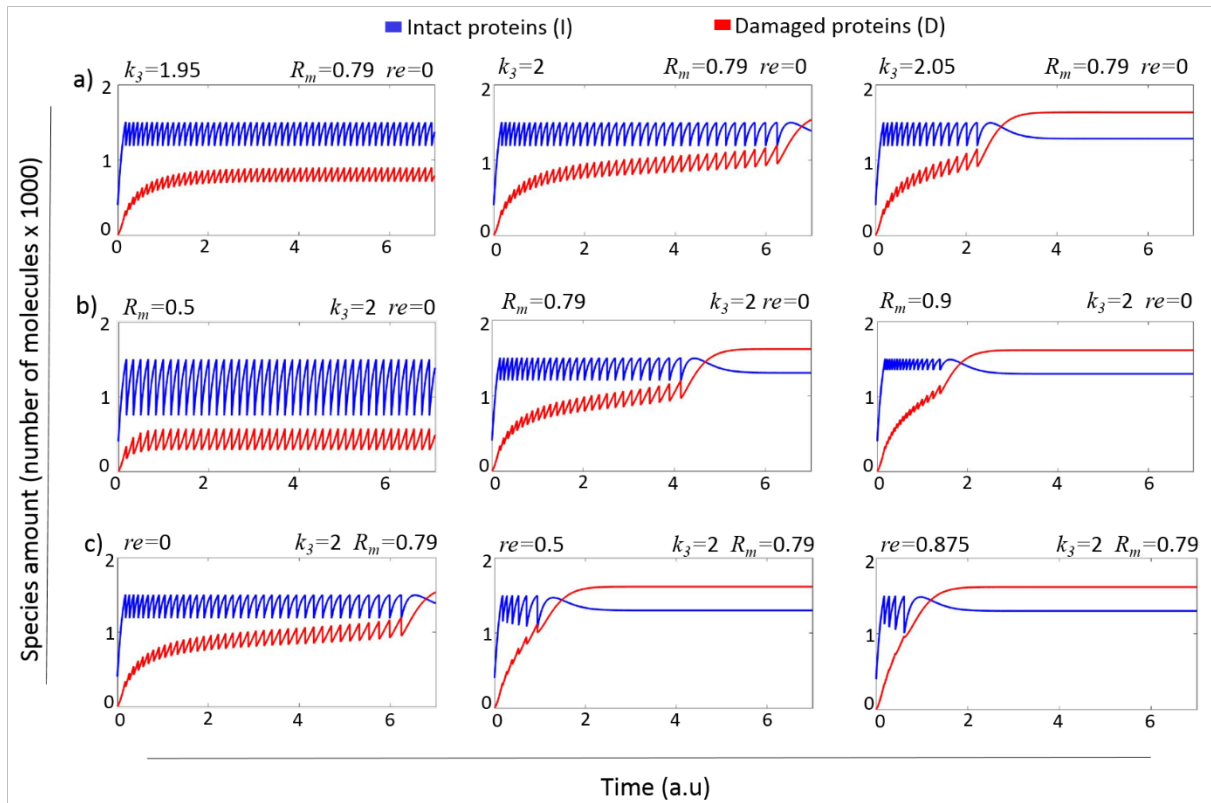


Figure S1: Intracellular species dynamics of a single cell a) damage accumulation rates b) size of the mother and c) retention coefficients. Red and blue lines describe the dynamics of damaged and intact cellular components, respectively.  $re(g) = Re$  (a constant).

## Pedigree-Tree Diagram

Pedigree-tree model follows the growth and division process of each individual cell. The process starts with a single cell that grows its intact and damaged component. At the growth threshold, cell buds its first daughter cell. At this time point, the budding cell is considered as a mother while the budded cell is considered as a daughter cell. Now, mother cell and daughter cell both undergo the growth process to reach the division threshold, see Figure S2. Hence cell population increases while each cell is tracked during its replicative lifespan or until the simulation ends. The population is discretely distributed over the total intact and damage portions of each cell as described in the main text.



660

Appendix 2

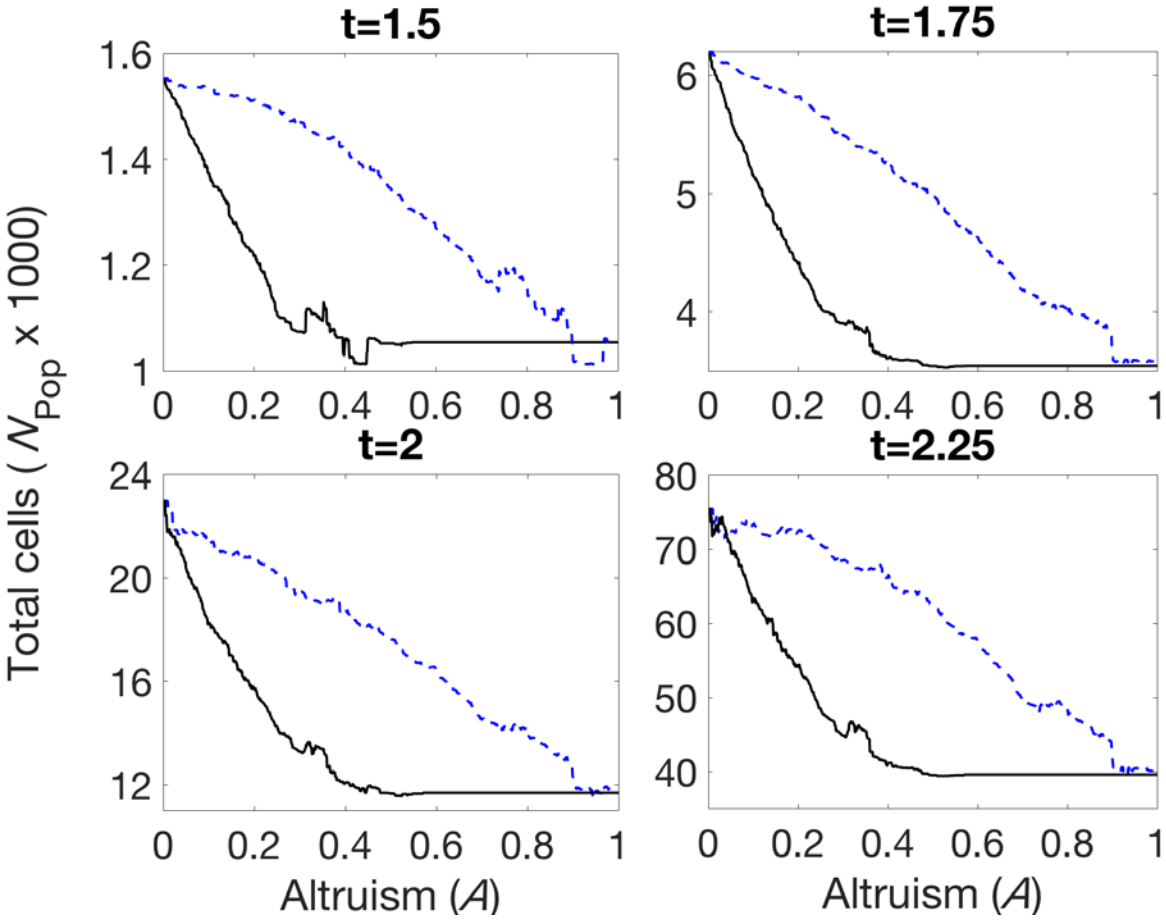


Figure S3: Total number of cells against the altruism values at four simulation times  $t = 1.5, 1.75, 2, 2.25$ . Lines represents population with distance strategy whereas the dashed lines represent the population with division strategy.



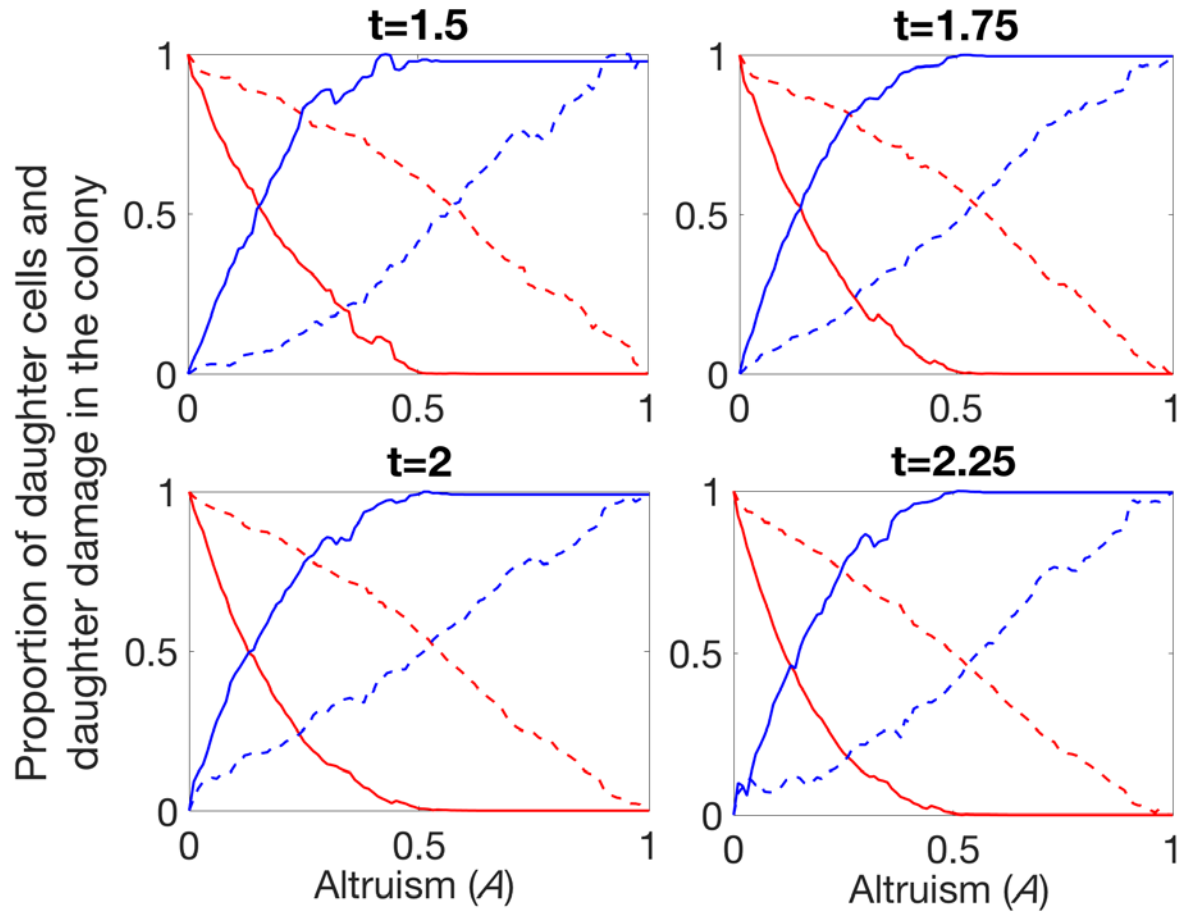


Figure S4: Proportion of daughter cells and their damage in the population for time  $t = 1.5, 1.75, 2$  and  $2.25$ . The continuous lines represent distance strategy while dashed lines represent division strategy. The lines moving from 0 to 1 are the daughter cells proportion while the lines moving from 1 to 0 are the damage proportion.

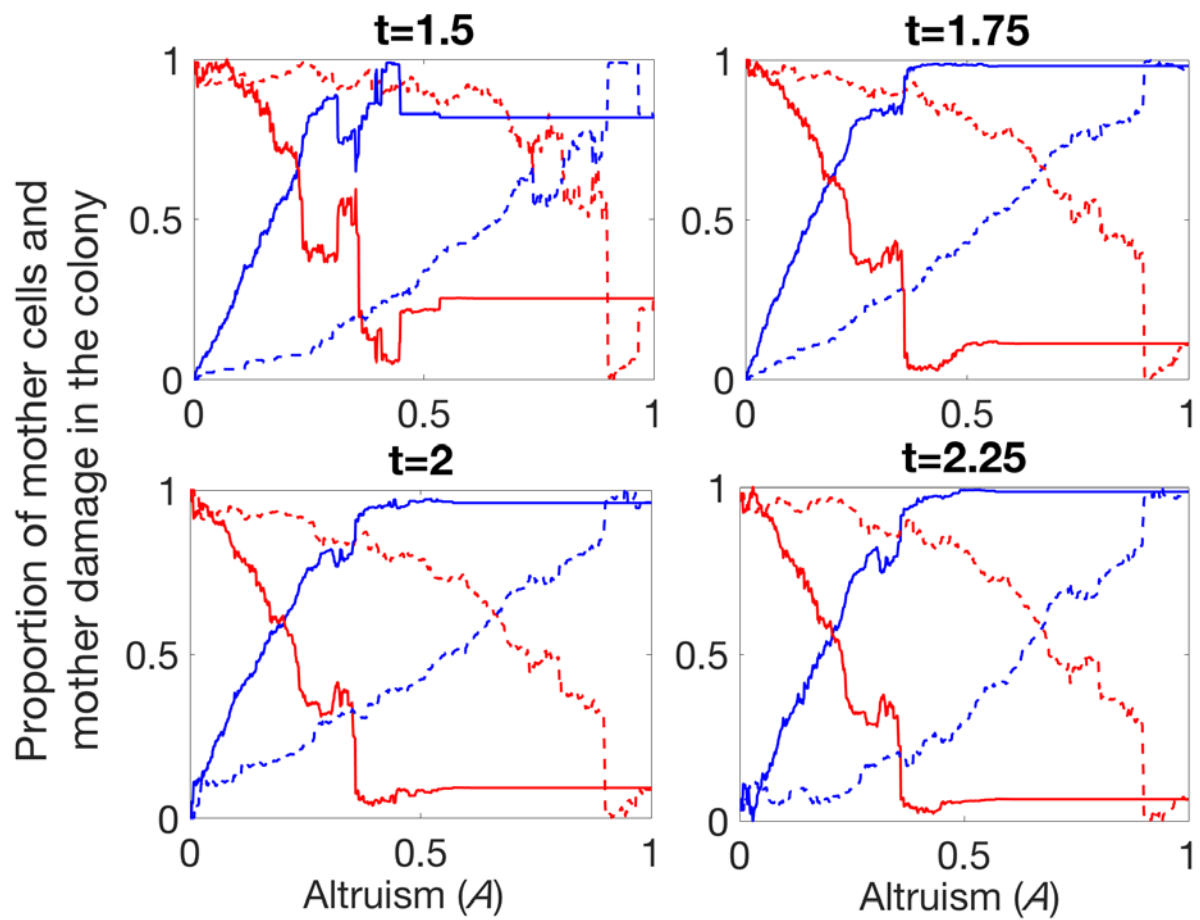


Figure S5: Proportion of mother cells and their damage in the colony at time  $t=1.5$ ,  $1.75$ ,  $2$  and  $2.25$ . The continuous lines represent distance strategy while dashed lines represent division strategy. The lines moving from 0 to 1 along y-axis are the mother cells proportion while the lines moving from 1 to 0 are the damage proportion.

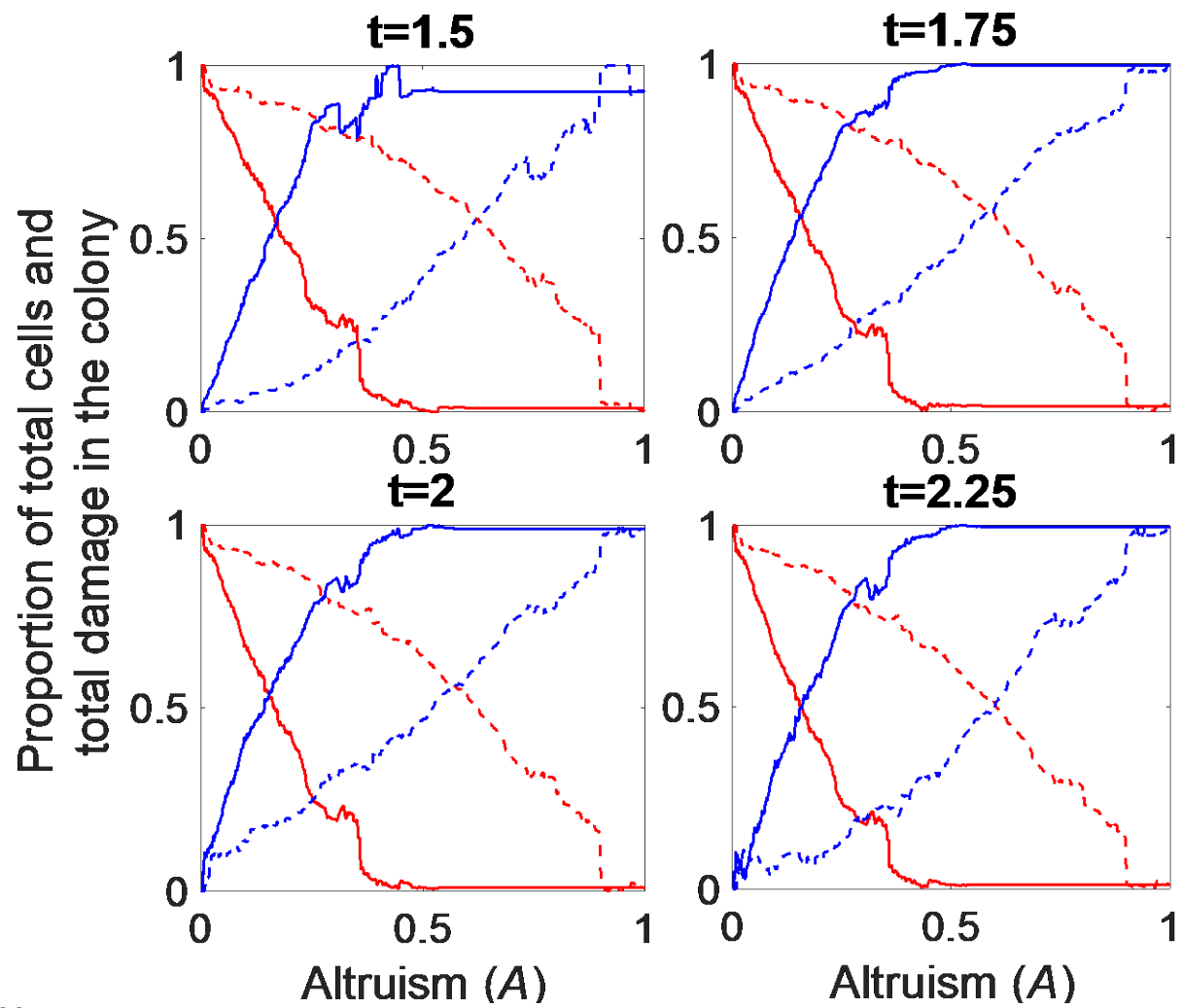


Figure S6: Proportion of total cells and their damage in the population for time  $t=1.5$ ,  $1.75$ ,  $2$  and  $2.25$ . The continuous lines represent distance strategy while dashed lines represent division strategy. The lines moving from  $0$  to  $1$  are the total cells proportion while the lines moving from  $1$  to  $0$  are the damage proportion.

## 722   **References**

- 723   Ackermann, M., Chao, L., Bergstrom, C.T., Doebeli, M., 2007. On the evolutionary origin of  
724       aging. *Aging Cell* 6, 235–244. <https://doi.org/10.1111/j.1474-9726.2007.00281.x>
- 725   Ackermann, M., Stearns, S.C., Jenal, U., 2003. Senescence in a bacterium with asymmetric  
726       division. *Science* 300, 1920. <https://doi.org/10.1126/science.1083532>
- 727   Aguilaniu, H., Gustafsson, L., Rigoulet, M., Nyström, T., 2003. Asymmetric inheritance of  
728       oxidatively damaged proteins during cytokinesis. *Science* 299, 1751–1753.  
729       <https://doi.org/10.1126/science.1080418>
- 730   Berg, J.M., Tymoczko, J.L., Stryer, L., 2002. *Evolution Requires Reproduction, Variation, and*  
731       *Selective Pressure.*
- 732   Biesalski, H.K., 2002. Free radical theory of aging. *Curr. Opin. Clin. Nutr. Metab. Care* 5, 5–10.
- 733   Brooks, R.C., Garratt, M.G., 2017. Life history evolution, reproduction, and the origins of sex-  
734       dependent aging and longevity. *Ann. N. Y. Acad. Sci.* 1389, 92–107.  
735       <https://doi.org/10.1111/nyas.13302>
- 736   Bufalino, M.R., DeVeale, B., van der Kooy, D., 2013. The asymmetric segregation of damaged  
737       proteins is stem cell-type dependent. *J. Cell Biol.* 201, 523–530.  
738       <https://doi.org/10.1083/jcb.201207052>
- 739   Chao, L., 2010. A model for damage load and its implications for the evolution of bacterial  
740       aging. *PLoS Genet.* 6. <https://doi.org/10.1371/journal.pgen.1001076>
- 741   Chao, L., Rang, C.U., Proenca, A.M., Chao, J.U., 2016. Asymmetrical Damage Partitioning in  
742       Bacteria: A Model for the Evolution of Stochasticity, Determinism, and Genetic  
743       Assimilation. *PLoS Comput. Biol.* 12. <https://doi.org/10.1371/journal.pcbi.1004700>
- 744   Clegg, R.J., Dyson, R.J., Kreft, J.-U., 2014. Repair rather than segregation of damage is the  
745       optimal unicellular aging strategy. *BMC Biol.* 12. [https://doi.org/10.1186/s12915-014-](https://doi.org/10.1186/s12915-014-0052-x)  
746       0052-x
- 747   Coelho, M., Lade, S.J., Alberti, S., Gross, T., Tolić, I.M., 2014. Fusion of protein aggregates  
748       facilitates asymmetric damage segregation. *PLoS Biol.* 12, e1001886.  
749       <https://doi.org/10.1371/journal.pbio.1001886>
- 750   de Grey, A.D., 1997. A proposed refinement of the mitochondrial free radical theory of aging.  
751       *BioEssays News Rev. Mol. Cell. Dev. Biol.* 19, 161–166.  
752       <https://doi.org/10.1002/bies.950190211>
- 753   Denoth Lippuner, A., Julou, T., Barral, Y., 2014. Budding yeast as a model organism to study  
754       the effects of age. *FEMS Microbiol. Rev.* 38, 300–325. [https://doi.org/10.1111/1574-](https://doi.org/10.1111/1574-6976.12060)  
755       6976.12060

756 Egilmez, N. K, and Jazwinski, S.M., 1989. Evidence for the involvement of a cytoplasmic factor  
757 in the aging of the yeast *Saccharomyces cerevisiae*. *J Bacteriol* 171: 37–42.

758 Erjavec, N., Cvijovic, M., Klipp, E., Nyström, T., 2008. Selective benefits of damage partitioning  
759 in unicellular systems and its effects on aging. *Proc. Natl. Acad. Sci. U. S. A.* 105, 18764–  
760 18769. <https://doi.org/10.1073/pnas.0804550105>

761 Erjavec, N., Larsson, L., Grantham, J., Nyström, T., 2007. Accelerated aging and failure to  
762 segregate damaged proteins in Sir2 mutants can be suppressed by overproducing the  
763 protein aggregation-remodeling factor Hsp104p. *Genes Dev.* 21, 2410–2421.  
764 <https://doi.org/10.1101/gad.439307>

765 Hill, S.M., Hanzén, S., Nyström, T., 2017. Restricted access: spatial sequestration of damaged  
766 proteins during stress and aging. *EMBO Rep.* 18, 377–391.  
767 <https://doi.org/10.15252/embr.201643458>

768 Hill, S.M., Hao, X., Grönvall, J., Spikings-Nordby, S., Widlund, P.O., Amen, T., Jörhov, A.,  
769 Josefson, R., Kaganovich, D., Liu, B., Nyström, T., 2016. Asymmetric Inheritance of  
770 Aggregated Proteins and Age Reset in Yeast Are Regulated by Vac17-Dependent  
771 Vacuolar Functions. *Cell Rep.* 16, 826–838.  
772 <https://doi.org/10.1016/j.celrep.2016.06.016>

773 Jazwinski, S.M., Wawryn, J., 2001. Profiles of random change during aging contain hidden  
774 information about longevity and the aging process. *J. Theor. Biol.* 213, 599–608.  
775 <https://doi.org/10.1006/jtbi.2001.2434>

776 Kaerberlein, M., 2010. Lessons on longevity from budding yeast. *Nature* 464: 513–519.

777 Katajisto, P., Döhla, J., Chaffer, C., Pentinmikko, N., Marjanovic, N., Iqbal, S., Zoncu, R., Chen,  
778 W., Weinberg, R.A., Sabatini, D.M., 2015. Asymmetric apportioning of aged  
779 mitochondria between daughter cells is required for stemness. *Science* 348, 340–343.  
780 <https://doi.org/10.1126/science.1260384>

781 Kennedy, B.K., Austriaco, N.R., Guarente, L., 1994. Daughter cells of *Saccharomyces cerevisiae*  
782 from old mothers display a reduced life span. *J. Cell Biol.* 127, 1985–1993.

783 Kirkwood, T.B., Rose, M.R., 1991. Evolution of senescence: late survival sacrificed for  
784 reproduction. *Philos. Trans. R. Soc. Lond. B. Biol. Sci.* 332, 15–24.  
785 <https://doi.org/10.1098/rstb.1991.0028>

786 Konieczny, L., Roterman-Konieczna, I., Spólnik, P., 2014. The Structure and Function of Living  
787 Organisms, in: *Systems Biology*. Springer, Cham, pp. 1–32.  
788 [https://doi.org/10.1007/978-3-319-01336-7\\_1](https://doi.org/10.1007/978-3-319-01336-7_1)

789 Kowald, A., Kirkwood, T.B., 2000. Accumulation of defective mitochondria through delayed  
790 degradation of damaged organelles and its possible role in the ageing of post-mitotic  
791 and dividing cells. *J. Theor. Biol.* 202, 145–160. <https://doi.org/10.1006/jtbi.1999.1046>

792 Kruegel, U., Robison, B., Dange, T., Kahlert, G., Delaney, J.R., Kotireddy, S., Tsuchiya, M.,  
793 Tsuchiyama, S., Murakami, C.J., Schleit, J., Sutphin, G., Carr, D., Tar, K., Dittmar, G.,  
794 Kaeberlein, M., Kennedy, B.K., Schmidt, M., 2011. Elevated proteasome capacity  
795 extends replicative lifespan in *Saccharomyces cerevisiae*. *PLoS Genet.* 7, e1002253.  
796 <https://doi.org/10.1371/journal.pgen.1002253>

797 Lindner, A.B., Madden, R., Demarez, A., Stewart, E.J., Taddei, F., 2008. Asymmetric segregation  
798 of protein aggregates is associated with cellular aging and rejuvenation. *Proc. Natl.*  
799 *Acad. Sci. U. S. A.* 105, 3076–3081. <https://doi.org/10.1073/pnas.0708931105>

800 Liu, B., Larsson, L., Franssens, V., Hao, X., Hill, S.M., Andersson, V., Höglund, D., Song, J., Yang,  
801 X., Öling, D., Grantham, J., Winderickx, J., Nyström, T., 2011. Segregation of protein  
802 aggregates involves actin and the polarity machinery. *Cell* 147, 959–961.  
803 <https://doi.org/10.1016/j.cell.2011.11.018>

804 Longo, V., Shadel, G. S., Kaeberlein, M., Kennedy, B., 2012. Replicative and Chronological Ageing  
805 in *Saccharomyces cerevisiae* *Cell Metab.* 16(1): 18-31 <https://doi.org/10.1016/j.cmet.2012.06.002>

807 Nyström, T., Liu, B., 2014. Protein quality control in time and space - links to cellular aging.  
808 *FEMS Yeast Res.* 14, 40–48. <https://doi.org/10.1111/1567-1364.12095>

809 Orgel, L.E., 1963. The maintenance of the accuracy of protein synthesis and its relevance to  
810 ageing. *Proc. Natl. Acad. Sci. U. S. A.* 49, 517–521.

811 Rujano, M.A., Bosveld, F., Salomons, F.A., Dijk, F., van Waarde, M.A.W.H., van der Want, J.J.L.,  
812 de Vos, R.A.I., Brunt, E.R., Sibon, O.C.M., Kampinga, H.H., 2006. Polarised asymmetric  
813 inheritance of accumulated protein damage in higher eukaryotes. *PLoS Biol.* 4, e417.  
814 <https://doi.org/10.1371/journal.pbio.0040417>

815 Spokoini, R., Moldavski, O., Nahmias, Y., England, J.L., Schuldiner, M., Kaganovich, D., 2012.  
816 Confinement to organelle-associated inclusion structures mediates asymmetric  
817 inheritance of aggregated protein in budding yeast. *Cell Rep.* 2, 738–747.  
818 <https://doi.org/10.1016/j.celrep.2012.08.024>

819 Stewart, E.J., Madden, R., Paul, G., Taddei, F., 2005. Aging and Death in an Organism That  
820 Reproduces by Morphologically Symmetric Division. *PLoS Biol.* 3.  
821 <https://doi.org/10.1371/journal.pbio.0030045>

822 Tyedmers, J., Mogk, A., Bukau, B., 2010. Cellular strategies for controlling protein aggregation.  
823 *Nat. Rev. Mol. Cell Biol.* 11, 777–788. <https://doi.org/10.1038/nrm2993>

824 Vedel, S., Nunns, H., Košmrlj, A., Semsey, S., Trusina, A., 2016. Asymmetric Damage  
825 Segregation Constitutes an Emergent Population-Level Stress Response. *Cell Syst.* 3,  
826 187–198. <https://doi.org/10.1016/j.cels.2016.06.008>

827 Zhou, C., Slaughter, B.D., Unruh, J.R., Guo, F., Yu, Z., Mickey, K., Narkar, A., Ross, R.T., McClain,  
828 M., Li, R., 2014. Organelle-based aggregation and retention of damaged proteins in

829           asymmetrically           dividing           cells.           Cell           159,           530–542.  
830           <https://doi.org/10.1016/j.cell.2014.09.026>

831

# Adaptive damage retention mechanism enables healthier yeast population

Qasim Ali<sup>1,2</sup>, Riccardo Dainese<sup>1,3</sup>, Marija Cvijovic<sup>1\*</sup>

<sup>1</sup>Department of Mathematical Sciences, Chalmers University of Technology and University of  
Gothenburg, Gothenburg, Sweden

<sup>2</sup> Department of Mathematics, North Carolina State University, NC 27607, USA (current  
affiliation)

<sup>3</sup> Laboratory of Systems Biology and Genetics, Institute of Bioengineering, School of Life  
Sciences, École Polytechnique Fédérale de Lausanne (EPFL), Lausanne, Switzerland (current  
affiliation)

\*Corresponding author

Marija Cvijovic

Department of Mathematical Sciences

Chalmers University of Technology and University of Gothenburg

Chalmers tvärgata 3

SE-41296 Gothenburg, Sweden

Phone: +46 31 772 53 21

Email: marija.cvijovic@gu.se



## 24 Highlights

- 25       ▪ retaining more damage by a yeast cell during the early divisions increases the number of  
26       healthy daughters in the population
- 27       ▪ a rapid decrease in the efficiency of damage retention, at the time when the mother cell is  
28       almost exhausted, produces fewer daughters with high levels of damage
- 29       ▪ fluctuations in the cost function allow yeast cell to continuously vary its strategy, suggesting  
30       that optimal reproduction success is a local minimum of the cost function

31

32 Keywords: yeast, asymmetrical division, damage retention, dynamical modelling, pedigree-  
33 tree model

34

35

36

## Abstract

37 During cytokinesis in budding yeast (*Saccharomyces cerevisiae*) damaged proteins are  
38 distributed asymmetrically between the daughter and the mother cell. Retention of damaged  
39 proteins is a crucial mechanism ensuring a healthy daughter cell with full replicative potential  
40 and an ageing mother cell. However, the protein quality control (PQC) system is tuned for  
41 optimal reproduction success that suggests optimal health and size of the population, rather  
42 than long-term survival of the mother cell. Modelling retention of damage as an adaptable  
43 mechanism, we propose two damage retention strategies to find an optimal way of decreasing  
44 damage retention efficiency in order to maximize population size and minimize the damage  
45 in the individual yeast cell. A pedigree model is used to investigate the impact of small  
46 variations in the strategies over the whole population. These impacts are based on the  
47 altruistic effects of damage retention mechanism and are measured by a cost function whose  
48 minimum value provides the optimal health and size of the population. We showed that  
49 fluctuations in the cost function allow yeast cell to continuously vary its strategy, suggesting  
50 that optimal reproduction success is a local minimum of the cost function. Our results suggest  
51 that a rapid decrease in the efficiency of damage retention, at the time when the mother cell  
52 is almost exhausted, produces fewer daughters with high levels of damaged proteins. In  
53 addition, retaining more damage during the early divisions increases the number of healthy  
54 daughters in the population.

55

Abbreviations	Description
$RE_{div/dist}$	Division / distance strategy of damage retention
$g$	Division number
$\alpha, n$	repressor activation constant, repressor Hill constant
$\tau_i, \tau_D$	Time required for intact/damage component to reach division/ death
$I_{div}$	Intact component threshold
$R_t$	Ratio between the times required for division and death threshold
$I_g$ and $D_g$	Intact and damage component of mother cell after division
$re$	Damage Retention with altruist effect
$re_{max}$	Maximum possible damage retention
$A$	Altruist value to make a variation in the strategy
$D, D_{death}$	Damage variable, Damage threshold
$N_{daugh/mot/pop}$	Daughter/mother/accumulated cells
$P_{daugh}, P_{mot}, P$	Population distribution for daughter/mother/accumulated
$D_{daugh/mot/pop}$	Damage in daughter/mother/accumulated cells population
$C_{daugh/mot/pop}$	Cost function for daughter/mother/accumulated cells population

## 59    **Introduction:**

60    Aging is a conserved scale-invariant phenomenon that exploits the entire organism  
61    simultaneously, from the organelles involved in the cellular processes to the organs and body  
62    structure. Aging factors like damage accumulation and its asymmetric segregation through  
63    retention mechanism during growth and division processes respectively have been frequently  
64    studied in the past few decades and are proposed to promote ageing from simple unicellular  
65    organism like budding yeast to higher eukaryotes (Bufalino et al., 2013; Erjavec et al., 2007;  
66    Hill et al., 2016; Katajisto et al., 2015; Kennedy et al., 1994; Kruegel et al., 2011; Zhou et al.,  
67    2014). Retention of damage during the process of cell division is an evolutionary conserved  
68    mechanism whose efficiency decreases gradually and leads to the senescence state where  
69    basic cellular processes are unable to produce enough proteins to have subsequent divisions  
70    (Aguilaniu et al, 2003; Ackermann et al., 2003; Erjavec et al., 2008; Rujano et al., 2006).  
71    Budding yeast, *Saccharomyces cerevisiae* (*S. cerevisiae*) has been widely studied in aging  
72    research and has contributed to the identification of many genes involved in mammalian aging  
73    (Longo et al, 2012). Ageing in yeast can be studied by two main approaches: replicative aging,  
74    which is measured by the number of divisions that a cell performs before senescence, and  
75    chronological aging, which corresponds to the time before a cell enters senescence in a non-  
76    dividing state (Longo, 2012). Experiments targeting replicative aging showed that yeast cells  
77    give rise to a limited number of daughter cells, usually around 20–25 (Mortimer and Johnson  
78    1959, Longo, 2012). Throughout its lifespan, a cell accumulates different types of ageing  
79    factors, like extra chromosomal RNA circles (ERCs), increased intracellular oxidative stress,  
80    mitochondrial dysfunctions and accumulation of damaged proteins (Aguilaniu 2003, Sinclair  
81    1998). It has been shown that asymmetric distribution of damaged proteins in the unicellular  
82    organisms is evolutionarily beneficial for the whole progeny thus ensuring the highest level of  
83    fitness for the daughter cells (Waddington, 1953; Eshel and Matessi, 1998; Crispo, 2007,  
84    Kaberlein, 2010). This unequal distribution of damage results in an ageing mother cell and a  
85    rejuvenated daughter with full replicative potential (Eglimetz and Jazwinski, 1989). In the early  
86    divisions, a mother cell is able to retain most of the damage, giving rise to fully healthy  
87    daughter cells. However, in the late stages of a mother cell's lifespan, damage retention  
88    becomes less effective, and aging factors begin to be passed to the daughters which, thus, are  
89    born prematurely old (Kennedy et al, 1994; Sinclair et al, 1998a; Sinclair et al, 1998b). This

trend reaches a climax in the last 5% of a mother's lifespan when divisions are often symmetric, and the daughter inherits a consistent amount of cellular damage from the mother. The gradual decline in the organelles performance during replicative aging results in cells with a unique way of damage retention that is well conserved across natural selection and provide a distinctive reproduction strategy among the different yeast strains (Erjavec et al., 2008; Kirkwood and Rose, 1991; Nyström and Liu, 2014).

From the evolutionary perspective of Darwinism, the variation in the genetic material of a trait is a random process that is passed on to its progeny by means of natural selection. These variations are negligible, preserving the structure and function during the lifespan of a particular species (Konieczny et al., 2014). However, there are several characteristics, e.g. age, size and reproduction, which are uniquely identifiable within the same species. Bringing all the characteristics together outlines an evolutionary survival strategy of the population that leads to its reproduction success (Berg et al., 2002; Brooks and Garratt, 2017).

Optimal reproduction success is a term used to define the replicative lifespan of a yeast cell that has evolved the organelles to adopt the finest route for the healthy survival of the yeast population. A success of the population is in the asymmetric distribution of damage during the cell division that ensures the low amount of damage in the progeny and its long replicative lifespan (Chao et al., 2016; Nyström and Liu, 2014). However, healthy progeny and long replicative lifespan are inversely proportional to each other since it is asserted that, during the replicative lifespan, yeast strains sacrifice their long-term survival over the health of their progeny by retaining the aging factors (Aguilaniu et al., 2003; Hill et al., 2017; Kirkwood and Rose, 1991). Therefore, it is interesting to find a strategy for optimal retention of aging factors in such a way that yeast population accumulates less damage in the living cells and provides maximum population.

Theoretical models have played a critical role in understanding the ageing process in the unicellular organisms (Ackermann et al., 2007; Chao, 2010; Chao et al., 2016; Clegg et al., 2014; Coelho et al., 2014; Erjavec et al., 2008; Lindner et al., 2008; Stewart et al., 2005; Vedel et al., 2016). A recent theoretical study has shown that symmetric division alone can lead to a senescence state where the cell can no longer divide while some stochastic effects on the damage distribution between mother and daughter cells can protect cells from early damage

(Chao et al., 2016). Moreover, natural selection adapts the protective mechanism into the subsequent progeny in a genetically controlled manner. Asymmetric division in yeast cells increases the population fitness in case of high damage propagation rates and therefore increases the proliferating capacity of the progeny (Erjavec et al., 2008). It has been suggested that the optimal aging strategy is to repair the transcriptional errors and mal-functionalities by recycling the damaged material to maintain the quality rather than segregating the damaged portions (Clegg et al., 2014). However, the protein quality control system is not sufficiently effective to maintain the proteostasis and therefore cellular health is sacrificed over the continuous production of proteins (Nyström and Liu, 2014; Orgel, 1963). Therefore, the segregation of damaged proteins in spatially sequestered regions of a cell becomes a necessity in order to maintain the performance of the organelles involved in the fundamental cellular processes (Hill et al., 2017; Tyedmers et al., 2010).

In previous computational models, retention of damage is, due to simplicity, assumed to have the same efficiency throughout the cells replicative life, thus it is treated as a constant (Erjavec et al., 2008; Clegg et al., 2014). Here, based on several experimental evidences reported in yeast (Kennedy et al, 1994; Sinclair et al, 1998a; Sinclair et al, 1998b), we consider that damage retention, like many other processes, loses its efficiency during the replicative lifespan of the yeast cell. However, the exact mechanisms of damage retention remain unclear. We propose two strategies named as *distance strategy* and *division strategy*, to investigate the efficiency and stability of damage retention during the replicative lifespan of the single cell. We ask whether it be possible that any two yeast strains following different strategies of damage retention converge to a unique optimal reproduction success. We also investigate whether a yeast population following a well-defined strategy of damage retention reaches a specific optimal reproduction success that her fellow mutated species cannot reach until it follows the same strategy.

## **Mathematical Modelling**

Mathematical model presented here is built on a model published by Erjavec et al, 2008 and comprises of division and growth processes for each cell using the discrete-continuous model. We provide here an abbreviated summary (for detailed derivation and parameters see Appendix 1).

150 Each cell increases its intact ( $I$ ) and damaged ( $D$ ) components during the growth process (Eq.  
 151 1) and asymmetrically distributes these components between mother  $R_m$  (Eq.2) and daughter  
 152  $R_d$  (Eq.3) cells during the division process.

$$\begin{aligned} \dot{I} &= k_1 \left( 1 - \frac{I + D}{K} \right) - k_2 I - k_3 I \\ \dot{D} &= k_3 I - k_4 D \end{aligned} \quad (1)$$

$$\begin{aligned} I_{in}(g+1) &= I_{end}(g) \cdot R_m - D_{end}(g) \cdot R_d \cdot re(g) \\ D_{in}(g+1) &= D_{end}(g) \cdot R_m + D_{end}(g) \cdot R_d \cdot re(g) \end{aligned} \quad (2)$$

$$\begin{aligned} I_{in}(g+1) &= I_{end}(g) \cdot R_d + D_{end}(g) \cdot R_d \cdot re(g) \\ D_{in}(g+1) &= D_{end}(g) \cdot R_d - D_{end}(g) \cdot R_d \cdot re(g) \end{aligned} \quad (3)$$

153 The damage retention mechanism allows mother cell to retain part of the damaged proteins  
 154 from the daughter cell and, in return, give part of the intact portion. The efficiency of damage  
 155 retention decreases during the whole replicative lifespan in a specified manner termed as a  
 156 strategy of premiere cell. This strategy is followed by the cell and its whole progeny during  
 157 their respective replicative lifespans. A pedigree-tree model follows the whole population and  
 158 provides a discrete population distribution function over the damaged component.

159 In this work, we consider two yeast strains following distinct strategies of decreased efficiency  
 160 of damage retention during the cell division. These strategies are based on the assumption  
 161 that each strain is tuned for a long replicative lifespan and not for its own long-term survival  
 162 (Kirkwood and Rose, 1991; Nyström and Liu, 2014). Small variations in a strategy are  
 163 implanted to alter the way of decreasing the efficiency of damage retention. It is considered  
 164 that each variation in the strategy represents an altruistic behaviour of a mother cell for her  
 165 progeny. However, for each variation, the whole pedigree-tree model is simulated, and cost  
 166 functions are calculated. These cost functions are based on the damage proportion of the alive  
 167 cells and their population size.

## 168    **Damage retention strategies**

169    Retention parameter can be varied considerably in multiple ways while each one can provide  
170    a significant effect on the population in the long run. However, it is not feasible to follow all  
171    plausible ways of reducing the efficiency of damage retentions due to computational limits.  
172    Therefore, it is inevitable to develop strategies by means of well-defined functions for the  
173    efficiency of damage retention. Two strategies, named as *division strategy* and *distance*  
174    *strategy*, are defined to investigate the efficiency of damage retention during the replicative  
175    lifespan of the single cell. Strategies have been developed in such a way that a mother cell  
176    following distance strategy retains more damage than a mother cell following division strategy  
177    during the early divisions.

### 178    **Division Strategy**

179    In a division strategy, we define retention efficiency as a repressor Hill function in the  
180    following way

$$RE_{div}(g + 1) = 1 - \frac{g^n}{g^n + \alpha^n} \quad (4)$$

181    where  $\alpha > 0$  and  $n \geq 1$  are constants. Increasing these constant values can slow down the  
182    decrease in the efficiency of damage retention in the subsequent divisions of the mother cell  
183    (Figure 1).



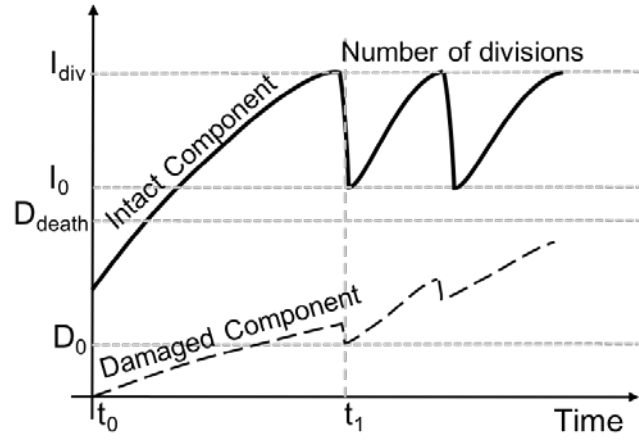


Figure 1: Division strategy: Efficiency in damage retention decreases with the increase in number of divisions. Mother cell is able to retain maximum damage in the beginning but loses its efficiency of damage retention as the number of divisions increases. The intact component decreases from its threshold  $I_{div}$  to  $I_{g=0}$  after division and the damaged component decreases to  $D_{g=0}$ . The cell death threshold is represented by  $D_{death}$ .

## Distance Strategy

In distance strategy, the efficiency of retaining damage (RE) decreases with the increase in the number of cell divisions and is also modelled by repressor Hill function as:

$$RE_{dist}(g + 1) = 1 - \frac{R_t^n(g)}{R_t^n(g) + \alpha^n} \quad (5)$$

The parameters  $n > 1$  and  $\alpha > 0$  can be set according to the  $R_t$  value; however, these parameters are the same as in the previous strategy (see Appendix 1). The variable  $R_t$  is the ratio between the time required for the intact component to reach division level ( $\tau_I$ ) and the time required for damage component to reach cell death ( $\tau_D$ ).

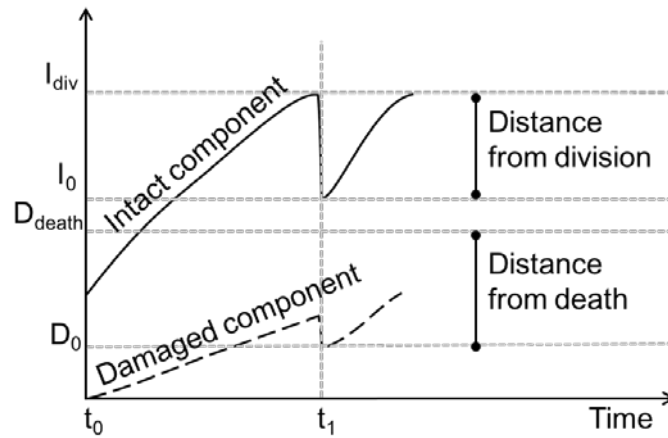
$$R_t = \frac{\tau_I}{\tau_D} \quad (6)$$

Due to the increase in damage during the replicative lifespan of a cell, the retention becomes more difficult. After every division cell anticipates the possibility of the next division. If the damage is high enough such that the next division is not possible then cell further decreases

its retention to the minimum level ( $RE_{\text{dist}} = 0$ ) as in the division strategy. The required times ( $\tau_I$  and  $\tau_D$ ) are calculated by taking the ratio between remaining distance and the mean rate of change in the corresponding intact ( $Avg(\dot{I})$ ) and damage ( $Avg(\dot{D})$ ) component.

$$\tau_I = \frac{I_{\text{div}} - I_g}{Avg(\dot{I})}, \tau_D = \frac{D_{\text{death}} - D_g}{Avg(\dot{D})} \quad (7)$$

In the distance strategy (Figure 2), cell composition is divided into two components which are increasing during their growth process. The increase in the damage component is represented by long-dashed lines (— —) that starts from zero and passes through  $D_0$  and intact component by continuous lines that starts from a minimum amount of intact proteins. At time  $t_1$ , the cell reaches the division threshold ( $I_{\text{div}}$ ) where it is ready to bud a daughter with asymmetric distribution of intact and damage component. After division, mother cell has intact component  $I_g$  and damage component  $D_g$ . At this point, the distance strategy comes into action. The parametric value of retention set by the strategy is used to anticipate the success in completing the next division by the above-defined procedure (see Eq. 5). If the next division is possible then the cell will divide according to the defined strategy. Otherwise, the cell will decrease the retention to its minimum value so that the next division becomes possible.



209

210 *Figure 2: Mother cell decreases damage retention by anticipating her next reproduction success. Cell increases its*  
 211 *initial intact and damage component from  $t_0$  and divides at time  $t_1$ . The intact component decreases from its*  
 212 *threshold  $I_{\text{div}}$  to  $I_{g=0}$  after division and the damaged component decreases to  $D_{g=0}$ . The cell death threshold is*  
 213 *represented by  $D_{\text{death}}$ .*

## 214 Altruistic Variation in the Efficiency of Damage Retention

215 The strategies provide a unique way of decreasing the efficiency of damage retention which  
216 can be varied by using an altruist factor ( $A$ ) as defined in Eq. (8). The parameter  $A$  is based on  
217 the consequences of the actions performed for the replicative lifespan of a mother cell and  
218 for the reproductive fitness of the offspring that is measured by determining their health  
219 status. The parameter  $A = 0.5$  is defined as a neutral value when it has no effect on the  
220 strategies of damage retention and therefore follows the asymmetric division as defined in  
221 Eqs. (4) and (5). For  $A < 0.5$ , cells show selfish behaviour to their progeny by retaining less  
222 damage than being neutral during their replicative lifespan, whereas for  $A > 0.5$ , cells show  
223 selfless behaviour by retaining more damage than the one defined in a neutral strategy. At  
224 the extreme values, the cells show either no retention ( $re = 0$ ) or full retention ( $re = 1$ ) during  
225 their replicative lifespan.

226 At the time of division, damage retention is set in two stages. Firstly,  $RE(g)$  is calculated by  
227 means of a defined strategy (distance or division strategy). Secondly, altruism parameter is  
228 used to alter the strategy. When no more divisions are possible, the retention decreases to  
229 zero allowing another division without taking the altruist effect into account. The equation for  
230 altruist retention is written as:

$$re(A, g) = RE(g) + 2 \left( A - \frac{1}{2} \right) ((1 - A)RE(g) + A(re_{max} - RE(g))) \quad (8)$$

231 The parameter  $re$  is the altruism-dependent efficiency of damage retention and  $re_{max}$  is the  
232 maximum attainable retention, i.e. 1.

## 233 Pedigree-tree model

234 Here we develop a pedigree-tree model to follow the complete population with variable  
235 retention parameter (Eq(1-3) and Appendix 1). The cellular growth is represented by an  
236 increase in the number of intact and damage components and the division is represented by  
237 the asymmetric distribution of growth components (intact and damage) between mother and  
238 daughter cells. The advantage of this model is that the cells are instantly counted when bud  
239 out from their mothers while their growth components are tracked throughout their

240 replicative lifespan. At the end of the simulation, the cells are distributed according to their  
 241 intact and damage components in a discrete manner. Moreover, the variable retention of a  
 242 single cell during its lifespan can be applied over the whole population in an appropriate  
 243 manner. Following this procedure leads us to find the population distribution function for  
 244 damage component and to investigate the differences between strategies by using cost  
 245 functions.

## 246 **Population distribution function for intact/damage component**

247 Each cell is born with a specific level of damage and intact components and grows accordingly  
 248 until it reaches the division threshold that leads to its asymmetric binary division. The division  
 249 leads to a new daughter cell which follows the same growth and division strategy as her  
 250 mother. During this process the population increases, generating cells with a diverse level of  
 251 intact/damage components. These components can be distributed over the whole population  
 252 at any time  $t = t_0$  and can be represented by a population distribution function  $P(A, D)$ .  
 253 Therefore, for each altruist value  $A$  and accumulated damage  $D$ , the population distribution  
 254 function for the damaged component is written as,

$$P(A, D) = \frac{\sum_{D=a}^{D=b} (N_{daugh}(A, D) + N_{mot}(A, D))}{N_{pop}(A)}. \quad (9)$$

255 where  $a$  and  $b$  are the minimum and maximum accumulated damage, respectively. The  
 256 functions  $N_{daugh}(A, D)$  and  $N_{mot}(A, D)$  represent the number of daughter and mother cells with  
 257  $D \in [0, D_{death}]$  amount of damage component at a given altruist value  $A$ . The population  
 258 distribution function is normalized by total population of alive cells  $N_{pop}(A) = \sum (N_{daugh}(A, D) +$   
 259  $N_{mot}(A, D))$ . The variation in  $N_{pop}$  due to altruism  $A$  is well-intended to ensure the total size of  
 260 the population at any time  $t = t_0$ . Similar kind of distribution functions can be defined for the  
 261 normalized population distribution of daughter cells,  $P_{daugh}(A, D)$ , and mother cells,  $P_{mot}(A, D)$   
 262 as follows:

$$P_{mot}(A, D) = \frac{\sum_{D=a}^{D=b} N_{mot}(A, D)}{\sum_D N_{mot}(A, D)},$$

$$P_{daugh}(A, D) = \frac{\sum_{D=a}^{D=b} N_{daugh}(A, D)}{\sum_D N_{daugh}(A, D)}. \quad (10)$$

## 263 Cost Functions

264 The calculation of cost function is performed at the end of the discrete-continuous model  
 265 while the objective is to find the minimum cost function so that smallest amount of damage  
 266 and a maximum number of cells exist in the population. The damaged component and the  
 267 total population is calculated for the virgin cells – the cells that have not undergone any  
 268 division yet, for the mother cells and for the whole population. These calculations are then  
 269 normalized, defined by  $\tilde{N}(X)$ , where  $X$  is any population distribution of either mother, daughter  
 270 or total cells with a given altruist value and damage  $D$ . This helps to eliminate the redundancy  
 271 between the cellular components and the population.  $\tilde{N}(X)$  can be defined as,

$$272 \quad \tilde{N}(X) = \frac{X - X_{min}}{X_{max} - X_{min}}$$

273 The normalization is carried out by finding the extreme values from the deterministic model  
 274 for the total damage in the cells and the total population. The extreme values for each cost  
 275 function exist at unique values of altruism  $A \in [0,1]$ .

276 Cost function at any given altruism value  $A$  in case of daughter cells is the sum of normalized  
 277 accumulated damage of all the daughter cells,  $\tilde{N}(\sum_{D_{daugh}} D_{daugh}(A))$ , and difference between  
 278 normalized maximum number of daughter cells during  $A \in [0,1]$ , i.e. equals to 1, and  
 279 normalized alive daughter cells,  $\tilde{N}(N_{daugh}(A, D))$ , present in the system at any time  $t = t_0$ .

$$C_{daugh}(A) = \tilde{N}\left(\sum_{D_{daugh}} D_{daugh}(A)\right) + \left(1 - \tilde{N}\left(\sum_D N_{daugh}(A, D)\right)\right) \quad (11)$$

280 The cost function for damage component in the mother cells at a given value of  $A$  is similar to  
 281 the cost function defined for damage component in the daughter cells. The only difference is  
 282 that we calculate damage in those cells that have been divided at least once. We write this  
 283 cost function as,

$$C_{mot}(A) = \tilde{N} \left( \sum_{D_{mot}} D_{mot}(A) \right) + \left( 1 - \tilde{N} \left( \sum_D N_{mot}(A, D) \right) \right) \quad (12)$$

284 Damage in a mother cell is denoted by  $D_{mot}$  and a total population of the mother cells is  $N_{mot}$ .  
 285 For the damage proportion in the total yeast population at a given altruism  $A$ ,  $N_{pop}(A)$ , the cost  
 286 function is the sum of the normalized damage in the total population,  $\tilde{N}(D_{pop})$ , and the  
 287 difference between the normalized maximum and the normalized current population sizes,  
 288 i.e.  $1 - \tilde{N}(N_{pop})$ . It is given by the following formula,

$$C_{pop}(A) = \tilde{N} \left( \sum_{D_{pop}} D_{pop}(A) \right) + \left( 1 - \tilde{N}(N_{pop}(A)) \right) \quad (1)$$

## 289 Variation in Altruism

290 Altruism parameter  $A$  is varied deterministically as well as stochastically. The deterministic  
 291 way is quite straightforward as it formulates the normalized distribution of cells at discrete  
 292 values of  $A$  and calculates cost functions for each value of  $A$  that varies in the interval  $[0,1]$ .  
 293 These cost functions are further used in the stochastic model to help find the minimum value  
 294 of cost function.

295 The stochastic settings involve individual-based modelling approach in which altruist  
 296 parameter  $A$  is randomly chosen from its neighbouring values. Small variations bring changes  
 297 in the strategy of damage retention and mimic the concept of mutation which directly affects  
 298 the cost function. The cost of following an individual's strategy of damage retention by its  
 299 progeny is deterministically calculated using Eqs. (11), (12) and (13) which involves simulation  
 300 of the pedigree-tree model for a specific period of time. The method allows the cell to follow  
 301 the direction where it finds minimum cost function. The direction of the altruist value is  
 302 chosen on the basis of current and preceding cost functions by using the signum function while  
 303 the magnitude of the variation is set by choosing a random value in the interval of  $[0, \varepsilon]$ .

$$A_{i+1} = A_i \pm \text{rand}(0, \varepsilon) \text{sgn}(C(A_{i-1}) - C(A_i)) \quad (14)$$

304 This process continues for a set period of time and is terminated by the following criteria,

$$\sum_{i=S_N+l}^{S_N+j+l} |A_{i-j} - A_{i-(j+k)}| < \varepsilon. \quad (15)$$

305 In the above equation, sign  $\pm$  are set according to the direction of altruist value and the index  
 306 of altruism  $A$  indicates the strategy variation number. The positive sign is used when the  
 307 direction of altruism is upward, i.e.  $A_{i-1} < A_i$ , whereas the negative sign is used in case altruism  
 308 is decreasing, i.e.  $A_{i-1} > A_i$ .

## 309 **Results:**

310 Initially, there is a single daughter yeast cell present in the system that has a sufficient amount  
 311 of intact proteins to grow and doesn't contain any damaged proteins. A general behaviour of  
 312 the model is described in Figure S1.

313 In the course of this work, we sought to establish a relationship between strategies followed  
 314 by distinct yeast strains and relationship among yeast strains following the same strategy. The  
 315 former is followed deterministically to find the reproduction success by using the given cost  
 316 functions whereas in the later the optimality is investigated by making stochastic variations in  
 317 the strategies.

## 318 **Relation Between Strategies**

319 Damage retention strategies follow a defined way to decrease the retention efficiency of a  
 320 mother cell. However, there are unique routes associated with each value of altruism that is  
 321 followed according to their intrinsic behaviour represented by Eqs. (4) and (5). The distance  
 322 strategy keeps the damage retention high and decreases the efficiency at an increasing rate  
 323 whereas the division strategy was defined in an opposite fashion by showing a sharp decrease  
 324 during the early replicative lifespan of a mother cell.

325 The strategies are defined using Hill function in the equations (4) and (5) with  $\alpha = 1$  (Figure  
 326 3). A comparison between the symmetric and asymmetric cell divisions has been performed  
 327 to observe the effect of strategies over the number of divisions while choosing different sizes  
 328 of the cells. The variations in the strategies are given by altruist parameter  $A$  with  $A_{max} = 1$ . It  
 329 is interesting to note that both strategies provide the same behaviour at the endpoints of  $A$ ,  
 330 i.e. 0 and 1 (Figure 3).

331

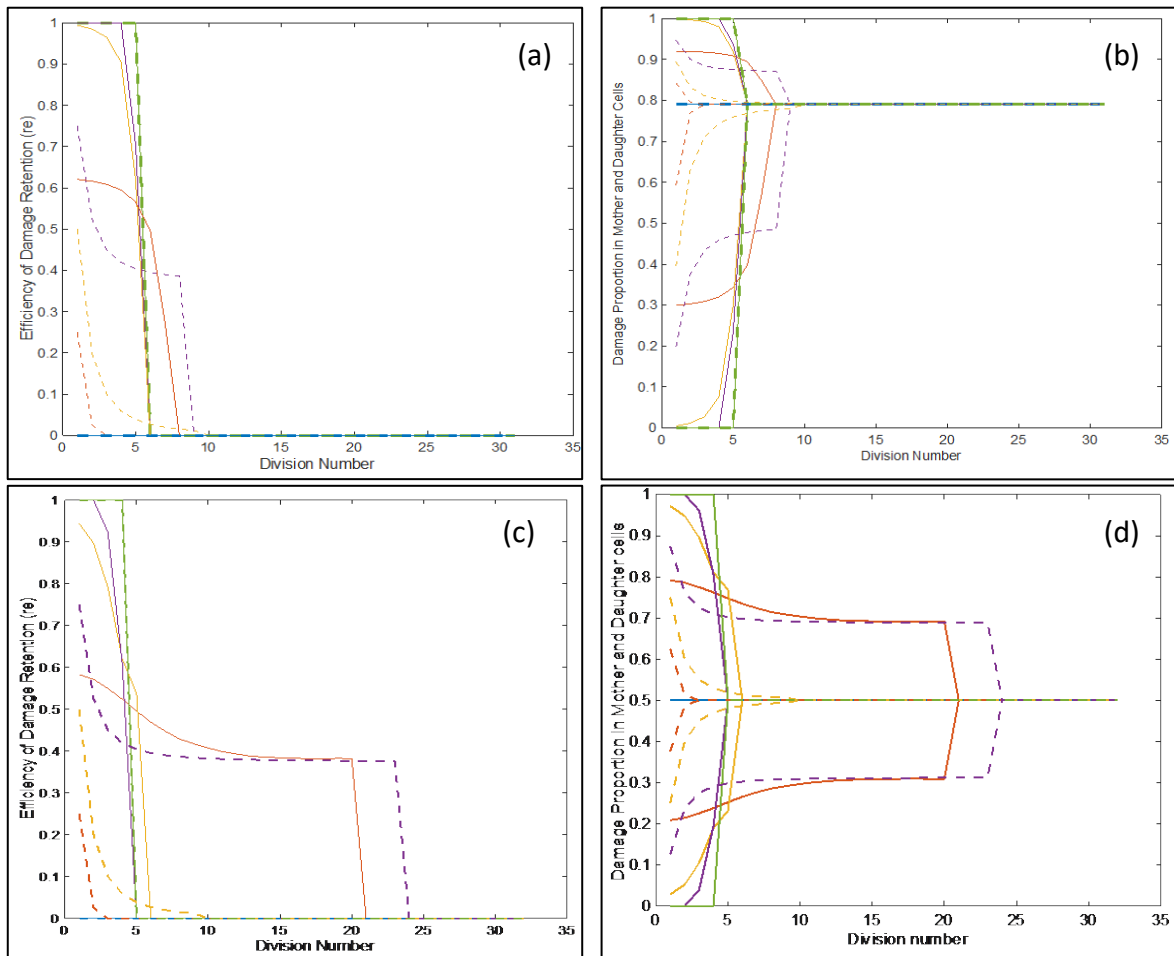


Figure 3: Damage retention efficiency ( $RE$ ) for altruist parameter values  $A = 0$  (blue), 0.25 (red), 0.5 (yellow), 0.75 (violet) and 1 (green). The dashed lines represent division strategy and continuous lines represent distance strategy. Colours are drawn to match the altruist parameter values between the two strategies. Left hand side panels (a) and (c) shows the damage retention by mother cell while the right-hand side panels (b) and (d) are obtained by relating size-wise damage distribution among mother and daughter cells. The cell sizes after division of cells are chosen asymmetric ( $R_m = 0.79$ ) for panel (a) and (b) and symmetric ( $R_m = 0.5$ ) for panel (c) and (d).



At  $A = 0$ , yeast cell does not retain any damaged portion ( $re(0, g) = 0$ ) during its replicative lifespan and therefore share damage with her daughter according to the division size of the cell  $R_m$ . Consequently, yeast survives for a longer replicative time and buds off 31 daughters when  $R_m = 0.5$  and 32 daughters when  $R_m = 0.79$  (Figure 3). On the other hand, at  $A = 1$ , yeast cell retains all the damage ( $re(1, g) = 1$ ) and buds a completely healthy daughter cell each time which affects its lifespan and brings it to 5 divisions. For all the other altruist values, i.e.  $0 < A < 1$ ,  $A$  does not provide the same retention function for both strategies. It can be observed that cell with division strategy retains less damage than distance strategy; however, the former retains damage for a longer period of time during its lifespan. After the critical damage level when no more retention possible, the cell loses all the retention and share the damage according to the cell sizes.

### **Population Distribution of Damaged Proteins**

The pedigree-tree model provides a large population of cells where intact and damage components are individually tracked throughout their replicative lifespan. This provides a non-uniform distribution of alive cells over damaged components. Therefore, the cell population is clustered according to the accumulated damage in each cell (with cluster size of 60 and number of clusters of 10 in the interval  $[0, 600]$ ) for five values of altruism  $A = 0, 0.25, 0.5, 0.75$  and  $1$  (Figure 4, Figure 5 and Figure 6). The maximum attainable damage is bounded by the threshold  $D_{\text{death}} = 600$ ; however, the figures show that the cell could have accumulated damage at most in the interval  $[480, 540]$ . These clustered populations are normalized in order to calculate the proportion of cells with respect to the total population. Moreover, the error bars are drawn to find the mean and standard deviation of the proportion of cells attaining specific proportion of accumulated damage at the four simulation times  $t = 1.5, 1.75, 2$  and  $2.25$ .

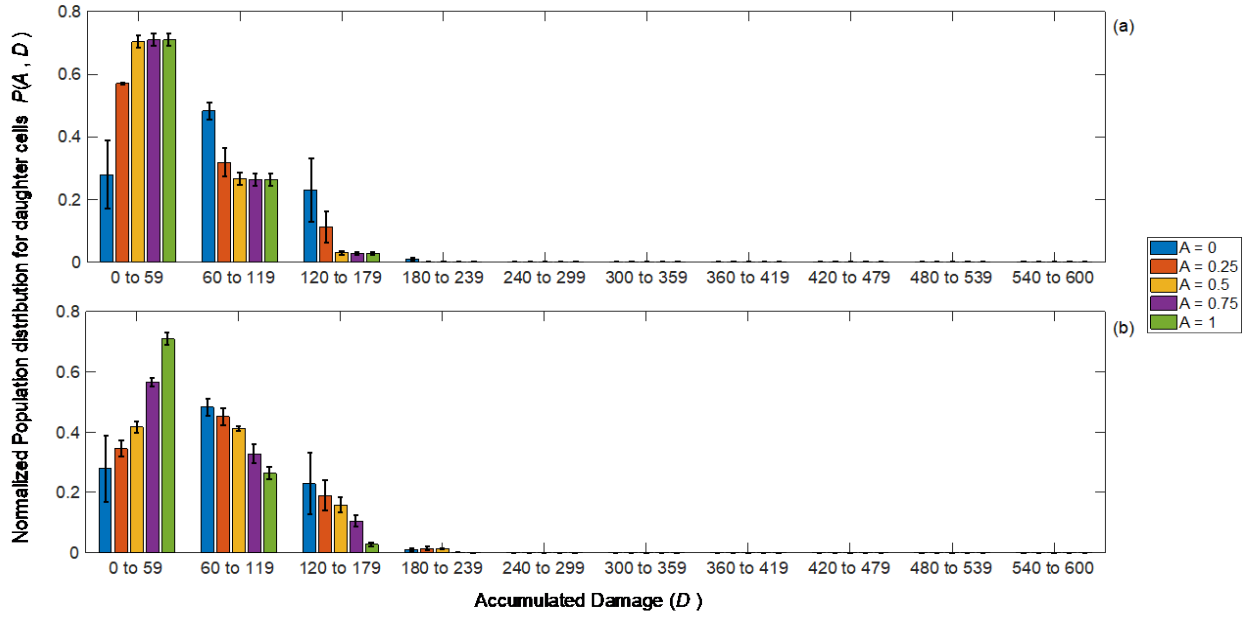


Figure 4: Mean and standard deviation of the daughter distribution of damaged proteins by using distance (a) and division (b) strategies, see Eq. (11). Mean of the distribution is taken for the simulation time  $t = 1.5, 1.75, 2, 2.25$ . The accumulated damage in the span of 600 is clustered into subintervals each of length 60.

The population distribution of daughter cells is present only in the first three clusters of damage component (Figure 4). In the first cluster,  $D_{\text{daugh}} \in [0, 59]$ , the mean proportion of cells,  $P(A, D)$ , increases when altruism  $A$  goes from 0 to 1 while the succeeding clusters show a reverse behaviour. The error bars represent the standard deviation of the mean distribution values for simulation time  $t = 1.5, 1.75, 2, 2.25$ . For  $A = 0$ , the standard deviation is quite high because the cell proportion was higher in the first and third clusters ( $P(A = 0, D = [0, 60]) \approx 0.38$ ) during the early simulation time,  $t = 1.5$ . However, it decreased to below 0.2 in the later simulation time,  $t = 2.25$ . Moreover, for  $A \geq 0.5$ , the proportion of cells with least damage is much high and have a very small standard deviation.

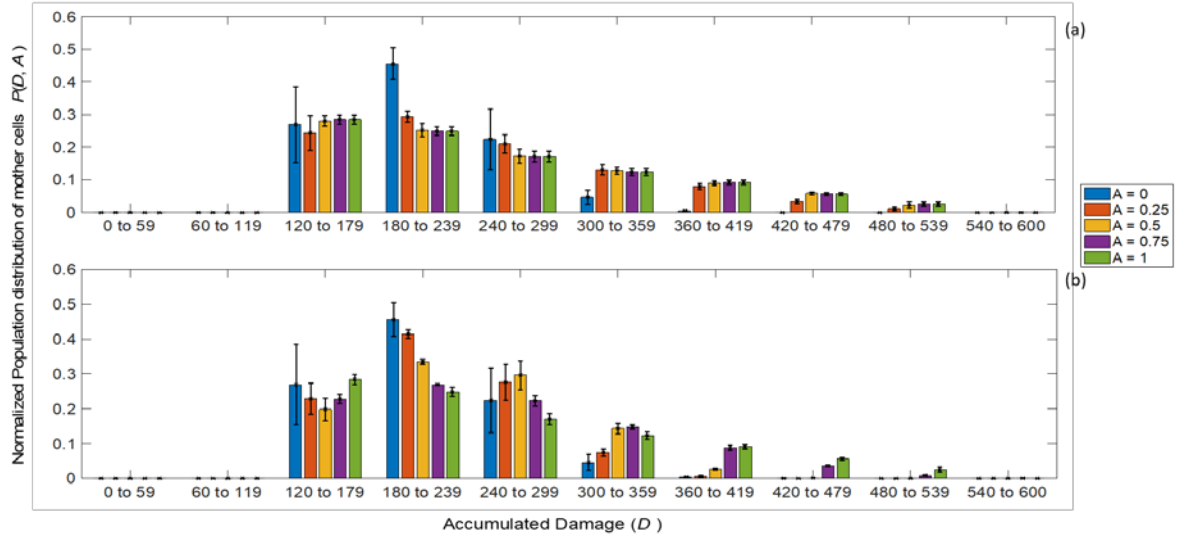


Figure 5: Mean and standard deviation of the mother distribution of damaged proteins by using distance (a) and division (b) strategies, see Eq. (10). Mean of the distribution is taken for the simulation time  $t = 1.5, 1.75, 2, 2.25$ . The accumulated damage in the span of 600 is clustered into subintervals each of length 60.

The number of daughter cells gradually increases in the first cluster of accumulated damage as  $A$  goes from 0 to 1 however it shows opposite behaviour in the second and third cluster (Figure 4b). It can be observed that the mean proportion of daughter cells following the distance strategy is higher than the mean proportion following the division strategy in the first cluster for all values of  $A$ , except the extreme values where both strategies provide the same result. However, the behaviour is opposite in the next two clusters. This suggests that the distance strategy, i.e. keeping the retention high in the early divisions, accumulates less damage in the population.

Mother cells distribution for damaged component is also normalized and its mean and standard deviation is calculated for the given simulation times  $t = 1.5, 1.75, 2$  and  $2.25$  and altruism values  $A = (0, 0.25, 0.5, 0.75, 1)$  and accumulated damage component in mother cells is shown in the third and succeeding clusters (Figure 5). This means that cells become a mother in the third cluster of damage accumulation however the highest proportion of cells are present in the fourth cluster where damage is in the interval  $[180, 240)$ . The standard deviation of the mean proportion of mother cells is similar to the mean proportion of daughter cells and therefore cellular health becomes better as  $A$  goes from 0 to 1. In comparison between the two strategies, the mothers following the distance strategy have higher damage than mothers

following division strategy. In addition, the mean proportion of mother cells containing high damage is comparatively lower than the ones containing the low damage.

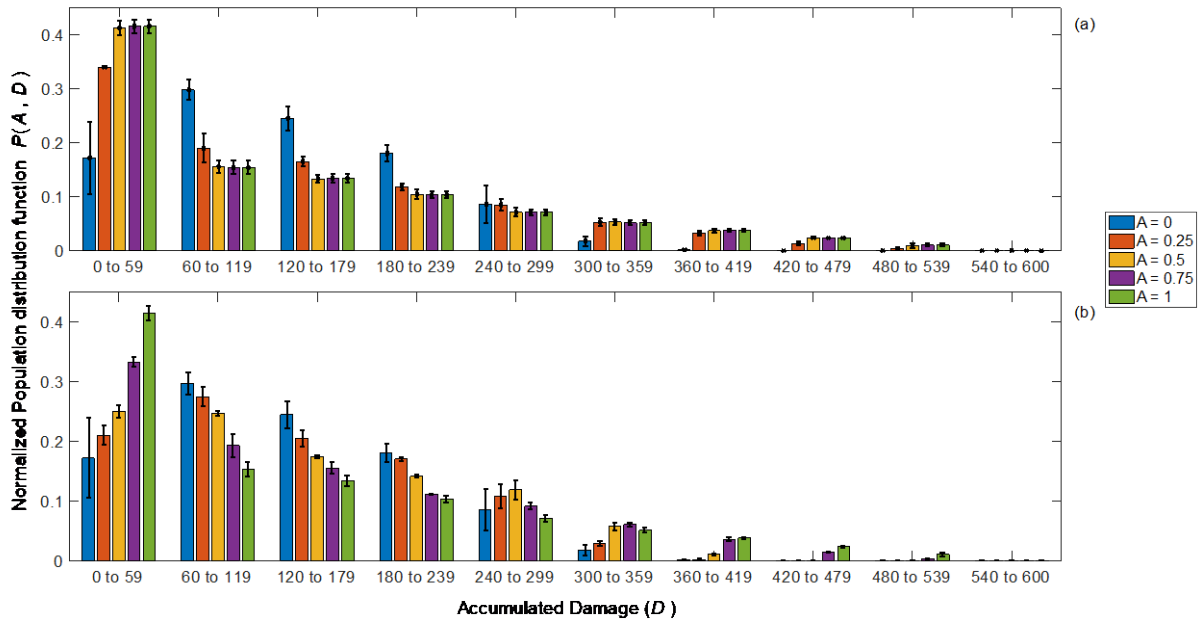


Figure 6: Mean and standard deviation of the normalized population distribution of damaged proteins by using (a) distance and (b) division strategies as defined in Eq. (9). Mean of the distribution is taken for the simulation time  $t = 1.5, 1.75, 2, 2.25$ . The accumulated damage in the span of 600 is clustered into subintervals each of length 60.

Mean and standard deviation of the normalized distribution of cells over the accumulated damage in alive cells show the behaviour similar to the above distributions at different values of  $A$ , however, there is a significant decline in the proportion of healthy cells, i.e. first cluster (Figure 6). At  $A = 0$ , the standard deviation gives comparatively high values. This is due to the fact that premier cells do not have enough damage to share with their daughter cells for short time scale ( $t = 1.5$ ) and therefore most of the daughter cells born with damage are grouped in clusters 1 and 2. Moreover, the proportion of cells is significantly decreased to below 0.2 when time duration is increased to  $t = 2.25$ .

### Optimal Reproduction success

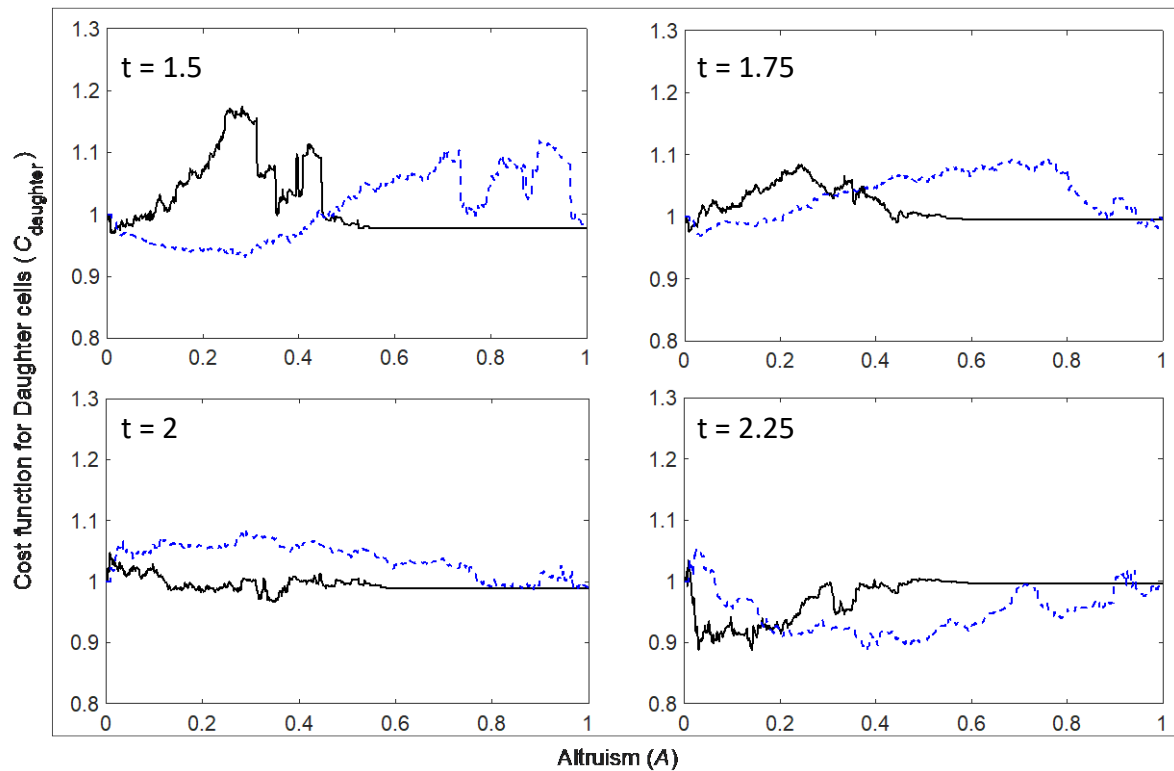
Models are simulated in deterministic as well as stochastic settings to find the cost functions. These cost functions represent reproduction success by taking into account the cellular health status and population size. The deterministic model provides a cost for predefined values of

411 altruism  $A$  whereas the stochastic model tracks the minimum value for cost function by taking  
412 random steps towards the lowest value of the cost function.

### 413 Deterministic outcomes

414 The deterministic modelling approach is used to evaluate the cost functions by varying the  
415 altruist parameter  $A$  between 0 and 1 with the step size  $\Delta A = 10^{-3}$ . The results are obtained for  
416 the cost functions defined in Eqs. (11), (12) and (13) and are presented in Figure 7 (for  
417 daughter cells), in Figure 8 (for mother cells) and in Figure 9 (for a total number of alive cells)  
418 respectively each at four different times  $t = 1.5, 1.75, 2$  and  $2.25$ . Computationally, it becomes  
419 very expensive to go beyond the time point  $t = 2.25$ . Therefore, this is the maximum time point  
420 chosen. Other time points are chosen to understand the behaviour of cost function over the  
421 altruism parameter  $A$ . The cost function is modelled by taking this fact into consideration that  
422 the replicative lifespan decreases with the increase in damage retention by the cell. In such a  
423 scenario, it would be interesting to see the effect of replicative lifespan over the damage  
424 accumulation in the population.

425 Altruistic effects on the daughter cells provide a time-variant response to its cost function.  
426 Due to asymmetric division, mother cells require less time to reproduce than the daughter  
427 cells. Therefore, the longer lifespan of mother cells will quickly increase the population;  
428 however, in case of low damage retention, high amount of damage is passed on to the newly  
429 born daughter cells. In case of distance strategy, this phenomenon quickly increases the  
430 damage in the population and raises the cost function to a high level during the early time, i.e.  
431  $t = 1.5$  and  $1.75$  (Figure 7, Figure 8 and Figure 9). However, with the progression of time, i.e.  $t$   
432 goes to  $2$  and  $2.25$ , the cost function gives a surprising outcome by replacing the high values  
433 with the lower ones, exposing that for large time scale, population size can dominate over the  
434 total damage present in the population. For instance, the distance strategy (continuous lines)  
435 near  $A = 0.3$ , the cost function that was at maximum, i.e.  $C_{\text{daugh}} = 1.2$  at time  $t = 1.5$ , goes below  
436 the value of  $C_{\text{daugh}} = 1$  at time  $t = 2.25$ .



438 Figure 7: Cost function for the distance (continuous lines) and division (dashed lines) strategies of  
 439 daughter cells  $C_{Daugh}$  at four time-points  $t = 1.5, 1.75, 2$  and  $2.25$  against the altruist values  $A$  in the  
 440 interval  $[0,1]$  and step size  $0.001$ . The cost function is defined in Eq. (11) while the deterministic model  
 441 used to simulate the results is described in Appendix 1.

442 Division strategy provides the opposite response than the distance strategy during the early  
 443 simulation time by showing a small decrease in the payoff function for early altruism values.  
 444 The reason is clearly that the proportion of cells in the population decreases slightly slower  
 445 than the increase in the proportion of damage accumulation (Figure S2). For a longer period  
 446 of time,  $t = 2.25$ , both strategies decrease their cost function for early values of  $A$ , however,  
 447 their optimal reproduction success varies.

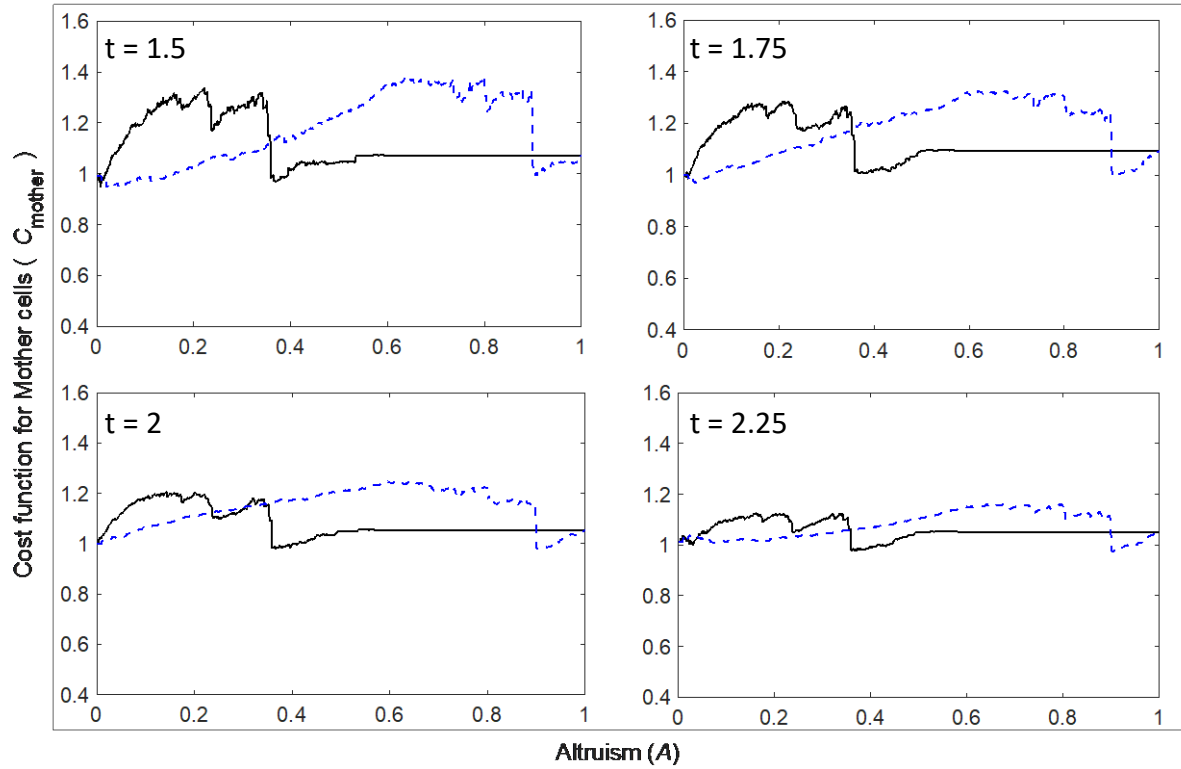


Figure 8: Cost function for the distance (continuous lines) and division (dashed lines) strategies of mother cells  $C_{\text{Mot}}$  at four time-points  $t = 1.5, 1.75, 2$  and  $2.25$  against the altruist values  $A$  in the interval  $[0,1]$  and step size  $0.001$ .

Taking the final time into consideration, the results provide several interesting outcomes regarding the least value for the cost function, i.e. the optimal reproduction success. Firstly, the optimal reproduction success for both strategies requires selfish behaviour of mother cells when altruism parameter  $A < 0.5$ . However, a complete selfish behaviour is not a good strategy which may increase the damage in the population. It is important to note that the cost function varies significantly from one simulation time to the next one, e.g.  $t = 2$  to  $2.25$  which means that the cost function is not in an equilibrium state. Conversely, it is interesting to note that the cost function is squeezing around  $C_{\text{Daugh/Mot/Tot}} = 1$  by reducing the drastic changes. These drastic changes cause fluctuations in the cost function whose local minimum is termed as “evolutionary ditch”. These ditches may not provide the least cost function; however, it becomes difficult to come out from such ditches since these are surrounded by high values of cost functions.

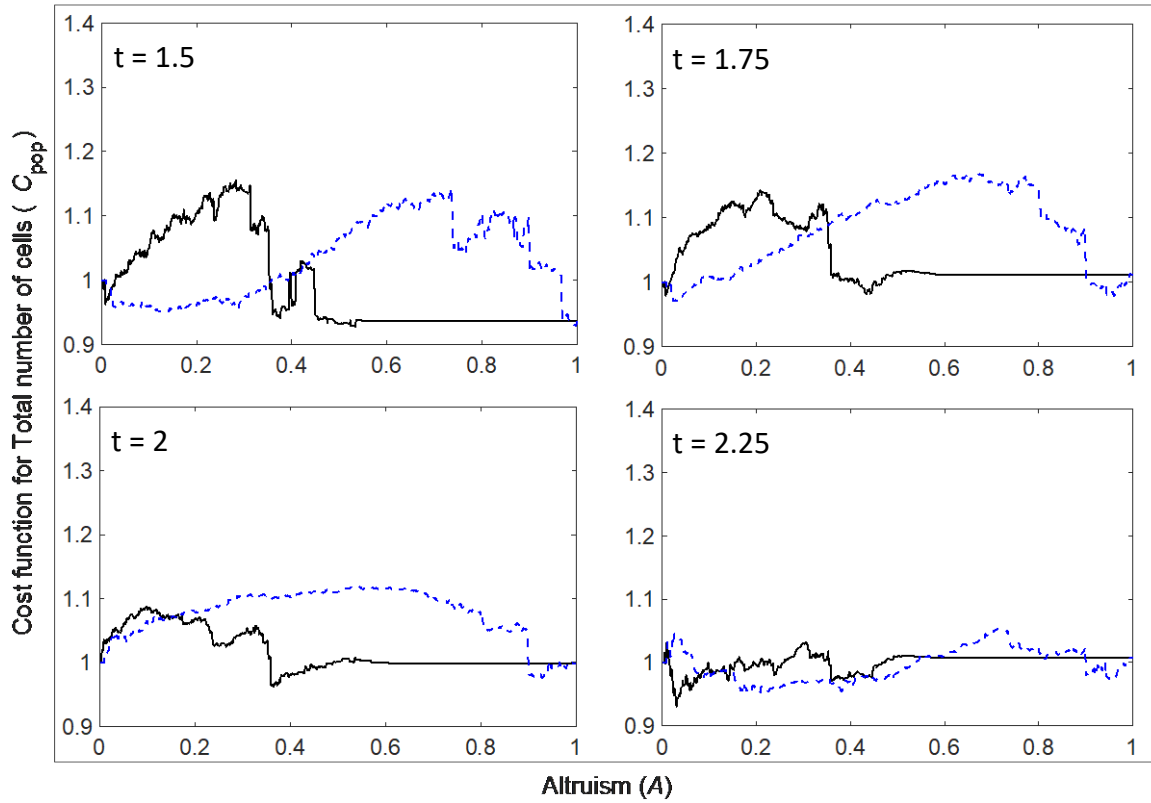


Figure 9: Cost function for the distance (continuous lines) and division (dashed lines) strategies of total cells  $C_{pop}$  at four time-points  $t = 1.5, 1.75, 2$  and  $2.25$  against the altruist values  $A$  in the interval  $[0,1]$  and step size  $0.001$ .

#### Stochastic Simulations

Stochastic settings are implemented to observe the behaviour of the cost function for total cells calculated at the simulation time  $t = 1.5$ . The strategies starting points are chosen for altruist values  $A$  between  $0$  and  $1$  with a step size of  $0.1$  (Figure 10). At each altruist value, cost functions are calculated which are then compared to their previous values. The strategies vary in the direction where small values of cost function are found by using Eq. (14). However, the least value is not predefined in the stochastic settings and therefore the simulation continues even after reaching the least cost function. The cost function is very sensitive in the sense that a small variation in altruist parameter can vary the yeast efficiency of retaining damage which may result in the decrease/increase in the yeast cell population and damage accumulation in the population. This fallouts fluctuation in the cost function which sets the direction by varying altruism values as shown in Figure 10. In the simulations, an important aspect to analyse is that most of the fluctuations occurred at some specific altruism values. The stopping criteria



481 is implemented after 1000 variations, strategy variation number ( $S_N$ ) = 1000, by the following  
482 inequality

$$\sum_{i=S_N+l}^{S_N+j+l} |A_{i-j} - A_{i-(j+k)}| < \varepsilon \quad (15)$$

483 The index values are  $j = k = 10$  and the epsilon  $\varepsilon = 0.02$ . The parameter epsilon provides the  
484 maximum possible variation in the altruism value and is used in the Eq. (14). The stopping  
485 criteria are defined by the summation expression that stops the simulation if the  $\varepsilon$  condition  
486 is fulfilled consecutively for five values of index  $l$ .

487 The altruist effects on distance strategy (Figure 10a), have revealed clear differences between  
488 the values of  $A$  chosen above and below the neutral one, i.e. 0.5. For a yeast population  
489 following its strategy with altruism  $A \geq 0.5$ , the cost function decreases as  $A$  increases and  
490 eventually,  $A$  reaches to the maximum value. On the other hand, when  $A < 0.5$ , the strategy  
491 varies most of the time around the values  $A = 0$  and 0.4 that are surrounded by evolutionary  
492 ditches. Since strategies are tuned to keep varying  $A$  in the direction where least value of cost  
493 function (minimum of the cost function) is found, therefore, the sensitivity in cost function  
494 against the altruist values allows cells to alter their strategy which creates a safe escape from  
495 the evolutionary ditch. In a similar way, these strategies escape from the least values of the  
496 cost function. Such escapes are made possible due to the involvement of randomness in the  
497 altruism.

498 The division strategy also shows similar behaviour as distance strategy however the strategy  
499 is more frequently observed around the extreme values of altruism, i.e.  $A = 0, 0.1, 0.9$  and 1  
500 (Figure 10b). The simulations show that strategy started around  $A \leq 0.4$  could not escape from  
501 the local minimum of the cost function while the starting value of  $A$  above 0.8 eventually  
502 reached to their evolutionary ditch.

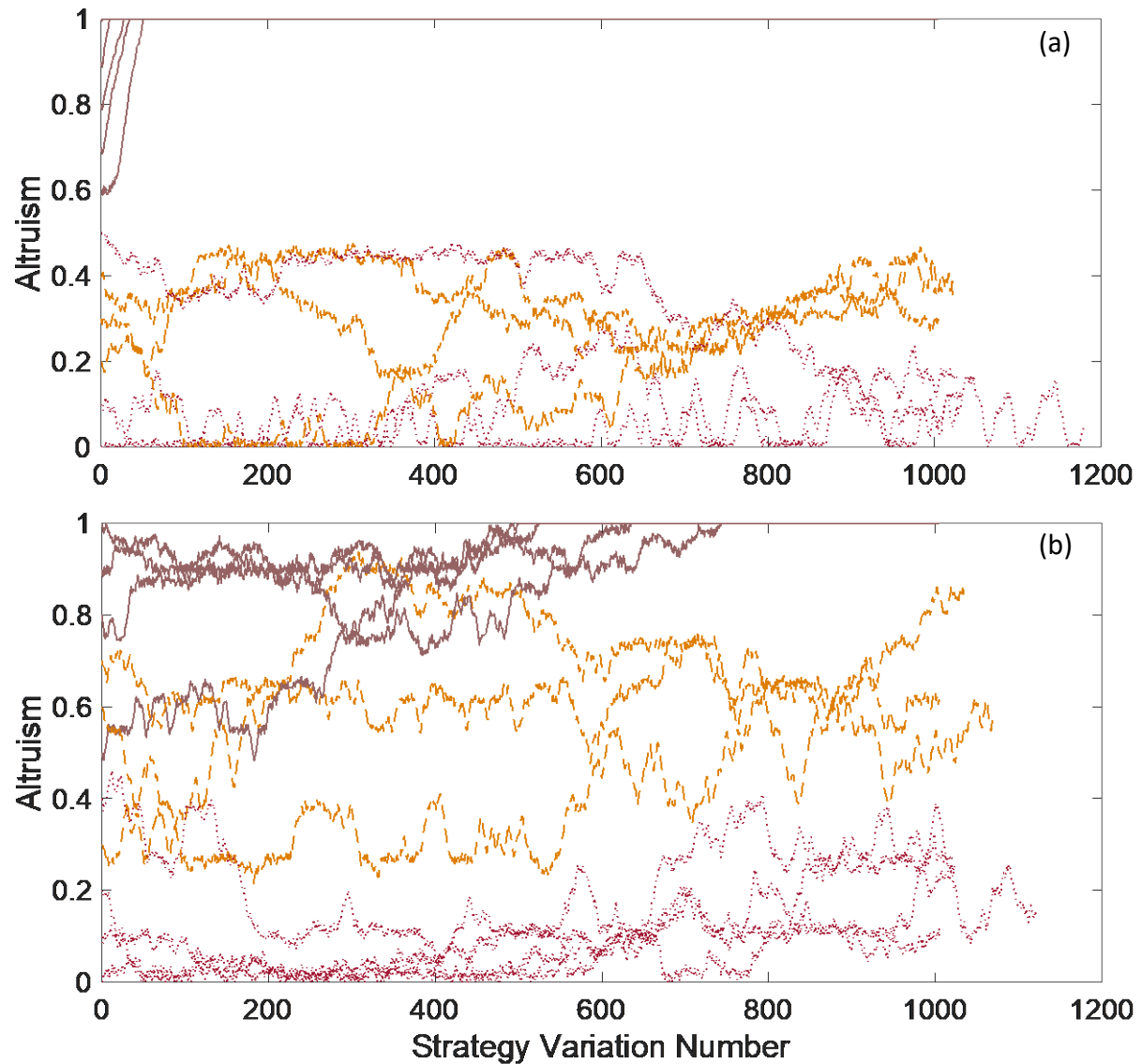


Figure 10: Stochastic simulations of (a) distance and (b) division strategies at time  $t = 1.5$ . The altruism parameter  $A$  is varied randomly for each strategy variation number in the interval  $[0, \varepsilon = 0.02]$ . The lines styles are used to clear up the tracking of each simulation.

## Conclusions

The efficiency of damage retention provides a monotonically decreasing function in which a mother cell retains lower amounts of damage in each subsequent division. The defined strategies have provided unique ways for decreasing the efficiency during cell replicative lifespan of a budding yeast while the altruism factor was used to make deviations in the strategy. For each deviation, a well-defined cost function is computed. Deterministic settings were adopted to analyse the behaviour of cost functions for each strategy. It has also provided the extreme values of the cost function which were further used under the stochastic settings. The cost functions were varied by means of random altruistic effects given to the strategies.

These variations were tuned to find the optimal reproduction success of the population. However, the strategies that started at different altruist values, ended up optimizing in a local fashion rather than approaching a global minima of the cost function.

### **Distance vs Division Strategy**

Our results show that retaining more damage, in the beginning, provides healthy daughter cells which plays a significant role in maintaining the accumulated health of the population. Moreover, the daughters born with high damage did not replicate as often as daughters born with low damage. In the case of division strategy, the mother cell shared more damage in the early divisions, leading to the poor health of progeny. At the later stage of replication, when the damage efficiency is low, the mother cell shared a high level of damage with its daughter cells. Consequently, these daughter cells could not provide healthy progeny to the population.

### **Altruism Provides Healthy but a Small Population**

Increase in the altruist values increases the efficiency of damage retention of the mother cell. A complete altruist behaviour allows a mother cell to retain all the damage at the time of division which reduces its replicative lifespan while giving birth to completely healthy daughter cells (Figure 3). In the case of whole pedigree, the same phenomenon is followed (Figures S1). When both factors, health and population size are considered (Figures 7 – 9), the cost functions of each strategy provided different global minima, while the distance strategy provides lower cost than the division strategy. This shows that a yeast following division strategy can never achieve a better health and population status than a yeast following a distance strategy.

Population size and population health have shown reverse behaviours. Increasing population size affects the health of the population and brings more damage to the cells while a better health keeps the population size small. In addition, yeast cells with altruistic behaviour do not give a boost to the population health as compared to selfish yeasts who although increase the damage but doubles the size of the population. Providing good health to new buds significantly increases damage in the mother cells which results in an early senescence state where no more replications are possible (Aguilaniu et al., 2003; Denoth Lippuner et al., 2014;

543 Jazwinski and Wawryn, 2001; Liu et al., 2011; Spokoini et al., 2012). On the other hand, selfish  
544 behaviour allows a long replicative lifespan.

### 545 **Optimal Reproduction Success represents Local Minima of Cost Function**

546 Strategies were adopted for the continuous search for the minimal value of the cost function.  
547 Since the function values could not be anticipated in the stochastic simulations, the altruist  
548 value varied continuously to search for it. Therefore, the cost function never converged to any  
549 specific value. This interprets the physical phenomenon where mutations in a yeast strain  
550 could vary the strategy that is followed by its progeny. It is observed that when yeast varied  
551 its state from the minima of the cost function, the subsequent mutations could not reverse  
552 mutation due to stochastic effects and therefore the trait is able to reach local minima of the  
553 cost function. Thus, the optimal reproduction success would never be able to show stable  
554 behaviour near the minima of the cost function. At the same time, when cells opted for a  
555 minimum value of cost function, the optimal reproduction success trapped for a long period  
556 of time to local minima which were surrounded by high cost functions.

### 557 **Evolutionary Ditches can make a Trait Maladaptive**

558 Evolutionary ditches became evolutionary traps in certain cases when the yeast species were  
559 unable to escape from local minima because the cost function is surrounded by higher values.  
560 With distance strategy, the cost function at  $A = 1$  is lower than  $0.5 < A < 1$ , however it is  
561 sufficiently higher than the minimum value of cost function (Figures 7 – 9). Consequently, in  
562 the stochastic simulation, the cells with  $A > 0.5$ , have rapidly adapted complete altruist  
563 behaviour,  $A = 1$ , and couldn't manage to escape from there. This behaviour showed sufficient  
564 potential in the yeast strategy to follow an extinction, especially when it is competing against  
565 the other species with lower values of the cost function. In summary, our results suggest that  
566 damage retention during the early divisions (distance strategy) increases the number of  
567 healthy daughters in the yeast population. In addition, a rapid decrease in the efficiency of  
568 damage retention, at the time when the mother cell is almost exhausted, produces fewer  
569 daughters with a very high amount of damage. Next, the two proposed strategies have distinct  
570 cost functions, implying that a strategy may not attain the same minima of cost function as  
571 the other. The minimum value attained by distance strategy has provided the minimal value

572 of cost function. And finally, fluctuations in the cost function allow yeast cell to continuously  
573 vary its strategy, suggesting that optimal reproduction success is a local minimum of the cost  
574 function.

575 Acknowledgement

576 This work was supported by the Swedish Foundation for Strategic Research.

577

## 578 **Appendix 1**

### 579 **A mathematical model for yeast cell growth and division processes**

580 The replicative lifespan of a yeast cell is comprised of two major processes: cellular growth in  
581 which the intact and damage components of a cell increase, and cell asymmetric division in  
582 which cell buds out a new daughter cell. A pedigree-tree modelling approach is used so that  
583 the cellular processes can be tracked for each cell individually. A similar modelling approach  
584 has been used in the literature where the retention parameter was kept constant (Erjavec et  
585 al., 2008), however, it followed the fate of the progenitor and the progeny, separately,  
586 through a number of generations. We could thus draw a “mother lineage” and a “daughter  
587 lineage”, whereby we would, after every division, follow respectively the next generation of  
588 mothers only, or the next generations of daughters only. However, these do not represent a  
589 realistic population that consists of intermediated branches as well. Thus, in the model  
590 presented here, we simulate the realistic population, including all intermediated branches and  
591 mixed-linages.

592 During the growth process, the number of healthy protein (intact protein) molecules increases  
593 in the cell at the rate constant  $k_1$  and dissolves into the system due to half-life phenomenon  
594 at the rate equals to  $k_2$ . At the rate,  $k_3$  damage proteins are formed. The degradation rate for  
595 damaged molecules is denoted by  $k_4$ . The modelled equations can, therefore, be written as,

$$\begin{aligned} \dot{I} &= k_1 \left( 1 - \frac{I + D}{K} \right) - k_2 I - k_3 I \\ \dot{D} &= k_3 I - k_4 D \end{aligned} \quad \text{Eq. 1}$$

596 The increase in the number of damaged proteins  $D$  becomes lethal if the cell reaches death  
597 threshold value  $D = D^*$  whereas the intact component  $I$  increases inside the cell to division  
598 threshold  $I = I^*$ . If the cell reaches division threshold first, the cell divides and produces a  
599 daughter cell with a mother to daughter cell size ratio  $R_m : 1 - R_m$ . During the early cell  
600 divisions, the mother cell retains maximum damage while its retention efficiency decreases in  
601 the later divisions until it reaches the minimum value  $re(g)=0$ , i.e. no retention.

602

Parameter	Description	Values	Assumptions and source
$I^*$	cell division threshold, in the number of intact proteins	1500	amount of intact proteins (Erjavec et al., 2008)
$D^*$	cell death threshold, in number of damaged proteins	600	
$k_1$	rate maximal protein production	$1.5 \times 10^4$	adjusted by hand to allow steady-state (Erjavec et al., 2008)
$k_2$	the rate of degradation of intact proteins	$\ln 2$	the half-life of 1 time unit (Erjavec et al., 2008)
$k_3$	rate of damaging of intact proteins	[0.1,2.3] by 0.75	(Erjavec et al., 2008)
$k_4$	the rate of degradation of damaged proteins	$\ln 2$	the half-life of 1 time unit (Erjavec et al., 2008)
$K$	carrying capacity	2500	adjusted by hand
$re$	retention coefficient	[0, 1] by 0.125	(Erjavec et al., 2008)
$R_m$	size of the progenitor after division	0.79	$R_m + R_d = 1$ (Erjavec et al., 2008)
$R_d$	size of the progeny after division	0.21	$R_m + R_d = 1$ (Erjavec et al., 2008)

Table 1: **Model parameters with default values and assumptions made**

606 The division process is modelled as a discrete set of equations for mother and daughter cells.

607 For the mother cell, the intact and damage portions can be calculated as:

$$\begin{aligned} I_{in}(g+1) &= I_{end}(g) \cdot R_m - D_{end}(g) \cdot R_d \cdot re(g) \\ D_{in}(g+1) &= D_{end}(g) \cdot R_m + D_{end}(g) \cdot R_d \cdot re(g) \end{aligned} \quad \text{Eq. 2}$$

608 The intact and damage portions for daughter cells have the similar equations

$$\begin{aligned} I_{in}(g+1) &= I_{end}(g) \cdot R_d + D_{end}(g) \cdot R_d \cdot re(g) \\ D_{in}(g+1) &= D_{end}(g) \cdot R_d - D_{end}(g) \cdot R_d \cdot re(g) \end{aligned} \quad \text{Eq. 3}$$

609 where the parameter  $R_d = 1 - R_m$  size of the daughter cell after division and  $g$  is division  
610 number. The index terms *in* and *end* are the initial value after division and end value before  
611 division respectively. The equations 2 and 3 are based on the principle of mass conservation  
612 over generations (Erjavec et al., 2008). In particular, this means that the total cellular content  
613 ( $I+D$ ), in the original cell equal the sum of the total cellular content of the mother and daughter  
614 cell. The conditions are also based on mass conservation with respect to intact component  $I$   
615 and damage  $D$ .

## 616 The general behaviour of Model

617 The processes described in the above model involving cell growth and division are simulated  
618 in the Figure S1. The figure describes a general behaviour of the modelled system without  
619 including the strategies and their altruist behaviour. Three parameters are investigated at  
620 different values to understand their effect on the overall dynamics of the modelled system.  
621 We observe that cell undergoes more divisions with the decrease in the values of  $k_3$ ,  $R_m$  and  
622  $re$ . In the case of finite replications, cell generally takes more time in the later divisions to grow  
623 and reach the division threshold. On the other hand, increasing the cell size ratio from mother  
624 to daughter cells ( $R_m$ ) decreases the time to the next division. Damage retention also plays an  
625 important role in the replicative lifespan of a cell. However, this parameter is chosen constant  
626 here for the sake of simplicity. It is interesting to observe that a total number of divisions  
627 drastically decreases with the increase in retention parameter. We study the retention  
628 parameter as a variable, dependent upon a number of divisions of the mother cell.

629

630

631

632

633



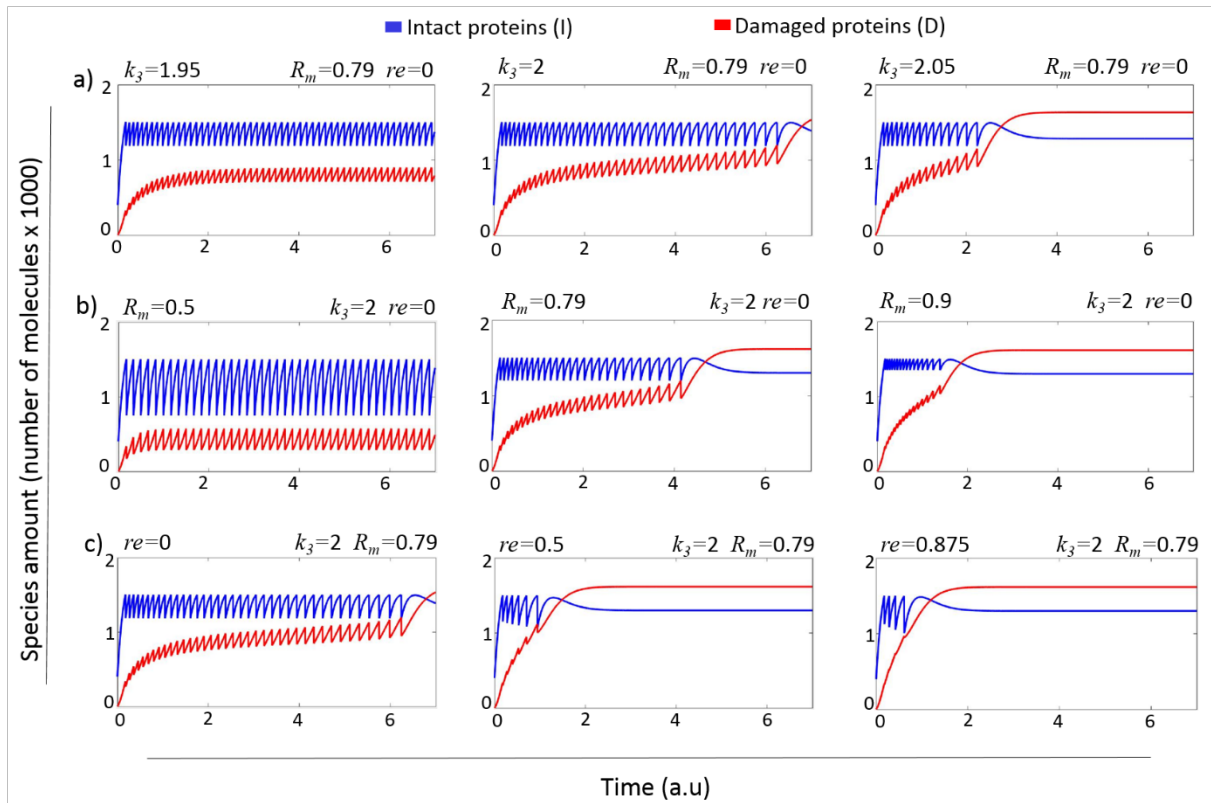


Figure S1: Intracellular species dynamics of a single cell a) damage accumulation rates b) size of the mother and c) retention coefficients. Red and blue lines describe the dynamics of damaged and intact cellular components, respectively.  $re(g) = Re$  (a constant).

## Pedigree-Tree Diagram

Pedigree-tree model follows the growth and division process of each individual cell. The process starts with a single cell that grows its intact and damaged component. At the growth threshold, cell buds its first daughter cell. At this time point, the budding cell is considered as a mother while the budded cell is considered as a daughter cell. Now, mother cell and daughter cell both undergo the growth process to reach the division threshold, see Figure S2. Hence cell population increases while each cell is tracked during its replicative lifespan or until the simulation ends. The population is discretely distributed over the total intact and damage portions of each cell as described in the main text.

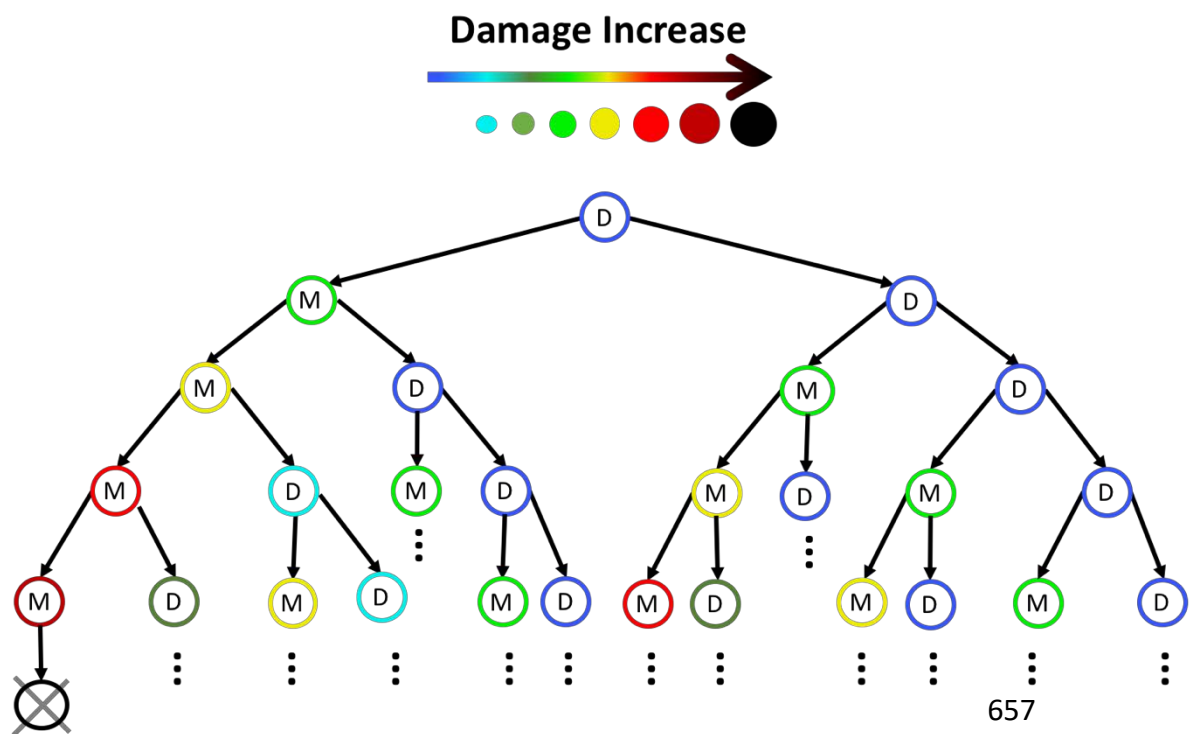


Figure S2: Schematic representation of pedigree-tree model. Each circle represents a cell. D stands for daughter whereas M stands for mother. Blue color is damage free cells while black color is for dead cells (no more divisions possible).

Appendix 2

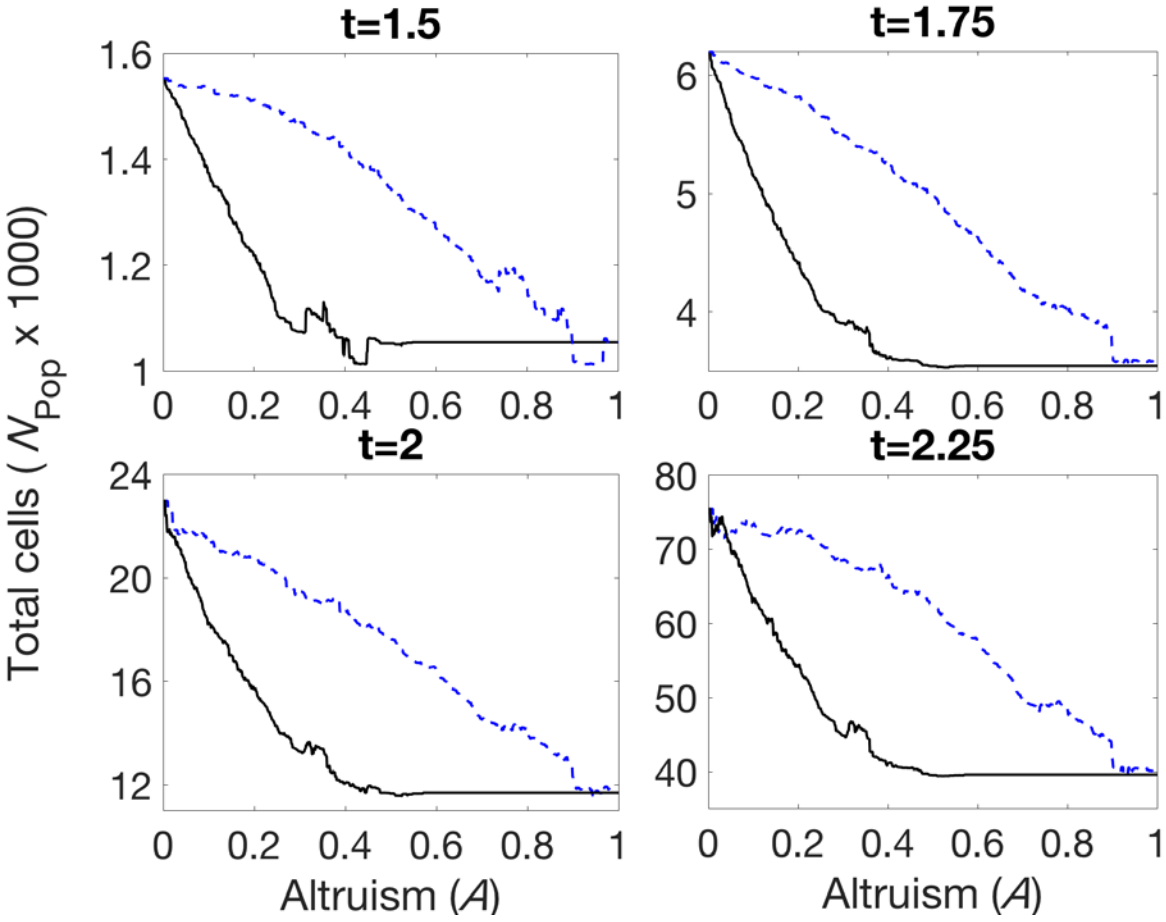


Figure S3: Total number of cells against the altruism values at four simulation times  $t = 1.5, 1.75, 2, 2.25$ . Lines represents population with distance strategy whereas the dashed lines represent the population with division strategy.

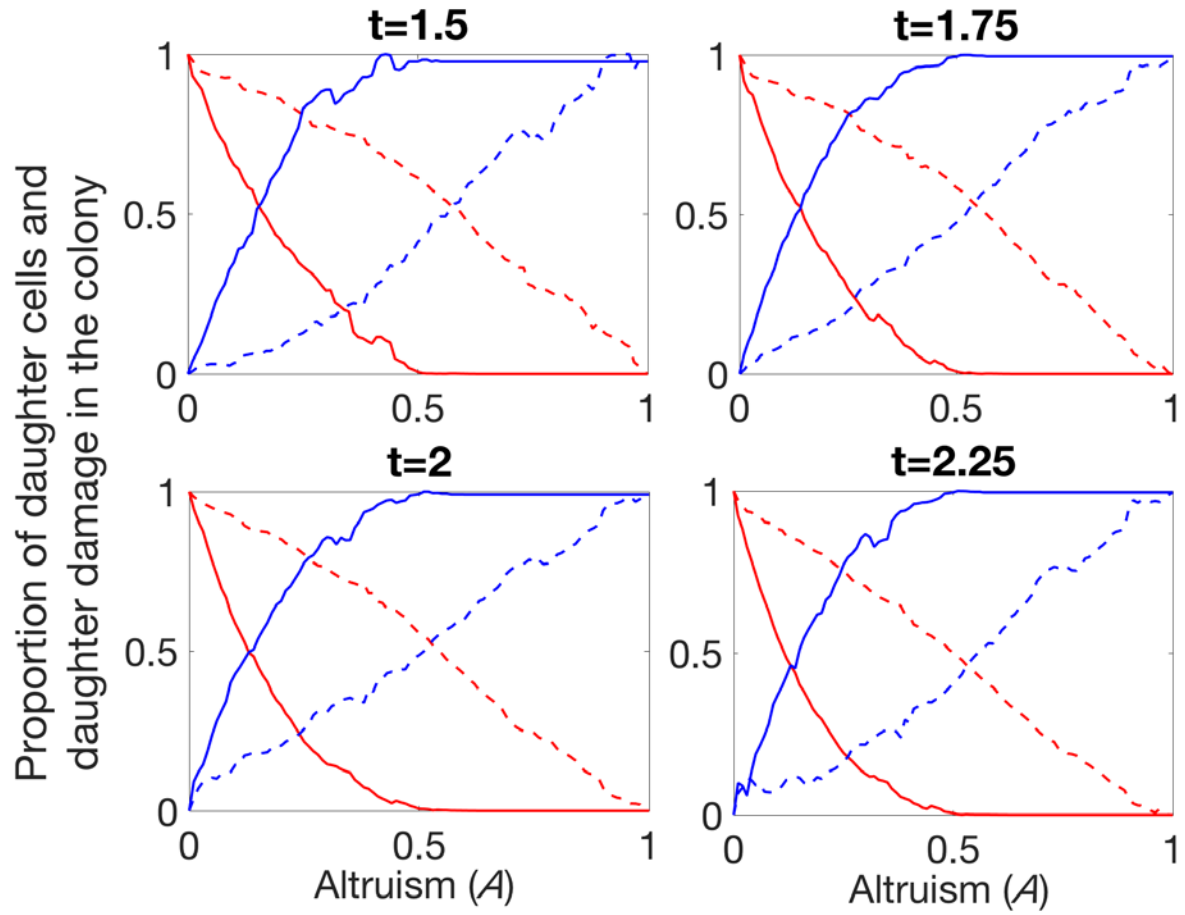


Figure S4: Proportion of daughter cells and their damage in the population for time  $t = 1.5, 1.75, 2$  and  $2.25$ . The continuous lines represent distance strategy while dashed lines represent division strategy. The lines moving from 0 to 1 are the daughter cells proportion while the lines moving from 1 to 0 are the damage proportion.

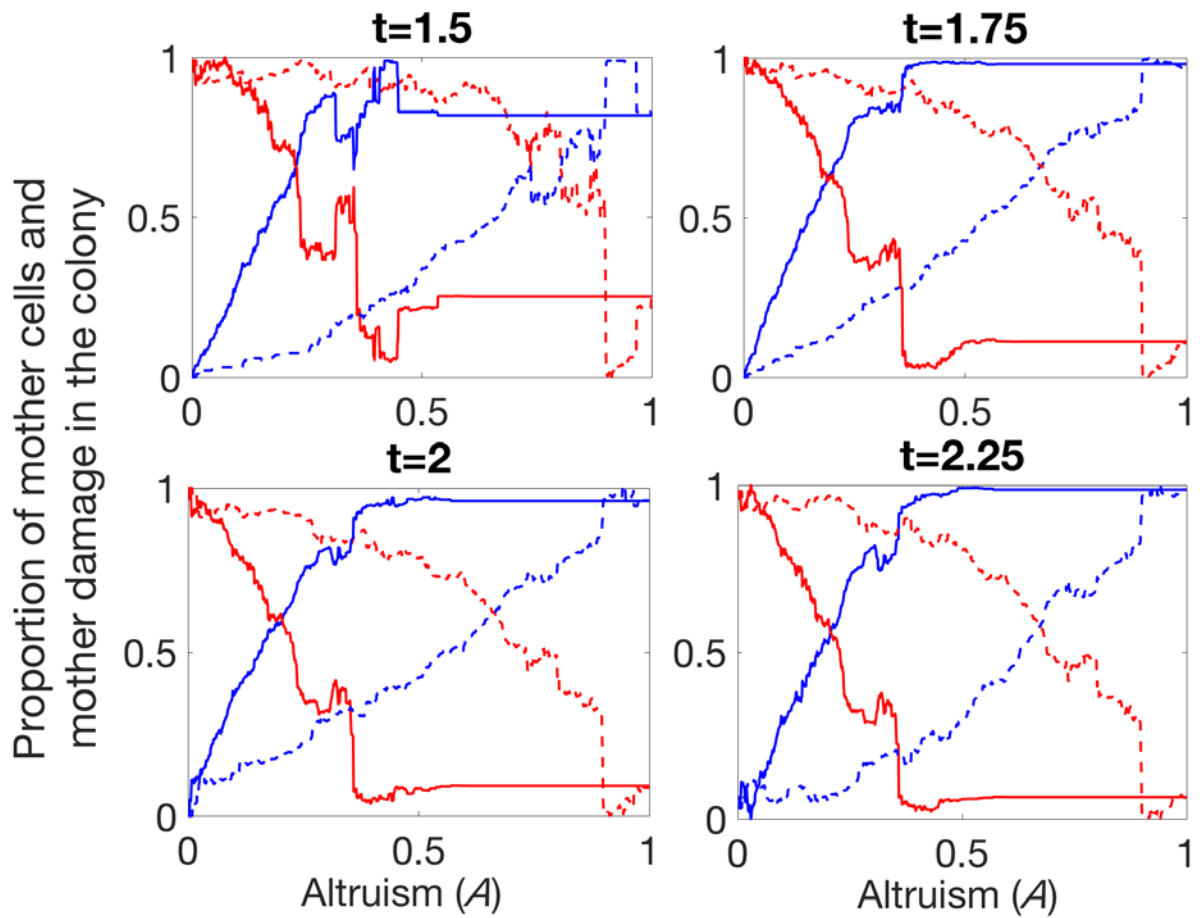


Figure S5: Proportion of mother cells and their damage in the colony at time  $t=1.5$ ,  $1.75$ ,  $2$  and  $2.25$ . The continuous lines represent distance strategy while dashed lines represent division strategy. The lines moving from 0 to 1 along y-axis are the mother cells proportion while the lines moving from 1 to 0 are the damage proportion.

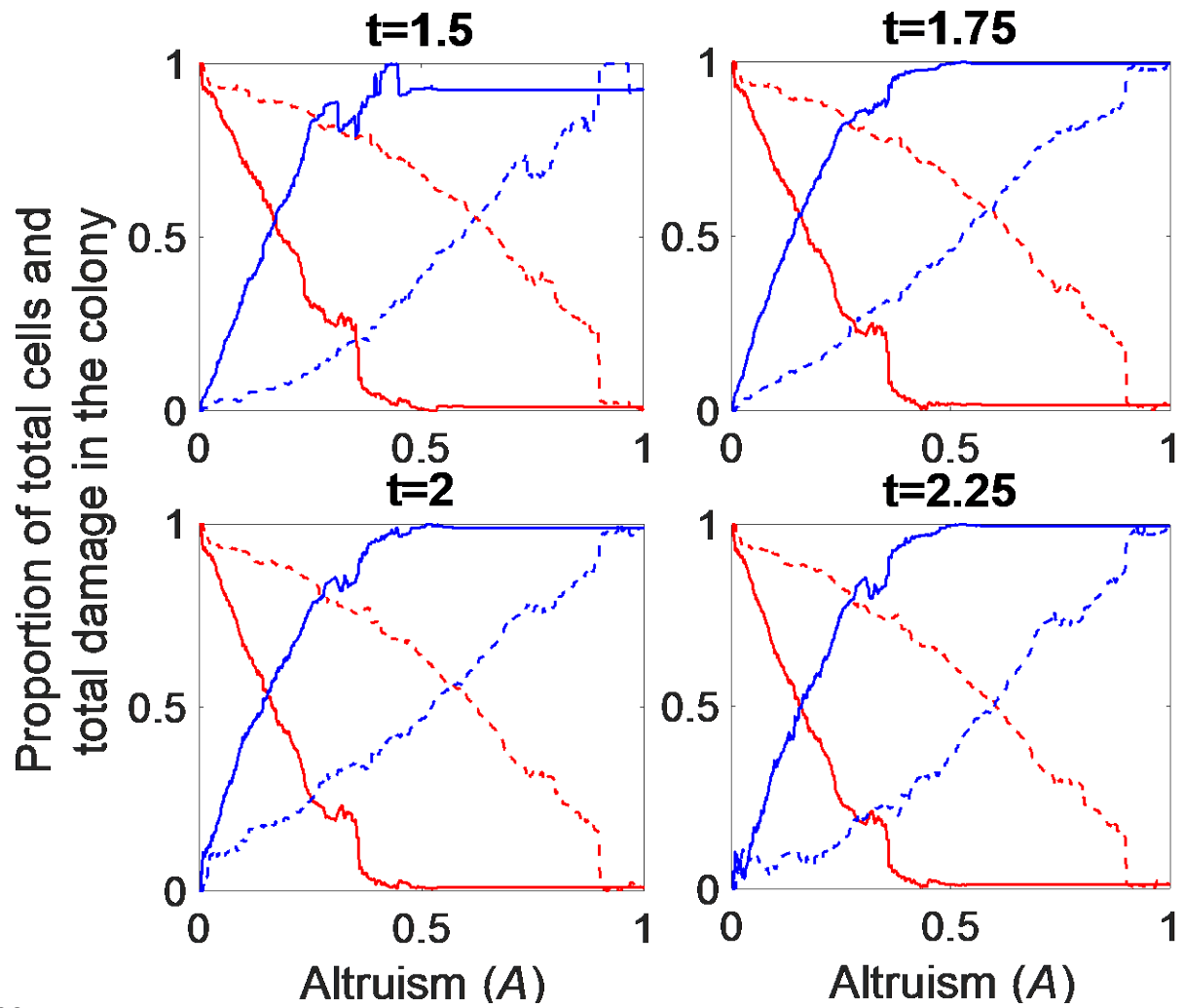


Figure S6: Proportion of total cells and their damage in the population for time  $t=1.5, 1.75, 2$  and  $2.25$ . The continuous lines represent distance strategy while dashed lines represent division strategy. The lines moving from 0 to 1 are the total cells proportion while the lines moving from 1 to 0 are the damage proportion.

## 722   **References**

- 723   Ackermann, M., Chao, L., Bergstrom, C.T., Doebeli, M., 2007. On the evolutionary origin of  
724       aging. *Aging Cell* 6, 235–244. <https://doi.org/10.1111/j.1474-9726.2007.00281.x>
- 725   Ackermann, M., Stearns, S.C., Jenal, U., 2003. Senescence in a bacterium with asymmetric  
726       division. *Science* 300, 1920. <https://doi.org/10.1126/science.1083532>
- 727   Aguilaniu, H., Gustafsson, L., Rigoulet, M., Nyström, T., 2003. Asymmetric inheritance of  
728       oxidatively damaged proteins during cytokinesis. *Science* 299, 1751–1753.  
729       <https://doi.org/10.1126/science.1080418>
- 730   Berg, J.M., Tymoczko, J.L., Stryer, L., 2002. *Evolution Requires Reproduction, Variation, and*  
731       *Selective Pressure.*
- 732   Biesalski, H.K., 2002. Free radical theory of aging. *Curr. Opin. Clin. Nutr. Metab. Care* 5, 5–10.
- 733   Brooks, R.C., Garratt, M.G., 2017. Life history evolution, reproduction, and the origins of sex-  
734       dependent aging and longevity. *Ann. N. Y. Acad. Sci.* 1389, 92–107.  
735       <https://doi.org/10.1111/nyas.13302>
- 736   Bufalino, M.R., DeVeale, B., van der Kooy, D., 2013. The asymmetric segregation of damaged  
737       proteins is stem cell-type dependent. *J. Cell Biol.* 201, 523–530.  
738       <https://doi.org/10.1083/jcb.201207052>
- 739   Chao, L., 2010. A model for damage load and its implications for the evolution of bacterial  
740       aging. *PLoS Genet.* 6. <https://doi.org/10.1371/journal.pgen.1001076>
- 741   Chao, L., Rang, C.U., Proenca, A.M., Chao, J.U., 2016. Asymmetrical Damage Partitioning in  
742       Bacteria: A Model for the Evolution of Stochasticity, Determinism, and Genetic  
743       Assimilation. *PLoS Comput. Biol.* 12. <https://doi.org/10.1371/journal.pcbi.1004700>
- 744   Clegg, R.J., Dyson, R.J., Kreft, J.-U., 2014. Repair rather than segregation of damage is the  
745       optimal unicellular aging strategy. *BMC Biol.* 12. [https://doi.org/10.1186/s12915-014-](https://doi.org/10.1186/s12915-014-0052-x)  
746       0052-x
- 747   Coelho, M., Lade, S.J., Alberti, S., Gross, T., Tolić, I.M., 2014. Fusion of protein aggregates  
748       facilitates asymmetric damage segregation. *PLoS Biol.* 12, e1001886.  
749       <https://doi.org/10.1371/journal.pbio.1001886>
- 750   de Grey, A.D., 1997. A proposed refinement of the mitochondrial free radical theory of aging.  
751       *BioEssays News Rev. Mol. Cell. Dev. Biol.* 19, 161–166.  
752       <https://doi.org/10.1002/bies.950190211>
- 753   Denoth Lippuner, A., Julou, T., Barral, Y., 2014. Budding yeast as a model organism to study  
754       the effects of age. *FEMS Microbiol. Rev.* 38, 300–325. [https://doi.org/10.1111/1574-](https://doi.org/10.1111/1574-6976.12060)  
755       6976.12060

756 Egilmez, N. K, and Jazwinski, S.M., 1989. Evidence for the involvement of a cytoplasmic factor  
757 in the aging of the yeast *Saccharomyces cerevisiae*. *J Bacteriol* 171: 37–42.

758 Erjavec, N., Cvijovic, M., Klipp, E., Nyström, T., 2008. Selective benefits of damage partitioning  
759 in unicellular systems and its effects on aging. *Proc. Natl. Acad. Sci. U. S. A.* 105, 18764–  
760 18769. <https://doi.org/10.1073/pnas.0804550105>

761 Erjavec, N., Larsson, L., Grantham, J., Nyström, T., 2007. Accelerated aging and failure to  
762 segregate damaged proteins in Sir2 mutants can be suppressed by overproducing the  
763 protein aggregation-remodeling factor Hsp104p. *Genes Dev.* 21, 2410–2421.  
764 <https://doi.org/10.1101/gad.439307>

765 Hill, S.M., Hanzén, S., Nyström, T., 2017. Restricted access: spatial sequestration of damaged  
766 proteins during stress and aging. *EMBO Rep.* 18, 377–391.  
767 <https://doi.org/10.15252/embr.201643458>

768 Hill, S.M., Hao, X., Grönvall, J., Spikings-Nordby, S., Widlund, P.O., Amen, T., Jörhov, A.,  
769 Josefson, R., Kaganovich, D., Liu, B., Nyström, T., 2016. Asymmetric Inheritance of  
770 Aggregated Proteins and Age Reset in Yeast Are Regulated by Vac17-Dependent  
771 Vacuolar Functions. *Cell Rep.* 16, 826–838.  
772 <https://doi.org/10.1016/j.celrep.2016.06.016>

773 Jazwinski, S.M., Wawryn, J., 2001. Profiles of random change during aging contain hidden  
774 information about longevity and the aging process. *J. Theor. Biol.* 213, 599–608.  
775 <https://doi.org/10.1006/jtbi.2001.2434>

776 Kaerberlein, M., 2010. Lessons on longevity from budding yeast. *Nature* 464: 513–519.

777 Katajisto, P., Döhla, J., Chaffer, C., Pentinmikko, N., Marjanovic, N., Iqbal, S., Zoncu, R., Chen,  
778 W., Weinberg, R.A., Sabatini, D.M., 2015. Asymmetric apportioning of aged  
779 mitochondria between daughter cells is required for stemness. *Science* 348, 340–343.  
780 <https://doi.org/10.1126/science.1260384>

781 Kennedy, B.K., Austriaco, N.R., Guarente, L., 1994. Daughter cells of *Saccharomyces cerevisiae*  
782 from old mothers display a reduced life span. *J. Cell Biol.* 127, 1985–1993.

783 Kirkwood, T.B., Rose, M.R., 1991. Evolution of senescence: late survival sacrificed for  
784 reproduction. *Philos. Trans. R. Soc. Lond. B. Biol. Sci.* 332, 15–24.  
785 <https://doi.org/10.1098/rstb.1991.0028>

786 Konieczny, L., Roterman-Konieczna, I., Spólnik, P., 2014. The Structure and Function of Living  
787 Organisms, in: *Systems Biology*. Springer, Cham, pp. 1–32.  
788 [https://doi.org/10.1007/978-3-319-01336-7\\_1](https://doi.org/10.1007/978-3-319-01336-7_1)

789 Kowald, A., Kirkwood, T.B., 2000. Accumulation of defective mitochondria through delayed  
790 degradation of damaged organelles and its possible role in the ageing of post-mitotic  
791 and dividing cells. *J. Theor. Biol.* 202, 145–160. <https://doi.org/10.1006/jtbi.1999.1046>



792 Kruegel, U., Robison, B., Dange, T., Kahlert, G., Delaney, J.R., Kotireddy, S., Tsuchiya, M.,  
793 Tsuchiyama, S., Murakami, C.J., Schleit, J., Sutphin, G., Carr, D., Tar, K., Dittmar, G.,  
794 Kaeberlein, M., Kennedy, B.K., Schmidt, M., 2011. Elevated proteasome capacity  
795 extends replicative lifespan in *Saccharomyces cerevisiae*. *PLoS Genet.* 7, e1002253.  
796 <https://doi.org/10.1371/journal.pgen.1002253>

797 Lindner, A.B., Madden, R., Demarez, A., Stewart, E.J., Taddei, F., 2008. Asymmetric segregation  
798 of protein aggregates is associated with cellular aging and rejuvenation. *Proc. Natl.*  
799 *Acad. Sci. U. S. A.* 105, 3076–3081. <https://doi.org/10.1073/pnas.0708931105>

800 Liu, B., Larsson, L., Franssens, V., Hao, X., Hill, S.M., Andersson, V., Höglund, D., Song, J., Yang,  
801 X., Öling, D., Grantham, J., Winderickx, J., Nyström, T., 2011. Segregation of protein  
802 aggregates involves actin and the polarity machinery. *Cell* 147, 959–961.  
803 <https://doi.org/10.1016/j.cell.2011.11.018>

804 Longo, V., Shadel, G. S., Kaeberlein, M., Kennedy, B., 2012. Replicative and Chronological Ageing  
805 in *Saccharomyces cerevisiae* *Cell Metab.* 16(1): 18-31 <https://doi.org/10.1016/j.cmet.2012.06.002>

807 Nyström, T., Liu, B., 2014. Protein quality control in time and space - links to cellular aging.  
808 *FEMS Yeast Res.* 14, 40–48. <https://doi.org/10.1111/1567-1364.12095>

809 Orgel, L.E., 1963. The maintenance of the accuracy of protein synthesis and its relevance to  
810 ageing. *Proc. Natl. Acad. Sci. U. S. A.* 49, 517–521.

811 Rujano, M.A., Bosveld, F., Salomons, F.A., Dijk, F., van Waarde, M.A.W.H., van der Want, J.J.L.,  
812 de Vos, R.A.I., Brunt, E.R., Sibon, O.C.M., Kampinga, H.H., 2006. Polarised asymmetric  
813 inheritance of accumulated protein damage in higher eukaryotes. *PLoS Biol.* 4, e417.  
814 <https://doi.org/10.1371/journal.pbio.0040417>

815 Spokoini, R., Moldavski, O., Nahmias, Y., England, J.L., Schuldiner, M., Kaganovich, D., 2012.  
816 Confinement to organelle-associated inclusion structures mediates asymmetric  
817 inheritance of aggregated protein in budding yeast. *Cell Rep.* 2, 738–747.  
818 <https://doi.org/10.1016/j.celrep.2012.08.024>

819 Stewart, E.J., Madden, R., Paul, G., Taddei, F., 2005. Aging and Death in an Organism That  
820 Reproduces by Morphologically Symmetric Division. *PLoS Biol.* 3.  
821 <https://doi.org/10.1371/journal.pbio.0030045>

822 Tyedmers, J., Mogk, A., Bukau, B., 2010. Cellular strategies for controlling protein aggregation.  
823 *Nat. Rev. Mol. Cell Biol.* 11, 777–788. <https://doi.org/10.1038/nrm2993>

824 Vedel, S., Nunns, H., Košmrlj, A., Semsey, S., Trusina, A., 2016. Asymmetric Damage  
825 Segregation Constitutes an Emergent Population-Level Stress Response. *Cell Syst.* 3,  
826 187–198. <https://doi.org/10.1016/j.cels.2016.06.008>

827 Zhou, C., Slaughter, B.D., Unruh, J.R., Guo, F., Yu, Z., Mickey, K., Narkar, A., Ross, R.T., McClain,  
828 M., Li, R., 2014. Organelle-based aggregation and retention of damaged proteins in

829           asymmetrically           dividing           cells.           Cell           159,           530–542.  
830           <https://doi.org/10.1016/j.cell.2014.09.026>

831

## Highlights

- Asymmetrically dividing budding yeast can increase the number of healthy daughters in the population by retaining more damage during the early divisions
- Retention of damaged proteins is a crucial mechanism ensuring a healthy daughter cell with full replicative potential and an ageing mother cell
- The protein quality control (PQC) system is tuned for optimal reproduction success that suggests optimal health and size of the population, rather than long-term survival of the mother cell
- A rapid decrease in the efficiency of damage retention, at the time when the mother cell is almost exhausted, produces fewer daughters with high levels of damage
- Fluctuations in the cost function allow yeast cell to continuously vary its strategy, suggesting that optimal reproduction success is a local minimum of cost function